

1994

A Dynamic model to study the influence of alpine ski boot characteristics on heel retention force

Elizabeth T. Hsiao

Follow this and additional works at: <http://scholarworks.rit.edu/theses>

Recommended Citation

Hsiao, Elizabeth T., "A Dynamic model to study the influence of alpine ski boot characteristics on heel retention force" (1994). Thesis. Rochester Institute of Technology. Accessed from

This Thesis is brought to you for free and open access by the Thesis/Dissertation Collections at RIT Scholar Works. It has been accepted for inclusion in Theses by an authorized administrator of RIT Scholar Works. For more information, please contact ritscholarworks@rit.edu.

**A DYNAMIC MODEL TO STUDY THE INFLUENCE OF ALPINE SKI BOOT
CHARACTERISTICS ON HEEL RETENTION FORCE**

ELIZABETH T. HSIAO

**A Thesis Submitted in Partial Fulfillment of the Requirements
for the Degree of Master of Science in Mechanical Engineering**

Approved by: Dr. Josef S. Torok (Advisor)

Dr. Jasper E. Shealy (Co-advisor)

Mr. Richard A. Schwartz (Xerox Corporation)

Dr. Charles Haines (Department Head)

Department of Mechanical Engineering
College of Engineering
Rochester Institute of Technology

July 1994

Permission Granted

I, Elizabeth T. Hsiao, do hereby grant Wallace Memorial Library of Rochester Institute of Technology permission to reproduce my thesis in whole or in part. Any reproduction by Wallace Memorial Library will not be used for commercial use or profit.

ACKNOWLEDGMENTS

My deepest appreciation to Dr. Török for readily providing support to me during all of my years at RIT and helping me through the most difficult part, the thesis. Thank you to Dr. Shealy for sharing his incredible knowledge and insight into the world of skiing and ski injury research. Thanks to Dick Schwartz for taking the time out of a very busy schedule to provide his usual thorough and intelligent input during the review of this work.

Additionally, thank you to Kathryn Playfoot for assisting with portions of the editing, typing, and curve fitting analysis.

I would also like to acknowledge and express my appreciation to my family, friends, and colleagues at Xerox. For without them, none of this would have been possible. Thank you to Ron Peck for his incredible patience and support. And of course, a very big thank you to Robin for being an amazing person.

ABSTRACT

A dynamic model representing an alpine ski boot under a forward leaning load was successfully developed. This model was based on the equations of motion for the defined system. The intent of this model was to provide an initial, first order investigation of the effect of variations in boot design. Specifically, it evaluated the influence of certain boot characteristics on the vertical heel force on the boot when it is captured in a conventional toe-heel ski binding. Boot stiffness, sole length, functional boot height, and initial forward lean angle were the chosen characteristics.

Functional boot height refers to a distance along the upper shaft of the boot. This distance is defined from the pivot point between the upper shaft and the lower base to a single loading point which is assumed to represent the concentration of the skier's forward load.

The initial forward lean angle is the angle formed by the centerline of the boot shaft and a vertical axis when the boot is in the unloaded condition.

This model considered the stiffness discontinuity which occurs if an increasing input force is applied even after the boot shaft is flexed forward far enough to a position that contacts the boot's built-in safety hard stop. As expected, greater heel forces were predicted for situations when the shaft was forced against the hard stop.

With respect to two of the characteristics, boot stiffness and initial forward lean angle, the results from the model suggested that very different phenomena occur to the heel force depending if it is examined before or after this discontinuity. For the first condition, which is the situation before the discontinuity, individual variation of either of these parameters caused distinctly different values in the heel force. But for the second condition, or situation after the discontinuity, variation of these parameters had no effect on the heel force. In fact, the force converged to the same value over time.

In contrast, variation of either of the two other parameters, sole length and functional boot height, caused distinctly different values in heel force during either condition.

The model found that if the range of the boot shaft motion was limited to within the first condition, then boot stiffness was the predominate parameter influencing the heel force. If the motion and loading went beyond this case, into the second condition range, then functional boot height became the most influential.

In addition to the model development, an exhaustive review of previous research was conducted on topics that pertained to alpine ski boot parameters and injuries to the lower extremities of the alpine skier. Research of particular interest was the efforts to characterize boot stiffness. Of particular note were the works by Walkhoff and Baumann (1987), Bonjour and Delouche (1989), and the long-term endeavor by a working group under the jurisdiction of the International Organization for Standards (ISO/TC83/SC3/WG14 1983 - 1993).

TABLE OF CONTENTS

ABSTRACT

LIST OF FIGURES iv

LIST OF TABLES iv

LIST OF SYMBOLS v

CHAPTER

1) INTRODUCTION	1
- Review of Previous Research	5
- Characterization of Boot Stiffness	5
- Forward Lean Angle	10
- Functional Boot Height	13
- Applied Skier Force	14
- Concern to Safety - Lower Extremity Injuries	15
2) PURPOSE	19
- Objectives	19
- Restrictions	20
3) DEVELOPMENT OF THE THEORETICAL MODEL	21
- The Dynamic Model	21
- Stiffness Discontinuity	22
- Model Parameters	24
- Model for First Condition	27
- Equations of Motion	28
- Generalized Forces	28
- Kinetic Energy	30
- Potential Energy	32
- Dissipation Function	35
- Combining Components into the Equations of Motion	35
- Application of Generalized Momenta	36
- Model for Second Condition	40
- Equations of Motion	41
- Generalized Forces	41
- Kinetic Energy	42
- Potential Energy	43
- Dissipation Function	43
- Combining Components into the Equations of Motion	44
- Application of Generalized Momenta	44

4)	DEVELOPMENT OF MODEL ANALYSIS TEST VALUES	45
-	Assessment of Dimensional Boot Properties	45
-	Approximation of Boot Stiffness	48
-	Dissipation Factor	54
-	Additional Analysis Constraints	56
-	Maximum Forward Lean Angle	56
-	Maximum Applied Force	57
-	Heel Force - Linear Spring Stiffness	57
5)	COMPUTER SIMULATION MODELS	58
-	First Condition Program	58
-	Combined First and Second Programs	59
6)	RESULTS OF COMPUTER MODELS	60
-	First Condition Program	60
-	Effects Due to Boot Parameters	60
-	Combined First and Second Programs	65
-	Effects Due to Boot Parameters	68
7)	CONCLUSIONS AND FUTURE RESEARCH	73
-	Conclusions	73
-	Future Research	75
	REFERENCE LIST	77

APPENDIX

A)	BACKGROUND WORK ON SKIER FORCE	
-	Principle of Conservation of Angular Momentum	A-I
-	Simple Case	A-III
-	Simplified Skier Case	A-IV
-	Average Skier Example	A-VI
B)	STATIC MODEL AT CONDITION OF MAXIMUM APPLIED LOAD	B-I
C)	COMPARISON BOOT DATA	C-I
-	Dolomite 65C Junior Racing, Front Entry	C-II
-	Trappeur Carbon, Front Entry	C-IV
-	Derivation of Mass Moments of Inertia Values	C-VI

APPENDIX (con't)

D)	ACSL PROGRAMS	D-I
	- "1STONLY.CSL": solves only first condition equations	D-II
	- "FIRST.CSL": solves only first condition eqns, use w/ Second.csl	D-III
	- "SECOND.CSL": solves only second condition eqns, use w/ First.csl	D-V
E)	ACSL PROGRAM RESULTS - NUMERICAL DATA	E-I
	- For 1STONLY.CSL	E-II
	- For FIRST.CSL and SECOND.CSL	E-XII

LIST OF FIGURES

<u>Figure #</u>		<u>Page</u>
1.1	Boot Parameters and Forces	4
1.2	Typical Applied Torque - Angular Deflection Response Curve	5
3.1	Typical Bending Moment - Angular Displacement Response Curve	23
3.2	Dynamic Model for the Boot	24
3.3	Free Body Diagram of Model in First Condition	27
3.4	Bending Moment-Angular Displacement Curves for Stiff and Soft Boots	33
3.5	Free Body Diagram of Model in Second Condition	40
4.1	Dimensional Data for Nominal Test Case (Nordica N955, Rear Entry)	46
4.2	Inertial Data for Nominal Test Case (Nordica N955, Rear Entry)	47
4.3	“Normal” Curve for Development of Nominal Test Case for K_o and ν	50
4.4	Screen Plot of Original Data vs. Approximation Curves	51
4.5	Screen Plot of Fit Results After Convergence	52
4.6	Screen Plot of Results from Varying K_o and ν Test Values	53
4.7 (a-d)	Plots Illustrating Effect of Modifying Dissipation Factor, “DAMP”	55
6.1	Plots Comparing F and F_{HEEL} as Functions of t and α	62
6.2 (a-d)	Plots Illustrating Influence of Characteristic Boot Properties on F_{HEEL}	63
A.1	Body Acted Upon By an Impulse	A-II
A.2 (a-c)	Simple Rigid Body Model	A-III
A.3 (a-c)	Skier Model Hitting Obstacle at y	A-V
B.1	Free Body Diagram of Model at Condition of Maximum Applied Load	B-I
B.2	Static Model Diagram	B-II
C.1	Dimensional Data for Dolomite 65C, Front Entry	C-II
C.2	Inertial Data for Dolomite 65C, Front Entry	C-III
C.3	Dimensional Data for Trappeur Carbon, Front Entry	C-IV
C.4	Inertial Data for Trappeur Carbon, Front Entry	C-V
C.5	Simplified Boot Base Used to Approximate J_T	C-VI
C.6	Simplified Boot Shaft Used to Approximate I_G	C-VII
C.7	Simplified Total Boot Used to Approximate J_{TOT}	C-VIII

LIST OF TABLES

<u>Table #</u>	
4.1	Boot Parameters and Test Values

LIST OF SYMBOLS

<u>Symbol</u>	<u>Description</u>
A	Location of center of mass of shaft
c	Damping Constant
D	Dissipation function due to damping of the boot structure
F_{HEEL}	Force Generated at the Heel Binding
$F, F(t)$	Applied Skier's Force
f_o	Maximum Force
H	Contact point of boot heel to binding
I_G	Moment of Inertia of the shaft
J_T	Polar Moment of Inertia of the base about T
J_{TOT}	Polar Moment of Inertia of the total boot about T
K_o	Boot Stiffness Linear Constant
k	Linear Spring Force, Allows for binding retention
L	Lagrangian = $T - V$
L_1	Boot Sole Length
L_2	Internal Model Parameter, Distance between boot toe and ankle pivot
L_3	Functional Boot Height
m_a	Mass of base
m, m_B	Mass of shaft
P	Pivot point of boot shaft
p_i	Generalized Momenta
q_i	Generalized Coordinates
Q_i^{**}, Q_i	Non-Conservative Generalized Forces
t	Time
T	Pivot point at boot toe
T	Kinetic Energy
V	Potential Energy
V_{LS}	Potential Energy due to linear spring
V_{TS}	Potential Energy due to torsional spring
v_{cm}, v_a	Absolute velocity of center of mass of shaft
α	Relative Shaft Flex Angle = $\theta - \psi$
β	Internal Model Parameter, Angle between L_1 and L_2
γ_{max}	Maximum Forward Lean Angle = $\phi_o + \alpha_{max, forward}$
ϕ_o	Initial Forward Lean Angle
θ	Absolute Shaft Flex Angle, independent generalized coordinate
v	Boot Stiffness Exponential Constant
ω	Angular velocity
ψ	Boot Sole Angle, independent generalized coordinate

CHAPTER 1

INTRODUCTION

Understanding and defining the effects of alpine ski boot characteristics on skiing performance and skier safety has been a topic of investigation among ski researchers in industry and academia for quite sometime. It will continue to be a topic of interest and research in the future due to a lack of fundamental quantitative knowledge and data.

Much of the current knowledge regarding boot characteristics and their effects on performance is the result of qualitative study and experience by researchers, manufacturers, retailers, and educated skiers. For example, it is known that a “stiffer” boot will provide better ski guidance control and a quicker response, and therefore would be the boot of choice for a more skilled skier. A “softer” boot will be more forgiving and will not respond as quickly to loads applied by a skier, and therefore, should be used by a beginner.

With regard to safety, numerous studies have been conducted to report the injury rate of the lower extremity during skiing. Some, like Shealy and Ettlinger’s study (1987), have even attributed certain fractures of the tibia to inadequate boot design.

However, even with all of this information, there still exists a vast number of unknowns with regard to how individual boot parameters such as stiffness, range of

forward flexure, initial forward lean, sole length, and functional boot height contribute to the performance of the ski-boot-binding system and the overall safety of the skier.

An example of the importance of improving this quantitative understanding to both the skiing research community and international monitoring agencies is the formation of a special working group within the International Organization for Standardization (ISO) to characterize the flexural properties of ski boots. This group, started in 1983, is classified as Technical Committee 83 / Subcommittee 3 / Working Group 14 (ISO/TC83/SC3/WG14). Its mission is “to evolve test methods for the flexural function of the upper and shaft parts of ski boots”.

After eleven years of activity, this working group is still grappling with satisfying its mission statement. This is due to the complexity and difficulty of finding a reproducible test method. Through their collaborative research, the group has found that characterization of a boot’s flexural, or stiffness, properties was not as simple as dropping a boot into any available testing fixture and reading off the same value every time. Rather, they found that measured values are dependent on a large number of parameters, such as testing method, testing fixture, use of human vs. prosthetic legs, type of prosthetic leg, closure tension, etc.

Although one of the main goals of the working group is to develop a flexibility measuring method, the group has also expanded its interests into studying the passive and active safety issues regarding the flexure of ski boots. Passive safety entails defining the physiological limits of ankle flexion during skiing. Active safety corresponds to defining

the relationship between flexural boot behavior, ski guidance/performance, and skier safety.

Research promoting the understanding of the active safety issue provided the motivation for this investigation. Researchers have gathered some experimental data on the effects of changing a few boot characteristic parameters, such as boot construction-front vs. rear entry, stiffness, and shaft height (Hauser, Asang, and Schaff 1985; Schaff, Schattner, and Hauser 1987; Walkhoff and Baumann 1987; Bonjour and Delouche 1989; Hall, Schaff, and Nelson 1991; Schaff and Hauser 1993). However, most of these works were not conducted with the expressed interest of understanding how changing a particular parameter would effect the boot / skier system. Rather the change in parameter was coincidental with changing test boots during research efforts to study areas such as contact pressure, stiffness, and flexibility.

Some of the researchers who have tried to model certain aspects of the boot and lower extremity interactions are Schattner, Hauser, and Asang (1985), Lyle and Hubbard (1985), Quinn and Mote (1993), and Yee and Mote (1993). No published work has been presented, however, that has directly addressed the issues of modeling both the details of the boot and the effects of varying a boot's design on the forces generated by the boot / skier system. The work developed in this paper is an initial, first-order attempt to develop a dynamic model that can represent such a relationship.

The relationship that will be investigated is the effect that certain boot parameters, namely boot stiffness, initial forward lean angle, functional boot height, and boot sole length, have on influencing the vertical force experienced at the heel of the boot when

captured in a conventional toe-heel ski binding. This relationship will be evaluated during the dynamic conditions encountered under a forward leaning movement and loading by the skier. See Figure 1.1.

Although this model only deals with the external heel force, further work on the model could allow it to be expanded to consider other external or internal forces and/or moments. For example, based on research conducted by Mote (1987) and colleagues (Mote and Hull 1978; Kuo, Louie, and Mote 1985), extended work in the area of forces and moments about the toe and ball of the foot would be necessary to correctly assess the implications that these boot parameters might have on the forward bending forces and moments with respect to binding release.

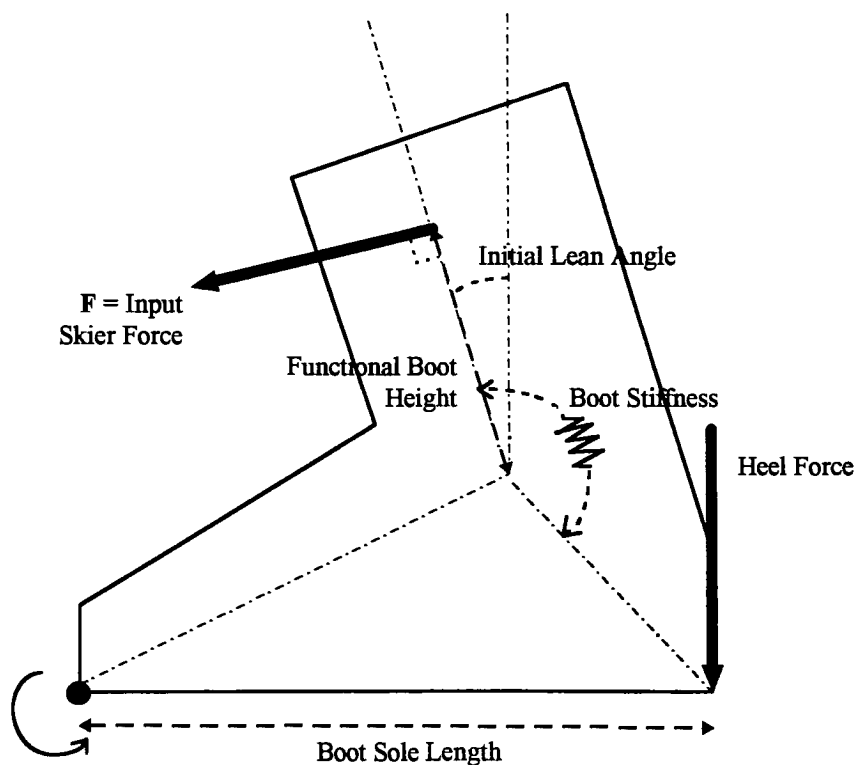


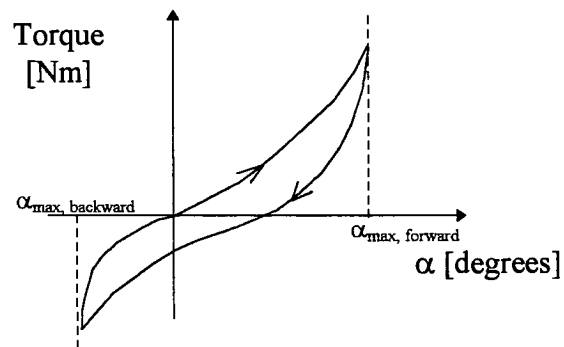
Figure 1.1 Boot Parameters and Forces. Note that boot stiffness is depicted as a torsional spring.

Review of Previous Research

Characterization of Boot Stiffness

The measurement of a boot's stiffness is currently made by flexing the upper shaft of a secured boot forward and backward and recording the angular deflection of the shaft versus the applied torque. This procedure creates a hysteresis curve similar to Figure 1.2. The stiffness of a boot is characterized by this torque-angle relationship. Stiffer boots tend to have steeper slopes and softer boots have gentler ones.

Figure 1.2 Typical Applied Torque - Angular Deflection Response Curve



The technique used in this measurement is not readily repeatable, standardized, nor consistent among researchers and manufacturers. As a result, the shape and slope of the curves varies from boot-to-boot and test-to-test. Numerous researchers (ISO/TC83/SC3/WG14, 1983 - 1993; Walkhoff and Baumann, 1987; Bonjour and Delouche, 1989) have attempted to develop a standardized, repeatable method to characterize a boot's inherent stiffness. Highlights of their work pertaining to boot stiffness follows.

After its initiation in 1983, the ISO working group set out to define a test method to define boot stiffness. During the first year, the group held four Round Robin meetings to share their experimental findings with regard to proposed testing methods. For the first

meeting, member labs measured three specified boots using their own testing method and fixtures on their own prosthesis or human leg. The results were scattered and were attributed to a variety of uncontrolled variables. Therefore, a second experiment was conducted and subsequent meeting was held. This time, they tried to identify an “ideal” prosthesis by comparing the different prostheses with human legs via x-rays and tested the different prostheses with the same method on the same machine. Again, the results were scattered.

A prosthesis made by TÜV (no.7 II) was chosen for testing and two more experiments were conducted. These results were presented at the third and fourth meetings. Both experiments were conducted at the different member labs on their different test machines and measured three and four specified test boots, respectively. The results were the same as before, scattered. The range of measurements varied from 4° to 7° at 100 Nm of applied forward torque and 4° to 10° at 200 Nm. At this point, the group decided to suspend its efforts at defining a test method and concentrate its activities on defining variables such as foot bed angle and forward lean angle, which contributed to some of the uncontrolled variables affecting the flex measurement.

In 1988, a detailed testing method proposal from Dr. C. Brown (ISO 1988) was submitted to conduct stiffness testing using human test subjects instead of prostheses. As of early 1991, a few labs had presented their results. Some of the conclusions that they found were that prostheses always recorded greater stiffness values than human testers; variables such as boot fit, ankle stiffness, and closure tension could still influence the results; and test methods could be reproducible, although some methods could be more

complicated than others. One method by C. Ettlinger (ISO 1992) seemed to have good promise and was being considered further.

Walkhoff and Baumann (1987) did lab testing at Raichle in order to understand hysteresis curve characteristics. Their experiments evaluated three types of boot construction - traditional overlapping front entry, three-piece, and rear entry. Either a prosthetic or human leg was considered under varying temperatures. From the hysteresis curves for different testing conditions, they compared characteristics such as “average stiffness”, “% energy dissipation to total energy input”, and an “energy dissipation factor” which was the actual dissipation energy divided by the average stiffness. Similar to the ISO group and work by Bonjour and Delouche (1989), their results also showed variability between prosthetic and human legs. They also concluded that test results can be significantly influenced by temperature changes (20°, 0°, and -10°C), boot construction, and the closure tension used around the foot or prosthesis.

Bonjour and Delouche (1989) performed stiffness testing in order to compare their results of using a prosthesis with those of the ISO working group and to gain knowledge on the effect of using a human leg. Their experiments were done on a test fixture developed in the Institute of Materials and Machines of Ecole Polytechnique Fédérale de Lausanne and used the same prosthesis as the ISO group, no.7 II. Tests were conducted on two different boots, one of which had stiffness adjustment capability. They made three observations based on their results. First, for the prosthesis, the stiffness curves were always shifted up and left such that the stiffness value determined from these curves was always greater in comparison to the results generated by the human testers. Second, the

human testers' curves had an average scatter of 40 - 50% of the mean value. And third, the influence of correctness of fit between the boot and foot was not readily apparent. Their overall conclusions were similar to the ISO group's: the boot alone cannot be measured for a specific stiffness; rather, it is a result of the combined boot/leg or boot/prosthesis system. Additionally, they said that stiffness values can only be compared, and only if under similar test conditions.

Observations about stiffness based on interpretation of research by investigators whose main objective was not stiffness characterization follow:

Asang and Hauser (1983) discussed experimental results that were used to demonstrate the International Association of Safety in Skiing's (IAS) standards #150 and #151. They looked at both the influence of the boot sole design on the torsional moment on the tibia and the influence of boot shaft design on the bending moment. In their research on boot shaft design which used a prosthetic leg, they showed that both the applied boot-top force and resulting heel force at a specified flexion angle varied depending on temperature and boot design. These experiments reaffirmed that stiffness increases with decreasing temperature (20° to -5°C) and different boots have different stiffnesses. Based on their research, they proposed different stiffness curves based on skiing ability.

Schattner, Hauser, and Asang (1985) developed a 3+1 degree of freedom, two dimensional point mass model of the skier from the knee down. Using their model they made conclusions regarding elastic (conservative) and inelastic (dissipative) boot stiffnesses with respect to the skier's mass, M , and size, L . They determined that elastic

stiffness was directly proportional to mass (M) and size (L). Inelastic stiffness was also linearly proportional to mass (M), but quadratically proportional to size (L^2). They also concluded that with increased speed and skill, the skier's generated torque increases, thereby increasing the need for higher stiffness. Thus, skilled or S-type skiers require stiffer boots with higher damping, and learner or L-type skiers need softer, low damping boots. Additionally, in order to ensure that maximal pressure and gradient are not beyond excessive limits, skiers which generate high moments; i.e. fast, tall, or heavy individuals, should use boot with relatively high shafts.

Schaff, Schattner, and Hauser (1987) did laboratory testing to measure the pressure distribution effects on the tibia using a pressure sensitive mat developed at TUEV Bayern. Additionally, they recorded the heel force. Test parameters were flexion, temperature, test subjects, boot size, gender by virtue of boot size selection, and boot construction - front vs. rear entry. They found that stiffness is temperature dependent; however, this temperature dependence could be reduced if a spring damping adjustment was incorporated in the boot. They also concluded that smaller sizes should be softer and boots should be classified according to gender and ability.

Shealy and Ettlinger (1987) investigated the effect that boot design had on causing the tibial bending injury known as "in-boot fractures" in five cases. They presented graphics representing typical hysteresis curves for recreational and racing ski boots. The recreational boot's large area within the loop was interpreted as typical of a boot that is softer and has more damping; one that does not have as lively a feeling. The racing boot

was said to feel more lively or springy because it acts more “like a spring than a damper.” (Note that this statement contradicts the one just made by Schattner, Hauser, and Asang.)

From the results of their study, they also proposed the need for additional standards for stiffness as a function of the skier’s mass and ability. Also there is a need to deal with gender differences in maximum dorsiflexion (although Shealy and Miller (1989), determined that gender is not an influencing factor for maximum flexion).

Yee and Mote (1993) performed field and laboratory testing to quantify and model the forces and moments at the boot top and knee. These factors are affected by boot stiffness and inertial forces. They had unexpected on-slope field results which found that the moment versus flexion response did not follow the typical laboratory hysteresis curve near the neutral flexion point (20° from vertical, for their model). Their lab curves, however, did follow typical hysteresis patterns as seen by others. They also found in their field data that the maximum bending moment did not occur at the expected maximum flexion, nor any large angle for that matter. It should be noted that their bending moment was the moment at the boot top, which is not the same as the typically measured moment at the distal end of the tibia. Additionally, in their lab testing, they observed that softer boots qualitatively have a greater nonlinear characteristic, and toward the forward limit of flex, the slope of the curve increased toward that of a stiffer boot.

Forward Lean Angle

The definition, method of measurement, and maximum range for the forward lean angle of the boot and skier’s leg are items under investigation by researchers. However,

there is disagreement as to how this angle should be defined. Is the angle measured from the vertical axis to the anterior blade of the tibia or the centerline of the calf, prosthesis or boot shaft? Is it measured from the horizontal axis to any of these reference points? What is the maximum angle or range of motion that a boot should be allowed to flex? Should the foot bed angle, which is within the inner boot, be considered?

Walkhoff and Baumann (1987) took x-rays of each boot construction with a human leg at the angles that they called “neutral position” and “40° forward flex position”. These angles were measured by potentiometers located at the ankle joint axis and were referenced from the vertical axis. The neutral position was basically measured in the unloaded condition.

For the overlap and three-piece designs at a 40° forward flex angle, they found that the tibial flexion angle was slightly greater than the boot shaft angle. Their study and observations were concerned with comfort and fit, but this example shows the potential difference which can occur between measured angles if based on the tibia or boot.

In 1986, after debating some of these questions, the ISO working group decided to define the forward lean angle with regard to their testing activities. They made two definitions, one for human legs and one for prostheses. For human legs, they chose the ASTM method (#F27.70, March, 1983) which measures the distance from the vertical axis to the line containing two points on the anterior tibia surface, 25% and 75% of the length. For a prosthesis, the angle is measured from the vertical to the central axis of the prosthesis. Later, the definition for the prosthesis was left open to the definition used by each prosthesis producer.

Hall, Schaff, and Nelson (1991) looked at angular displacement versus pressure distribution in skiers and non-skiers during flexion testing in a lab. They found that the rate of boot flexion is boot, not skier, dependent. Thus, they inferred that non-skiers and beginners need a soft boot and advanced skiers need a stiffer boot. However, both boots should allow a full flexion range, which would be 25° with a hard stop at approximately 40° from horizontal. They found that the actual range of motion for skiers is $16.64 \pm 1.15^{\circ}$ and $11.86 \pm 0.93^{\circ}$ for non-skiers.

Hauser, Asang, and Schaff (1985) made the following laboratory measurements: pressure, heel force, and lean angle. Three boots (A - which had a low shaft, B - which had a medium shaft and stiffness adjustment, and C - which had a high shaft) were used. They found that the range of motion of the ankle for optimal movement with no or minimal pain should be 0° to 30° from the vertical axis.

IAS #150 states that the maximum forward flex angle is 40° to 45° at 200 Nm, depending on interpretation, and minimum flex range should be up to 20° . Additionally, the angular deflection due to the maximum loading of 200 Nm should not change by more than 30% when testing in 0°C environment.

Based on their research, Shealy and Miller (1989) proposed that the maximum forward flex angle should not be greater than 30° in order to protect 93% of the population from injury due to excessive flexion. They also found no statistical difference in range of motion for age, gender, height, weight, and skiing experience. They quoted 1982 & 1983 *Skiing Magazine*'s test results which found at 200 Nm the maximum

forward flex angles for typical racing, recreational, and beginner boots were 27°, 30°, and 33°, respectively.

For the current investigation, which only considers the boot, the lean angle will be measured from the vertical axis to the centerline axis of the boot shaft.

Functional Boot Height

For the purpose of this investigation, the functional boot height is considered to be the distance along the boot shaft to the point of application of the forward load that is transferred from the skier. This load is assumed to act as a concentrated force.

Little research was found which tried to define this point. Many researchers just assume a point near the top of the boot.

One group of researchers (Schaff, Schattner, and Hauser 1987) were studying pressures along the tibia for front and rear entry boots. They identified the locations of maximum pressure for both constructions. For front entry boots, they found the maximum pressure to be generally located above the instep of the foot, or the lowest point on their pressure measuring mat which was located approximately 4 cm above the ankle joint. For rear entry boots, the location was at or near the boot top. Based on their evaluation, they stated a preference for a higher pressure location, similar to the rear entry results, and recommended that the maximum pressure also be distributed over a 4 cm² area.

Applied Skier Force

Initially, this investigation intended to model the loading condition on the boot by the skier as an impulse force similar to one that could be encountered during a forward fall. However, no published sources of experimental or theoretical data for such a force was found. Some studies were found that provided field data for normal cruising maneuvers (Hull and Mote 1982; Quinn and Mote 1993). Glenne and VonAllmen (1982) developed equations of motion from models for normal skiing activities such as fall line schussing, side slipping, and turning, but they did not address stopping or falling. Schaff and Hauser (1993) did conduct tests during falls and recorded force data; however, they only looked at backward falls.

Therefore, for this investigation, a simple sinusoidal forcing function was chosen to represent the input force. This function can be interpreted as a forward lean loading from an initially unloaded condition through an increasing force that may lead up to a force that is great enough to represent the same amount of force experienced in a forward fall. A more accurate forcing function or another forcing function that represents a different loading condition could always be added as future work.

Concern to Safety - Lower Extremity Injuries

To understand the impact that boot design may influence injuries during skiing, a literature search on lower extremity injuries was conducted. Researchers have found that the overall injury rate to the lower extremity has decreased, but the emphasis of injury type

and part of body injured have changed. The following are highlights of the findings from some major researchers.

In their study of four Norwegian ski areas from 1985-1986, Ekeland, Holtmoen, and Lystad (1993) found that 40% of all reported skiing injuries were classified as Lower Extremity Equipment Related (LEER) injuries. Of these LEER injuries, 56% were knee sprains and 14% were lower leg fractures, which were caused by a lack of or late binding release. Interestingly, 70% of the lower leg fractures were attributed to a lack of binding release.

Freeman et al. (1987) did a comparison study of data from four Aspen, Colorado ski areas for data collected from 1968-78 and 1982-84. They were interested only in understanding the changing patterns in tibial fracture incidences over the years. They found that there was a continual decline in tibial fractures from 12.9 injuries/100K skier days to 2.9/100K for 1968-69 to 1983-84, respectively. With regard to the population of all reported skiing injuries, the incidences of tibial fractures to other classifications of skiing injury also decreased (13% to 8% for 1968 to 1983, respectively).

They found that spiral tibial fractures, which are due to torsional forces, had reduced from 70.6% to 51.3% of all tibial fractures. They attributed this decrease to improvements, with regard to protection and release when under torsion, in the design and performance of both boots and bindings. Their hypotheses for why the incidences of spiral fractures were still comparatively higher than other tibial fracture types were because (a) ski injuries inherently have high rotational forces and (b) poor adjustment or maintenance of bindings may have also been a contributing factor.

Inversely, short oblique tibial fractures increased from 11.4% to 32.4%. These injuries are typically due to a high energy bending moment, which is often experienced during falls at high speeds. Freeman et al. concluded that this increase implies that the improvements made to binding designs were more effective in protection of torsional, than bending, forces.

Johnson, Ettlinger, and Shealy (1993) conducted, in Vermont, an eighteen season study (1972-1990) of all reported ski injuries. With regard to lower leg, or tibia, injuries, they found that the incidences decreased by 83% over the years. Specifically, twist-related injuries decreased by 90% and bending-related injuries decreased by 74%. Similar to the trends observed by Freeman et al., they found that tibial fractures decreased by 88%, and of these fractures, spiral fractures decreased by 94%.

They additionally reported knee sprains and found that grade I and II knee sprains (minor to moderate damage) decreased by 70% but grade III sprains (complete disruption) increased by 209%. Also, these grade III sprains now constituted 73%, up from 17%, of all knee sprains. Grade III sprains typically involve injury to the anterior cruciate ligament (ACL).

This increase in grade III sprains was also observed by other researchers and motivated Schaff and Hauser (1993) to perform laboratory and on-slope experiments to investigate the influence of ski boot construction on knee injuries such as severe knee lesions and, especially, isolated ACL ruptures. Their goal was to develop a measuring device for research using motion analysis, pressure and force measurement, and forward/backward motion examination via telemetry. Pending their results, they would

propose an improved safety concept. These experiments specifically looked at backward falls.

In their paper, Schaff and Hauser quoted numerous resources that proposed different theories on the mechanisms causing ACL ruptures. These include: hyperextension of the knee joint, hyperflexion of the knee joint, and backward falls. Additionally, they mention hybrid hyperflexion-backward fall mechanisms such as Johnson's "boot induced ACL injury", also known as the "big bump - flat landing" theory, and Ettlinger and Johnson's "phantom foot ACL injury", which is a backward fall with twisting. They also reference a model by Bally et al. which found that the load on the ACL increased if boot stiffness increased.

Shealy (1993) compared ski injury data for two sampling periods, 1978-81 and 1988-90, from fifteen ski areas across the United States. In general, he found that the overall injury rate decreased by 20% over the ten years. Specifically looking at lower extremity injuries, he found that tibial injuries had decreased 39% (from 12.6% to 7.7% of all injuries) and ankle injuries decreased 47% (11.5% to 6.1%), but knee injuries increased by 20% (27.2% to 32.7%). In fact, he found that knees were reportedly the most common body part injured, and the tibia and ankle had slipped from third and fourth to fourth and sixth most common part, respectively. Additionally, strains and sprains were the most common type of injury at 48.3%, while fractures were second at 13.5%.

Although Shealy found that the overall injury rate decreased, he indicated that this was a modest reduction in comparison with changes observed from the 1950s to the 1970s, and perhaps the injury rate had even reached a plateau with regard to current

equipment and tibial fractures and ankle injuries. He suggested that current skiing safety research should concentrate on areas such as design changes that could influence the reduction of knee injuries. He also proposed increased emphasis on the use of instruction to teach skiing safety.

(remainder of page is blank)

CHAPTER 2

PURPOSE

Objectives

The purpose of this investigation is to develop a dynamic model in order to assess certain characteristics of ski boots. In particular, the primary objective is to determine the influence of different ski boot characteristics on the heel hold-down force while a forward lean load is supplied. The development of this model may provide additional insight into the understanding of the dynamic properties of the alpine ski boot.

The developed model is based on the equations of motion for the boot in which certain boot characteristics are varied. Boot stiffness, functional boot height, initial forward lean, and boot sole length characteristics are evaluated.

The amount of forward lean load, or input force, is varied. The variation of this force approximates differences in skiers' strength, ability, body build, etc.

This model also considers the stiffness discontinuity that occurs when the maximum forward lean angle is achieved. This discontinuity occurs when the boot shaft reaches this point in its flexure path and can no longer proceed further due to the hard stop incorporated in the boot's design. Forces are now being transmitted more directly to the heel since energy is no longer being absorbed by the flexing of the boot shaft.

After developing the theoretical model, computer simulations were performed using several variations of the dynamic model. The equations of motion for the model, and consequently the heel force, were solved using programs written in the Advanced Continuous Simulation Language (ACSL).

Restrictions

Since this model is intended to be an initial, first order investigation of the influence of boot characteristics on heel force, it is restricted to a very simplified condition. In developing this model, only the case of a forward applied force is evaluated. The Principle of the Conservation of Angular Momentum had been attempted to approximate the impulse force that is generated at the ski boot by the skier in a forward fall. However, due to lack of data, the work in this area was suspended and a sinusoidal forcing function was chosen to actuate the model.

Additionally, only the bending characteristics in the sagittal plane and posterior-anterior movements are considered. Only forces and moments on the boot frame, or outer structure, are considered. No forces at the boot toe or under the ball of the foot are considered.

Additional assumptions include the boot sole as a rigid structure, the boot pivots about the toe, and the material properties of the boot (plastic shell and inner boot) are isotropic and can be combined into a homogeneous composite structure.

CHAPTER 3

DEVELOPMENT OF THE THEORETICAL MODEL

The Dynamic Model

The developed model was intended to provide an initial, first order investigation of the influence of ski boot characteristics on the vertical force generated at the boot heel. Many simplifying restrictions and assumptions were made when developing this model.

Restrictions and Assumptions:

- The skier's force is considered for the case of a leaning motion in the forward direction only. The force is applied normal to the tibial shaft and as a single point loading at the functional boot height. The forcing function is a sinusoidal function, $F(t) = f_0 \sin(\frac{t}{2})$, for $0 \leq t \leq \pi$. the case from an initial unloaded condition to a maximum forward leaning load is considered.
- Only the forces and moments in the sagittal plane are evaluated.
- Only the forces and moments applied to the boot frame or outer structure are evaluated. Bending moments on the tibia, forces at the boot toe, and forces under the ball of the foot are not considered.
- The boot sole is a rigid structure.
- The boot pivots about the toe, and therefore has no reaction forces but has a moment.

- The boot materials, a plastic shell and foam inner boot, are a homogeneous composite structure that is isotropic and follows the material properties of the shell.

Stiffness Discontinuity

The intention is to determine the heel force, F_{HEEL} . Two conditions need to be considered when determining this heel force profile. The first condition occurs while the shaft of the boot is still flexing and rotating about the pivot pins connecting the upper and lower plastic shells. The second occurs while the shaft has reached its maximum forward angular displacement, or hard stop, but an increasing input force is still being applied.

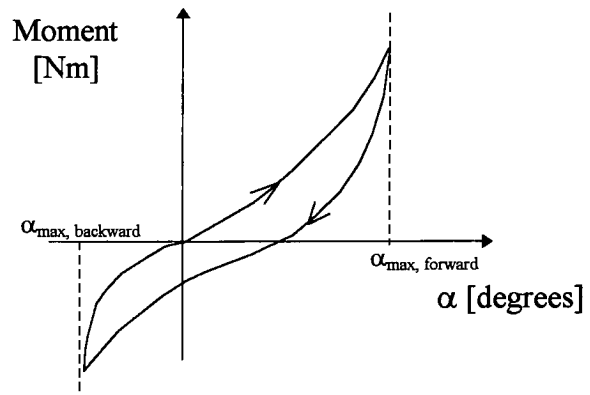
These two separate conditions result in a stiffness discontinuity. In the first condition, the boot stiffness can be approximated by the hysteresis relationship between the bending moment and angular displacement that was described in Chapter 1.

Using information from the hysteresis curves published by various researchers (ISO/TC83/SC3/WG14 1983-1993; Shealy and Ettlinger 1987; Walkhoff and Baumann 1987; Bonjour and Delouche 1989), the boot stiffness was chosen to be modeled as a nonlinear torsional spring¹ of stiffness K_0 . Figure 3.1 re-illustrates this condition, in which a boot is flexed forward and backward by either a human foot or prosthesis. During this flexing motion, the input force from the tester is not applied at a point beyond the forward or backward hard stops.

¹ A torsional spring behaves such that an angular deflection, α , [degrees or radians] will produce a change in torque, τ , [Nm] that is proportional to the spring's stiffness, k , [Nm/degrees or Nm, respectively]. This relationship can be represented as:

$$\begin{aligned}\tau &= k \cdot \alpha, \text{ for a linear spring, or} \\ \tau &= k \cdot \alpha^v, \text{ for a nonlinear spring.}\end{aligned}$$

Figure 3.1 Typical Bending Moment - Angular Displacement Response Curve

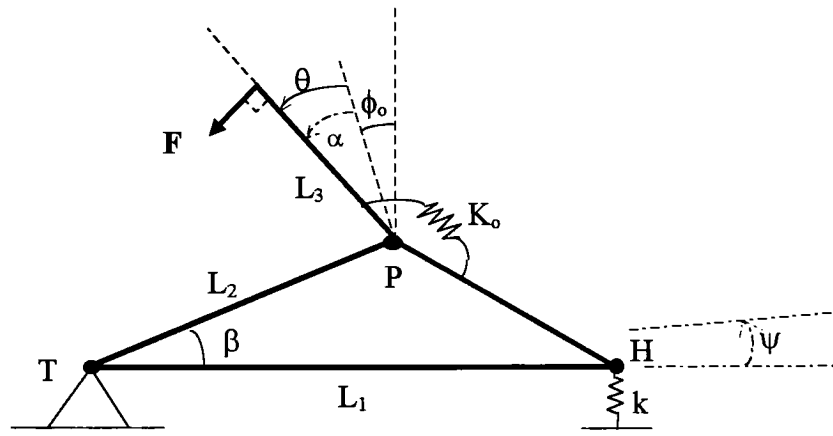


If the input force is continuously applied in a forward direction after reaching the hard stop, it is obvious that the response curve would follow the asymptote at $\alpha_{\max, \text{forward}}$, and the bending moment is no longer a function of angular displacement. At this point, the discontinuity in the boot stiffness occurs. The stiffness can no longer be determined from the bending moment - angular displacement relationship. This scenario describes the situation of the second condition.

In the second condition upon reaching the hard stop position, the entire boot is assumed to act like a rigid structure. The shaft and lower portion of the boot move as one unit pivoting about the toe. Thus, any applied force is transferred directly into the bending moment, and like-wise the heel force, without any of the energy attenuation that occurred when the shaft was rotating forward.

Because of this stiffness discontinuity, the model must consider both conditions. It should be noted that the second state requires information about the final conditions of the first state and therefore cannot be determined independently.

Model Parameters



for $t > t_0$

where

- F \equiv Applied Skier's Force
- H \equiv Contact Point of Boot Heel to Binding
- K_0 \equiv Absolute Boot Stiffness observed during shaft flexing
- k \equiv Allows for binding retention
- L_1 \equiv Boot Sole Length
- L_2 \equiv Local Variable
- L_3 \equiv Functional Boot Height
- P \equiv Pivot point of boot shaft
- T \equiv Pivot point at boot toe
- α \equiv Relative Shaft Flex Angle $= \theta - \psi$.
(Reference in diagram assumes $\psi = 0$.)
- β \equiv Local Variable
- ϕ_0 \equiv Initial Forward Lean Angle
- θ \equiv Absolute Shaft Flex Angle, independent generalized coordinate
- ψ \equiv Boot Sole Angle, independent generalized coordinate

Figure 3.2 Dynamic Model for the Boot

The input or Skier's Force, $F = F(t)$, is applied as a single point loading at the location of the functional boot height and is perpendicular to the boot shaft.

The Functional Boot Height, L_3 , is an assumed location for the concentration of the input force. This location has been designated as the top of the plastic shell for a rear entry boot or the middle of the top buckle on a front entry boot. Note that this location for the front entry boot is contrary to the pressure profiles found by Schaff, Schattner, and Hauser (1987).

The Initial Forward Lean Angle, ϕ_o , is the angle formed by the centerline of the boot shaft and a vertical axis perpendicular to the boot sole when the boot is in the unloaded condition. This point corresponds to the origin in Figure 3.1. The values used in the model were determined by visual inspection of the test boots. It should be noted that this choice in value is only an assumption made by the author. As has been stated by the ISO group (1985), the actual value of this “neutral” angle is imprecise due to the hysteresis effect of the prosthesis/boot system. They found that the range could be as large as 8° for rear entry boots and 11° for traditional boots.

The Boot Sole Angle, $\psi = \psi(t)$, measures the “theoretical” amount of global angular displacement that the boot sole experiences from the horizontal ground plane, or top surface of the ski. This value is theoretical because in reality, the boot sole is retained parallel to the ski by the heel binding during normal skiing conditions. However, in order to predict the heel force, a linear spring of stiffness, k , is used to approximate the binding retention effect and thus a measurement of deflection is necessary.

The Absolute Shaft Flex Angle, $\theta = \theta(t)$, measures the amount of global angular displacement that the boot shaft experiences beyond the initial forward lean angle, ϕ_o .

This statement means that θ always measures the absolute displacement of the centerline of the boot shaft from a constant reference axis that is relative to the ground. This axis is the one defined by the angle ϕ_o .

The Relative Shaft Flex Angle, α , represents the amount of local angular displacement of the boot shaft relative to the boot base, which flexes with ψ . This angle is defined as $\alpha = \theta - \psi$.

To better understand the difference between θ and α , consider these angles during the first and second conditions. During the first condition, both θ and α increase as the shaft rotates forward. However, during the second condition, α remains constant at $\alpha_{\max, \text{forward}}$ while θ is still increasing even though the boot shaft is no longer flexing forward with respect to the boot base.

The Boot Sole Length, L_1 , is length of the boot as determined from the outline contour of the sole of the boot.

For the case of the first condition in which the shaft is still flexing forward, the boot stiffness is modeled as a nonlinear torsional spring of stiffness K_o . Thus, as the shaft flexes forward, the torsional spring force and bending moment increase. Again, this characterization of the boot stiffness is an assumption made by the author since researchers are still undecided on the definition of stiffness and its measurement (ISO/TC83/SC3/WG14 1983-1993; Bonjour and Delouche 1989).

Model for First Condition

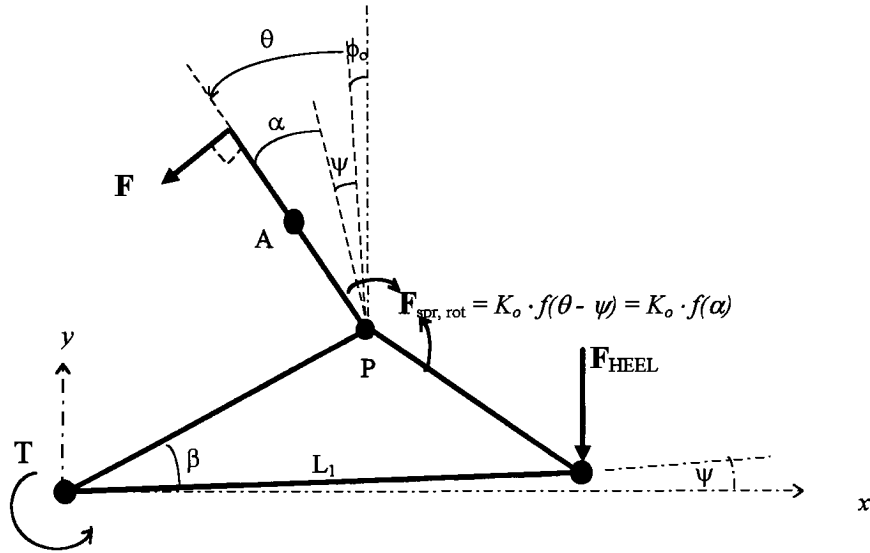


Figure 3.3 Free Body Diagram of Model in First Condition (flexure from ϕ_o to $\alpha_{\max, \text{forward}}$)

In this portion of the model, as the increasing input force is applied, the boot shaft is flexing forward from ϕ_o to its hard stop at $\alpha_{\max, \text{forward}}$. Meanwhile, the heel of the boot is “theoretically” rotating away from the top of the ski, and in reality would do so if the heel binding were not in place. Therefore, during this action, the torsional spring, which represents the boot’s stiffness properties, is angularly deflecting as a function of α .

The heel force, applied by the binding, is represented as the linear spring force generated by the vertical displacement caused by $\Delta\psi$. Therefore,

$$\begin{aligned} F_{HEEL} &= k \cdot L_1 \sin \psi \\ &= k \cdot L_1 \psi, \text{ for } \psi \ll 0. \end{aligned} \quad (3.1)$$

Thus $\psi = \psi(t)$ needs to be determined in order to solve for $F_{HEEL} = F_{HEEL}(t)$ at any time t .

The value of $\psi(t)$ is determined by developing the equations of motion for the system.

Equations of Motion

The equations of motion for this model were based on the application of Lagrange's equations for a system with dissipation and non-conservative forces which are not derivable from a potential function, V . Thus, the form of the Lagrange's equations, in terms of the Lagrangian, L , is

$$\frac{d}{dt} \left(\frac{\partial L}{\partial \dot{q}_i} \right) - \frac{\partial L}{\partial q_i} + \frac{\partial D}{\partial \dot{q}_i} = Q_i^{**} \quad i = 1, 2 \quad (3.2)$$

where

$$L = T - V$$

$T \equiv$ Kinetic Energy

$q_i \equiv$ generalized coordinates, $q_1 = \theta$ and $q_2 = \psi$

$D \equiv$ Dissipation function due to damping of the boot structure

$Q_i^{**} \equiv$ non-conservative generalized forces, $Q_1 = Q_\theta$ and $Q_2 = Q_\psi$.

Expanding Equation (3.2) by the Lagrangian, L , and noting that $V = V(q_i)$ and $\frac{\partial V}{\partial \dot{q}_i} = 0$,

produces the following form of the Equation of Motion:

$$\frac{d}{dt} \left(\frac{\partial T}{\partial \dot{q}_i} \right) - \left(\frac{\partial T}{\partial q_i} - \frac{\partial V}{\partial q_i} \right) + \frac{\partial D}{\partial \dot{q}_i} = Q_i^{**} \quad i = 1, 2 \quad (3.3)$$

Generalized Forces

The non-conservative generalized forces, Q_θ and Q_ψ , can be determined using the Principle of Virtual Work for a dynamic condition,

$$\delta W = \sum_{i=1}^{NDOF} Q_i \delta q_i,$$

where NDOF = number of degrees of freedom for the system (= 2).

These generalized forces consist of the forces not derivable from either a potential function, V , or a dissipation function, D .

Thus, for independent virtual displacements in the directions of the generalized coordinates, $\delta\theta$ and $\delta\psi$, the virtual work for each displacement is,

$$\begin{aligned}\delta W_\theta &= FL_3 \sin \delta\theta \\ &= FL_3 \delta\theta, \quad \text{for } \delta\theta \ll 0\end{aligned}$$

$$\begin{aligned}\delta W_\psi &= F \cos(\theta + \phi_0) \cdot L_2 \sin(\psi + \beta) \delta\psi + (-F \sin(\theta + \phi_0) \cdot L_2 \cos(\psi + \beta) \delta\psi) \\ &= [FL_2 \cos(\theta + \phi_0) \sin(\psi + \beta) - FL_2 \sin(\theta + \phi_0) \cos(\psi + \beta)] \delta\psi \\ &\quad \text{Apply: } \cos A \sin B - \sin A \cos B = \sin(B-A) = -\sin(A-B) \\ &= [-FL_2 \sin(\theta + \phi_0 - \psi - \beta)] \delta\psi\end{aligned}$$

Since the total virtual work is due to both components, the following relationship is derived.

$$\begin{aligned}\delta W &= \delta W_\theta + \delta W_\psi \\ \delta W &= [FL_3] \delta\theta + [-FL_2 \sin(\theta + \phi_0 - \psi - \beta)] \delta\psi\end{aligned}$$

Therefore applying the Principle of Virtual Work, $\delta W = \sum_{i=1}^{NDOF} Q_i \delta q_i$, the generalized forces

are:

$$\underline{Q_\theta = FL_3} \tag{3.4}$$

$$\text{and: } \underline{Q_\psi = -FL_2 \sin(\theta + \phi_0 - \psi - \beta)} \tag{3.5}$$

Kinetic Energy

The kinetic energy of the system is a combination of the linear and rotational kinetic energies of the boot's shaft and lower portion, or base.

For a system with translational and rotational components, the kinetic energy is described as:

$$T = \frac{1}{2}mv^2 + \frac{1}{2}I\omega^2.$$

Since the base of the boot only rotates about the toe at point T, it only has a rotational component of kinetic energy.

$$T_{BASE} = \frac{1}{2}J_T\dot{\psi}^2, \quad (3.6)$$

where $J_T \equiv$ Polar Moment of Inertia of the base about T

$\dot{\psi} \equiv$ angular velocity due to base rotation, ψ .

The shaft, however, rotates and translates as it flexes. The rotation is accounted for by the independent variable θ . The translation occurs because the center of mass moves due to the combined effect of the rotations from θ and ψ . Thus the kinetic energy for the shaft is,

$$T_{SHAFT} = \frac{1}{2}mv_{CM}^2 + \frac{1}{2}I_G\dot{\theta}^2,$$

where $m \equiv$ mass of the shaft,

$v_{cm} \equiv$ absolute velocity of the shaft's center of mass relative to the
inertial reference frame,

$I_G \equiv$ Moment of Inertia of the shaft, where point G \equiv point A,

$\dot{\theta} \equiv$ angular velocity due to shaft rotation, θ .

The value for v_{cm} can be determined by considering the relative velocities. Let point A represent the location for the center of mass of the shaft, such that $v_A = v_{cm}$.

Recall that point P is the pivot point of the boot shaft. (See Figure 3.3.)

Therefore,

$$\begin{aligned}\mathbf{v}_P &= \dot{\psi} \hat{\mathbf{k}} \times [L_2 \cos(\beta + \psi) \hat{\mathbf{i}} + L_2 \sin(\beta + \psi) \hat{\mathbf{j}}] \\ &= -\dot{\psi} L_2 \sin(\beta + \psi) \hat{\mathbf{i}} + \dot{\psi} L_2 \cos(\beta + \psi) \hat{\mathbf{j}} \\ \mathbf{v}_{A/P} &= \dot{\theta} \hat{\mathbf{k}} \times \left[-\frac{L_3}{2} \sin(\theta + \phi_0) \hat{\mathbf{i}} + \frac{L_3}{2} \cos(\theta + \phi_0) \hat{\mathbf{j}} \right] \\ &= -\frac{\dot{\theta} L_3}{2} \cos(\theta + \phi_0) \hat{\mathbf{i}} - \frac{\dot{\theta} L_3}{2} \sin(\theta + \phi_0) \hat{\mathbf{j}}\end{aligned}$$

Thus,

$$\begin{aligned}\mathbf{v}_A &= \mathbf{v}_P + \mathbf{v}_{A/P} \\ &= \left[-\frac{\dot{\theta} L_3}{2} \cos(\theta + \phi_0) + \dot{\psi} L_2 \sin(\beta + \psi) \right] \hat{\mathbf{i}} \\ &\quad + \left[-\frac{\dot{\theta} L_3}{2} \sin(\theta + \phi_0) + \dot{\psi} L_2 \cos(\beta + \psi) \right] \hat{\mathbf{j}} \\ v_A^2 &= |\mathbf{v}_A|^2 = \mathbf{v}_A \cdot \mathbf{v}_A \\ &= \left[\frac{\dot{\theta} L_3}{2} \cos(\theta + \phi_0) + \dot{\psi} L_2 \sin(\beta + \psi) \right]^2 \\ &\quad + \left[-\frac{\dot{\theta} L_3}{2} \sin(\theta + \phi_0) + \dot{\psi} L_2 \cos(\beta + \psi) \right]^2\end{aligned}\tag{3.7}$$

$$\therefore T_{SHAFT} = \frac{1}{2} m v_A^2 + \frac{1}{2} I_G \dot{\theta}^2, \text{ where } v_A^2 \text{ is from Equation (3.7).}\tag{3.8}$$

So, combining the kinetic energies from both parts of the boot (3.6) and (3.8), the total system kinetic energy is:

$$T = T_{BASE} + T_{SHAFT}$$

$$T = \frac{1}{2} J_T \dot{\psi}^2 + \frac{1}{2} I_G \dot{\theta}^2 + \frac{1}{2} m \left\{ \left[\frac{\dot{\theta} L_3}{2} \cos(\theta + \phi_0) + \dot{\psi} L_2 \sin(\beta + \psi) \right]^2 + \left[-\frac{\dot{\theta} L_3}{2} \sin(\theta + \phi_0) + \dot{\psi} L_2 \cos(\beta + \psi) \right]^2 \right\} \quad (3.9)$$

Now, in order to apply the kinetic energy to Lagrange's Equations of Motion, take the partial derivatives of T (3.9) for each generalized coordinate. Therefore after reduction, these partials are:

$$\frac{\partial T}{\partial \theta} = -\frac{m L_2 L_3}{2} \dot{\theta} \dot{\psi} [\cos(\theta + \phi_0 - \beta - \psi)] \quad (3.10)$$

and
$$\frac{\partial T}{\partial \psi} = \frac{m L_2 L_3}{2} \dot{\theta} \dot{\psi} [\cos(\theta + \phi_0 - \beta - \psi)] \quad (3.11)$$

Additionally, determine the time derivatives of the partial derivatives of T for each generalized coordinate, $\frac{d}{dt} \left(\frac{\partial T}{\partial \dot{q}_i} \right) = \frac{\partial T}{\partial \dot{q}_i}$.

$$\frac{\partial T}{\partial \dot{\theta}} = \left(I_G + \frac{m L_3^2}{4} \right) \dot{\theta} - \left(\frac{m L_2 L_3}{2} \sin(\theta + \phi_0 - \psi - \beta) \right) \dot{\psi} \quad (3.12)$$

$$\frac{\partial T}{\partial \dot{\psi}} = - \left(\frac{m L_2 L_3}{2} \sin(\theta + \phi_0 - \psi - \beta) \right) \dot{\theta} + (J_T + m L_2^2) \dot{\psi} \quad (3.13)$$

These terms are also referred to as the generalized momenta, p_i , such that

$$p_i = \frac{\partial L}{\partial \dot{q}_i} = \frac{\partial T}{\partial \dot{q}_i}, \quad \text{for } V = V(q_i).$$

Potential Energy

The potential energy of the boot system is due the effects of the linear spring at the heel (LS) and the nonlinear torsional spring connecting the shaft and base (TS).

For the linear spring, which follows Hooke's law as stated in Equation (3.1),

$\mathbf{F}_{\text{HEEL}} = k \cdot L_1 \psi$, the potential energy is:

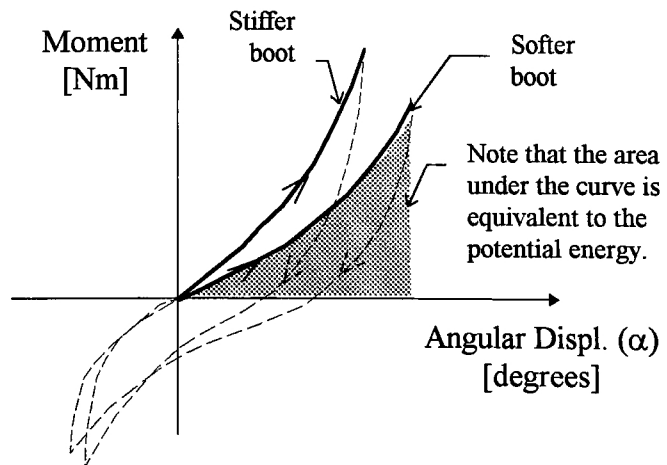
$$\begin{aligned} V_{LS} &= \frac{1}{2} k \left[(L_1) \sin \psi \right]^2 \\ &= \frac{1}{2} k \left[(L_1) \psi \right]^2, \quad \text{for } \psi \ll 0 \end{aligned}$$

Taking the partial derivatives of V_{LS} for each generalized coordinate gives:

$$\begin{aligned} \frac{\partial V_{LS}}{\partial \theta} &= 0 \\ \frac{\partial V_{LS}}{\partial \psi} &= k (L_1)^2 \psi \end{aligned} \tag{3.14}$$

The potential energy for the nonlinear torsional spring was derived using the condition for a conservative system which says that $Q_i = -\frac{\partial V}{\partial q_i}$, where Q_i are conservative generalized forces. Taking into account only the forward flexure portion of the bending moment - angular displacement response curve after the origin (solid line in Figure 3.4), a nonlinear relationship can be derived between bending moment - a generalized force - and angular displacement - interpreted as the combination of the angles θ and ψ .

Figure 3.4. Bending Moment - Angular Displacement curves for stiff and soft boots. Note that Angular Displacement is due to the combination of θ and ψ . ($\alpha = \theta - \psi$)



This relationship can be expressed as a polynomial function where the constant, K_o , and the polynomial multiplier, v , are determined by the boot's properties.

$$Q_i = -K_o \alpha^v, \text{ where } \alpha = (\theta - \psi).$$

Therefore, for in terms of the generalized coordinates, the generalized forces are,

$$Q_\theta = -K_o (\theta - \psi)^v, \text{ for } \theta > 0$$

$$Q_\psi = K_o (\theta - \psi)^v, \text{ for } \psi > 0$$

Values for K_o and v were approximated by using curve data presented by Bonjour and Delouche (1989). Curve fitting software was used to determine approximate values for this relationship. For stiffer or high performance boots, the values of K_o and v are higher. For softer or beginner boots, the values are lower.

Thus, the partial derivatives of V_{TS} with respect to the generalized coordinates are:

$$\begin{aligned} \frac{\partial V_{TS}}{\partial \theta} &= -Q_\theta = K_o (\theta - \psi)^v \\ \frac{\partial V_{TS}}{\partial \psi} &= -Q_\psi = -K_o (\theta - \psi)^v \end{aligned} \tag{3.15}$$

Therefore, the effects for the total potential energies from both springs gives the following equations,

$$\begin{aligned} \frac{\partial V}{\partial q_i} &= \frac{\partial V_{LS}}{\partial q_i} + \frac{\partial V_{TS}}{\partial q_i} \\ \frac{\partial V}{\partial \theta} &= K_o (\theta - \psi)^v \end{aligned} \tag{3.16}$$

$$\frac{\partial V}{\partial \psi} = k(L_1)^2 \psi - K_d(\theta - \psi)^p \quad (3.17)$$

Dissipation Function

The dissipation function, D , accounts for any damping effects of the boot. Damping in the boot can be related to the combined shock absorbing properties of the inner boot and plastic shell. For this model, these damping effects are combined into one value, c , which will be considered to be proportional to the angular velocities, $\dot{\theta}$ and $\dot{\psi}$. Therefore, the dissipation function is:

$$D = \frac{1}{2}c(\dot{\theta} - \dot{\psi})^2$$

So the non-conservative generalized force components, $\frac{\partial D}{\partial \dot{q}_i}$, are:

$$\frac{\partial D}{\partial \dot{\theta}} = c(\dot{\theta} - \dot{\psi}) \quad (3.18)$$

$$\frac{\partial D}{\partial \dot{\psi}} = -c(\dot{\theta} - \dot{\psi}) \quad (3.19)$$

Combining Components into the Equations of Motion

$$\text{Recalling Equation (3.3), } \frac{d}{dt} \left(\frac{\partial T}{\partial \dot{q}_i} \right) - \left(\frac{\partial T}{\partial q_i} - \frac{\partial V}{\partial q_i} \right) + \frac{\partial D}{\partial \dot{q}_i} = Q_i^{**} \quad i = 1, 2.$$

Now substitute into (3.3) all of the relationships that have been derived for each of the components. For $q_1 = \theta$, these would be (3.12), (3.10), (3.16), (3.18), and (3.4). For $q_2 = \psi$, these would be (3.13), (3.11), (3.17), (3.19), and (3.5), respectively.

Thus, the equations of motion for the boot are:

for $q_1 = \theta$,

$$\begin{aligned} \frac{d}{dt} \left[\left(I_G + \frac{mL_3^2}{4} \right) \dot{\theta} - \left(\frac{mL_2 L_3}{2} \sin(\theta + \phi_0 - \psi - \beta) \right) \dot{\psi} \right] \\ - \left[\left(-\frac{mL_2 L_3}{2} \dot{\theta} \dot{\psi} \cos(\theta + \phi_0 - \beta - \psi) \right) - \left(K_o(\theta - \psi)^v \right) \right] = FL_3 - c(\dot{\theta} - \dot{\psi}) \end{aligned} \quad (3.20)$$

and for $q_2 = \psi$,

$$\begin{aligned} \frac{d}{dt} \left[-\left(\frac{mL_2 L_3}{2} \sin(\theta + \phi_0 - \psi - \beta) \right) \dot{\theta} + (J_T + mL_2^2) \dot{\psi} \right] \\ - \left[\left(\frac{mL_2 L_3}{2} \dot{\theta} \dot{\psi} \cos(\theta + \phi_0 - \beta - \psi) \right) - \left(kL_1^2 \psi - K_o(\theta - \psi)^v \right) \right] \\ = -FL_2 \sin(\theta + \phi_0 - \psi - \beta) - (-c(\dot{\theta} - \dot{\psi})) \end{aligned} \quad (3.21)$$

However, these two equations have four (4) unknowns, θ , $\dot{\theta}$, ψ , and $\dot{\psi}$; therefore, two more equations are necessary. This dilemma is solved by using the relationship of the generalized momenta, $p_i = \frac{\partial L}{\partial \dot{q}_i} = \frac{\partial T}{\partial \dot{q}_i}$, for $V = V(q_i)$. (3.22)

Application of Generalized Momenta

After substituting the relationship described in Equation (3.22) into (3.20) and (3.21) and rearranging, the equations of motion can be rewritten as:

$$\begin{aligned} \frac{d}{dt} [p_\theta] = \dot{p}_\theta = \left[\left(-\frac{mL_2 L_3}{2} \dot{\theta} \dot{\psi} \cos(\theta + \phi_0 - \beta - \psi) \right) - \left(K_o(\theta - \psi)^v \right) \right] \\ + FL_3 - c(\dot{\theta} - \dot{\psi}) \end{aligned} \quad (3.23)$$

$$\begin{aligned} \frac{d}{dt}[p_\psi] = \dot{p}_\psi = & \left[\left(\frac{mL_2L_3}{2} \dot{\theta} \dot{\psi} [\cos(\theta + \phi_0 - \beta - \psi)] \right) - (kL_1^2 \psi - K_o(\theta - \psi)^\nu) \right] \\ & - FL_2 \sin(\theta + \phi_0 - \psi - \beta) - (-c(\dot{\theta} - \dot{\psi})) \end{aligned} \quad (3.24)$$

Additionally, recalling Equations (3.12) and (3.13) in terms of the general momenta give,

$$p_\theta = \frac{\partial T}{\partial \dot{\theta}} = \left(I_G + \frac{mL_3^2}{4} \right) \dot{\theta} - \left(\frac{mL_2L_3}{2} \sin(\theta + \phi_0 - \psi - \beta) \right) \dot{\psi} \quad (3.25)$$

$$p_\psi = \frac{\partial T}{\partial \dot{\psi}} = - \left(\frac{mL_2L_3}{2} \sin(\theta + \phi_0 - \psi - \beta) \right) \dot{\theta} + (J_T + mL_2^2) \dot{\psi} \quad (3.26)$$

Equations (3.25) and (3.26) can be rewritten as the following,

$$\begin{aligned} p_\theta &= A \dot{\theta} - B \dot{\psi} \\ p_\psi &= -B \dot{\theta} + D \dot{\psi} \end{aligned} \quad (3.27)$$

where $A = I_G + \frac{mL_3^2}{4}$

$$B = \frac{mL_2L_3}{2} \sin(\theta + \phi_0 - \psi - \beta)$$

$$D = J_T + mL_2^2$$

Equations (3.27) can be expressed in matrix notation as,

$$\begin{bmatrix} p_\theta \\ p_\psi \end{bmatrix} = \begin{bmatrix} A & -B \\ -B & D \end{bmatrix} \begin{bmatrix} \dot{\theta} \\ \dot{\psi} \end{bmatrix}, \quad \text{such that } \mathbf{M} = \begin{bmatrix} A & -B \\ -B & D \end{bmatrix}.$$

Using Cramer's rule², the solutions for $\dot{\theta}$ and $\dot{\psi}$ can be determined.

$$\begin{aligned}\dot{\theta} &= \frac{\begin{vmatrix} p_\theta & -B \\ p_\psi & D \end{vmatrix}}{|\mathbf{M}|} & \dot{\psi} &= \frac{\begin{vmatrix} A & p_\theta \\ -B & p_\psi \end{vmatrix}}{|\mathbf{M}|} \\ &= \frac{Dp_\theta + Bp_\psi}{|\mathbf{M}|} & &= \frac{Bp_\theta + Ap_\psi}{|\mathbf{M}|}\end{aligned}\quad (3.28) \text{ \& } (3.29)$$

$$\text{where } |\mathbf{M}| = AD - (-B)(-B) = AD - B^2$$

Thus, four dependent differential equations (3.23), (3.24), (3.28), and (3.29) were developed for \dot{p}_θ , \dot{p}_ψ , $\dot{\theta}$, and $\dot{\psi}$, respectively. These first order equations are recalled for reference.

$$\begin{aligned}\dot{p}_\theta &= \left[\left(-\frac{mL_2L_3}{2} \dot{\theta}\dot{\psi} [\cos(\theta + \phi_0 - \beta - \psi)] \right) - (K_\alpha(\theta - \psi)^\nu) \right] \\ &\quad + FL_3 - c(\dot{\theta} - \dot{\psi})\end{aligned}\quad (3.23)$$

$$\begin{aligned}\dot{p}_\psi &= \left[\left(\frac{mL_2L_3}{2} \dot{\theta}\dot{\psi} [\cos(\theta + \phi_0 - \beta - \psi)] \right) - (kL_1^2\psi - K_\alpha(\theta - \psi)^\nu) \right] \\ &\quad - FL_2 \sin(\theta + \phi_0 - \psi - \beta) - (-c(\dot{\theta} - \dot{\psi}))\end{aligned}\quad (3.24)$$

$$\dot{\theta} = \frac{Dp_\theta + Bp_\psi}{|\mathbf{M}|} \quad (3.28)$$

$$\dot{\psi} = \frac{Bp_\theta + Ap_\psi}{|\mathbf{M}|} \quad (3.29)$$

² Cramer's rule states that if $|\mathbf{A}| \neq 0$, a system $\mathbf{Ax} = \mathbf{b}$ of n linear equations in n unknowns has a unique solution whose j th component is given by

$$x_j = \frac{|\mathbf{D}_j|}{|\mathbf{A}|} \quad 1 \leq j \leq n$$

where the matrix \mathbf{D}_j has \mathbf{b} as its j th column and the corresponding columns of \mathbf{A} as its other columns. From Wylie and Barrett, p. 194.

However, there are still four unknowns, p_θ , p_ψ , θ , and ψ . By taking the integrals over time of the differential equations, these values can be determined. So, the four final equations are,

$$\underline{p_\theta = \int_{t_0}^t \dot{p}_\theta dt + p_\theta(t_0),} \quad (3.30)$$

$$\underline{p_\psi = \int_{t_0}^t \dot{p}_\psi dt + p_\psi(t_0),} \quad (3.31)$$

$$\underline{\theta = \int_{t_0}^t \dot{\theta} dt + \theta(t_0),} \quad (3.32)$$

$$\underline{\psi = \int_{t_0}^t \dot{\psi} dt + \psi(t_0),} \quad (3.33)$$

With these eight (8) dependent equations in hand, the equations of motion for the boot can be solved; and therefore, the values for $\psi = \psi(t)$ and, finally, $\mathbf{F}_{\text{HEEL}} = \mathbf{F}_{\text{HEEL}}(t)$ can be determined. These equations of motion will predict the activity of the boot system during the scenario of the first condition, that is when the shaft is rotating between ϕ_0 and

$\alpha_{\text{max, forward}}$.

Model for Second Condition

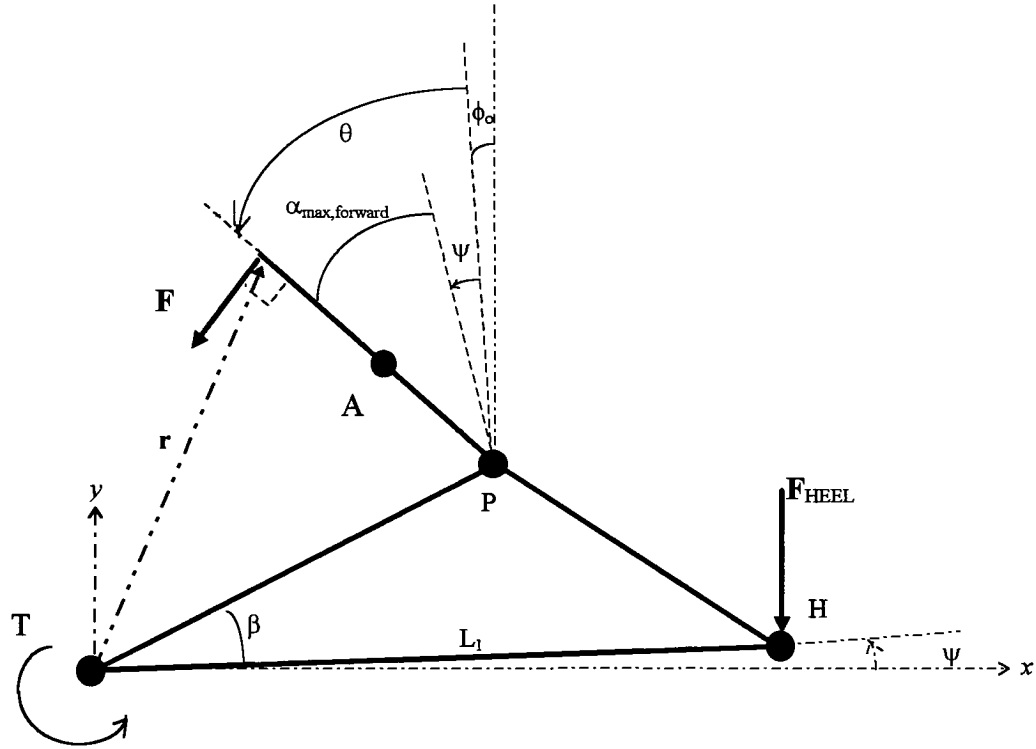


Figure 3.5 Free Body Diagram of Model in Second Condition
 Relative to the boot base, the shaft cannot rotate beyond $\alpha_{\max, \text{forward}}$.
 The entire boot rotates as a single rigid body about T, and $\Delta\theta = \Delta\psi$.

In this portion of the model, the input force is sufficient enough to cause the boot shaft to rotate until it reached its hard stop at $\alpha_{\max, \text{forward}}$. At this point, the boot shaft can no longer flex forward, relative to the boot base, even with additional loading. Therefore, the whole boot, shaft and base, are now considered a single rigid body. As an increasing input force is applied, the heel of the boot theoretically continues to rotate away from the top of the ski. Thus, the angular displacement, ψ , will continue to change. θ will also change but by the same amount as ψ because these variables are now constrained to each other, such that $\alpha \equiv \text{constant} = (\theta_{1\text{st con}} + \Delta\theta) - (\psi_{1\text{st con}} + \Delta\psi) \therefore \Delta\theta = \Delta\psi$.

Thus, the equations of motion developed for the first condition are no longer valid, and new equations of motion are necessary.

Equation of Motion

The equation of motion will be developed, using the same method as used for the first condition, from Lagrange's equation of motion. Equation (3.3) is repeated for reference:

$$\frac{d}{dt} \left(\frac{\partial T}{\partial \dot{q}_i} \right) - \left(\frac{\partial T}{\partial q_i} - \frac{\partial V}{\partial q_i} \right) + \frac{\partial D}{\partial \dot{q}_i} = Q_i^{**} \quad i = 1 \quad (3.3)$$

However in this portion of the model, only one variable ψ is considered because θ and ψ are constrained by $\Delta\theta = \Delta\psi$; therefore $i = 1$, and $q_1 = q_\psi$ and $Q_1^{**} = Q_\psi$.

Generalized Force

The non-conservative force, Q_ψ , is again derived by using the Principle of Virtual Work. $\delta W = \sum_{i=1}^{NDOF} Q_i \delta q_i$. Since the shaft is no longer rotating with respect to the base, a more convenient method for determining Q_ψ can be employed. This method utilizes the vector, \mathbf{r} , which extends from the boot toe, T, to the application point of the input force, \mathbf{F} . (See Figure 3.5.)

Virtual work can also be written as:

$$\delta W = \mathbf{F} \cdot \delta \mathbf{r}$$

where

$$\mathbf{r} = L_2 \cos(\beta + \psi) \hat{i} + L_2 \sin(\beta + \psi) \hat{j} - L_3 \sin(\alpha_{\max, \text{forward}} + \phi_0 - \psi) \hat{i} + L_3 \cos(\alpha_{\max, \text{forward}} + \phi_0 - \psi) \hat{j}$$

$$\mathbf{F} = -F \cos(\alpha_{\max, \text{forward}} + \phi_0 - \psi) \hat{i} - F \sin(\alpha_{\max, \text{forward}} + \phi_0 - \psi) \hat{j}$$

\therefore

$$\begin{aligned} \delta W &= \left\{ F \cos(\alpha_{\max, \text{forward}} + \phi_0 - \psi) \left[+L_2 \sin(\beta + \psi) + L_3 \cos(\alpha_{\max, \text{forward}} + \phi_0 - \psi) \right] \right. \\ &\quad \left. + F \sin(\alpha_{\max, \text{forward}} + \phi_0 - \psi) \left[-L_2 \cos(\beta + \psi) + L_3 \sin(\alpha_{\max, \text{forward}} + \phi_0 - \psi) \right] \right\} \cdot \delta \psi \\ &= \left\{ FL_3 - FL_2 \sin(\alpha_{\max, \text{forward}} + \phi_0 - \beta) \right\} \cdot \delta \psi \end{aligned}$$

This result gives the generalized force of

$$\underline{Q_\psi = FL_3 - FL_2 \sin(\alpha_{\max, \text{forward}} + \phi_0 - \beta)} \quad (3.35)$$

where $F = F(t)$ for $t \geq t_{1\text{st con, final}}$, $t_{1\text{st con, final}} \equiv$ time when $\alpha = \alpha_{\max, \text{forward}}$ and the first condition model no longer applies.

Kinetic Energy

The kinetic energy is now due to the rotational kinetic energy of the single rigid body of the combined shaft and base. Taking the moment of inertia about the toe at point T gives,

$$\begin{aligned} T &= \frac{1}{2} I \omega^2 \\ T &= \frac{1}{2} J_{TOT} \dot{\psi}^2 \end{aligned} \quad (3.36)$$

where $J_{TOT} \equiv J_T + \left(I_G + m_{\text{shaft}} \overline{AT}^2 \right)$, the combination of the Polar Moment of Inertia for the base, J_T , and the Moment of Inertia for the shaft modified by the Parallel Axis

Theorem from the center of gravity of the shaft to the boot toe, $\left(I_G + m_{shaft} \overline{AT}^2\right)$. Note: for the computer simulation model, J_{TOT} is assumed to be constant and \overline{AT} is based on the maximum lean condition.

The partial derivatives of T, for application into Lagrange's equation, are:

$$\frac{\partial T}{\partial \psi} = 0 \quad (3.37)$$

$$\frac{\partial T}{\partial \dot{\psi}} = J_{TOT} \dot{\psi} \quad (3.38)$$

Potential Energy

The potential energy is due only to the linear spring at the heel (LS).

$$V_{LS} = \frac{1}{2} k \left[(L_1) \psi \right]^2, \quad \text{for } \psi \ll 0$$

Therefore, the partial derivative for the total potential energy is the same as Equation (3.14-b),

$$\frac{\partial V}{\partial \psi} = \frac{\partial V_{LS}}{\partial \psi} = k (L_1)^2 \psi \quad (3.39)$$

Dissipation Function

Dissipation is considered for the ψ variable; therefore,

$$D = \frac{1}{2} c \dot{\psi}^2$$

$$\frac{\partial D}{\partial \dot{\psi}} = c \dot{\psi} \quad (3.40)$$

Combining Components into the Equation of Motion

Substitute Equations (3.35) through (3.40) into Equation (3.3) to get the equation of motion for the second condition.

$$\begin{aligned} \frac{d}{dt}[J_{TOT}\dot{\psi}] - (0 - kL_1^2\psi) + c\dot{\psi} &= FL_3 - FL_2 \sin(\theta_{max, forward} + \phi_0 - \beta) \\ \frac{d}{dt}[J_{TOT}\dot{\psi}] + kL_1^2\psi + c\dot{\psi} &= FL_3 - FL_2 \sin(\theta_{max, forward} + \phi_0 - \beta) \end{aligned} \quad (3.41)$$

Application of Generalized Momenta

Again, using the relationship of the generalized momenta, Equation (3.22)

$$p_i = \frac{\partial L}{\partial \dot{q}_i} = \frac{\partial T}{\partial \dot{q}_i}, \quad \text{for } V = V(q_i), \text{ and the same process as in the first condition, four}$$

dependent differential equations can be derived.

$$\dot{p}_\psi = \frac{d}{dt}[p_\psi] = FL_3 - FL_2 \sin(\theta_{max, forward} + \phi_0 - \beta) - kL_1^2\psi - c\dot{\psi} \quad (3.42)$$

$$\dot{\psi} = \frac{p_\psi}{J_{TOT}} \quad (3.43)$$

$$p_\psi = \int_{t_{1stcon, final}}^t \dot{p}_\psi dt + p_\psi(t_{1stcon, final}) \quad (3.44)$$

$$\psi = \int_{t_{1stcon, final}}^t \dot{\psi} dt + \psi(t_{1stcon, final}) \quad (3.45)$$

These four (4) dependent equations are solved after the boot shaft reaches its hard stop. They use the final conditions from the first state, $t_{1stcon, final}$, $F(t_{1stcon, final})$, $\psi(t_{1stcon, final})$, and $p_\psi(t_{1stcon, final})$ as initial conditions for solving this second state.

CHAPTER 4

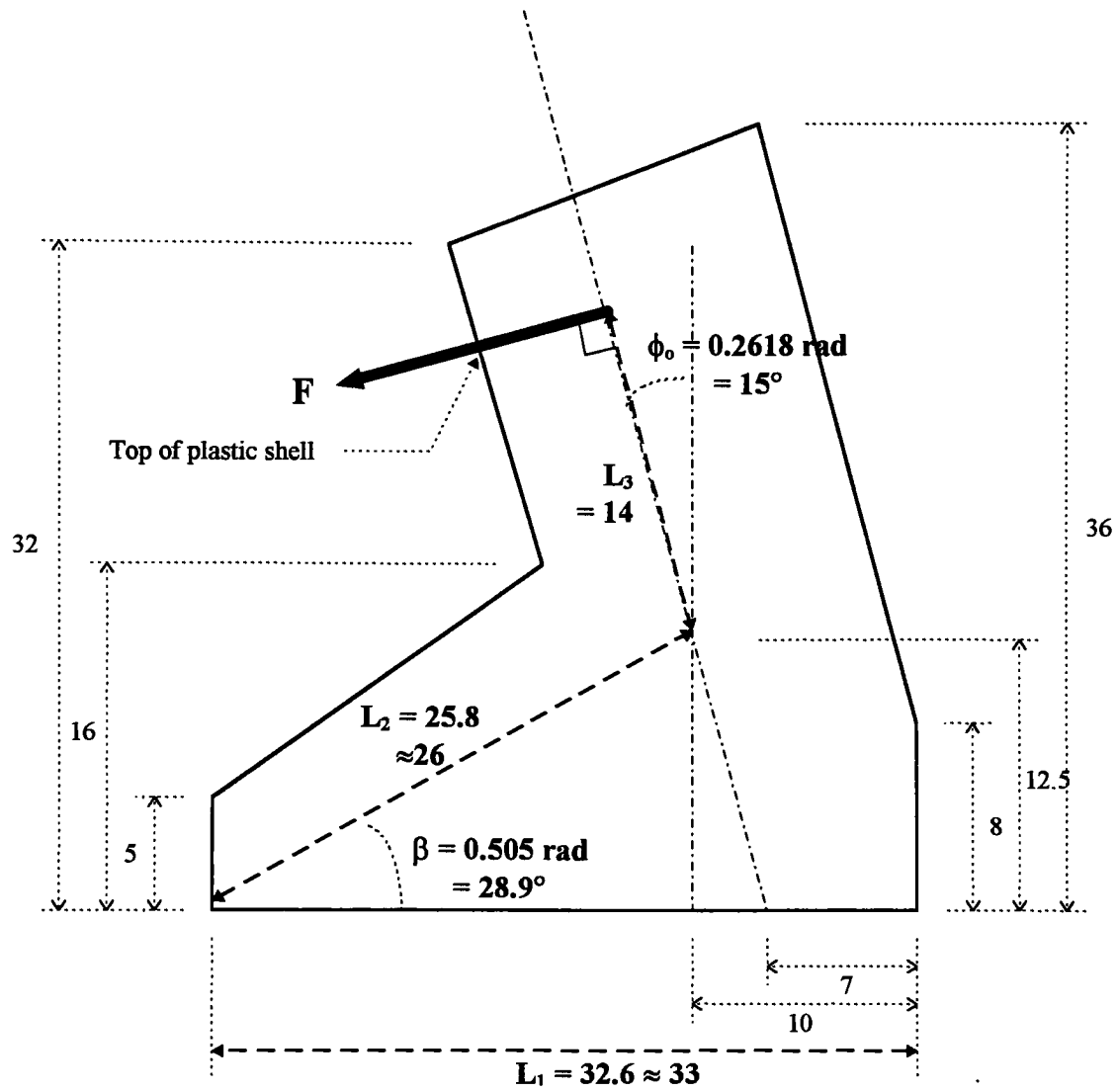
DEVELOPMENT OF MODEL ANALYSIS TEST VALUES

The model analysis was developed around a nominal test case and then each of the evaluated boot parameters were individually varied with respect to the nominal case. The varied parameters were boot sole length, L_1 , functional boot height, L_3 , initial lean angle, ϕ_o , and boot stiffness which is characterized by two values, K_o and ν . In addition to these originally planned test parameters, the dissipation factor, c , was also evaluated.

For the nominal case, the dimensional boot parameters were based on measurements made on a Nordica N955 rear entry boot. Values used to represent the boot stiffness parameters were derived using data from a hysteresis curve presented by Bonjour and Delouche (1989).

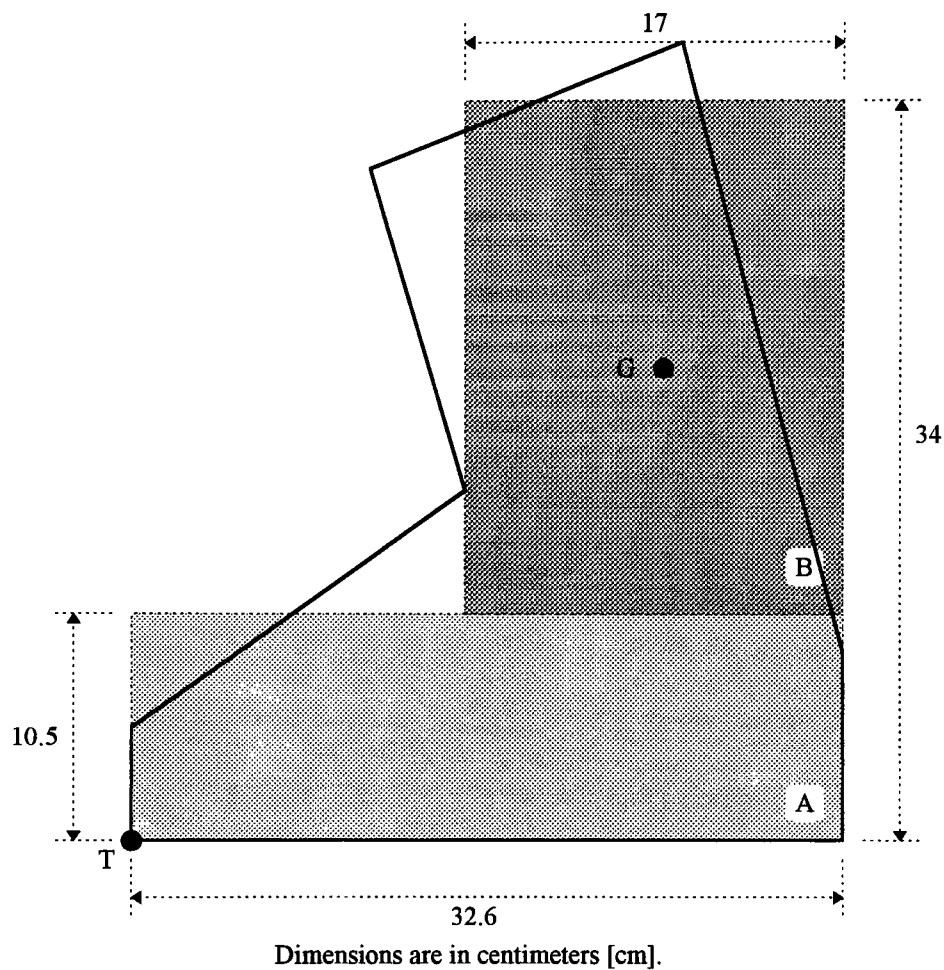
Assessment of Dimensional Boot Properties

A Nordica N955 rear entry boot, size 28.5, was chosen to be the test boot which provided the dimensional boot information for the nominal test case. The boot was chosen due to availability, knowledge of boot size, and similarity in dimension to boots used by other researchers. Figure 4.1 illustrates a rough outline for the boot and the visually measured approximations of the critical dimensional information, L_1 , L_2 , L_3 , β , and ϕ_o . Inertial data, J_T , J_{TOT} , and I_G , were approximated by using an even more simplified diagram of the boot profile, which is illustrated in Figure 4.2.



Dimensions are in centimeters [cm] unless noted.

Figure 4.1 Dimensional Data for Nominal Test Case (Nordica N955, Rear Entry, size 28.5). $L_1 = 33\text{cm}$, $L_2 = 26\text{cm}$, $L_3 = 14\text{cm}$, $\beta = 0.505 \text{ rad}$, $\phi_o = 0.2618 \text{ rad}$.



Base (A):

$$\text{Area}_A = 342.3 \text{ cm}^2$$

$$m_A = 1.010 \text{ kg}$$

$$J_T = J_{o, A} = 0.039 \text{ kg-m}^2$$

Shaft (B):

$$\text{Area}_B = 399.5 \text{ cm}^2$$

$$m_B = 1.178 \text{ kg}$$

$$I_G = I_{G, B} = 0.008 \text{ kg-m}^2$$

Total Boot (A+B):

$$\text{Area}_{\text{TOT}} = 741.8 \text{ cm}^2$$

$$m = 2.188 \text{ kg}$$

$$J_{\text{TOT}} = 0.127 \text{ kg-m}^2$$

Figure 4.2 Inertial Data for Nominal Test Case (Nordica N955, Rear Entry, size 28.5)
Calculations based on boot base (A) and shaft (B) represented as simple rectangles.

In addition to this boot, dimensional data for two other boots were recorded for comparison. These boots were a Dolomite 65C Junior Racing front entry, size 23.5, and a Trappeur Carbon front entry. The data for these boots are given in Appendix C.

Using these boots for comparison and picking realistic numbers, four (4) additional test values, two greater and two less than the nominal value, were evaluated for each parameter. The selected test values are given in Table 4.1, which is located on p. 56.

Approximation of Boot Stiffness

Since there is currently no specification for the definition nor measurement method to determine boot stiffness, it was necessary to derive an approximation based on knowledge of the hysteresis curves that have been presented by various researchers (ISO/TC83/SC3/WG14, 1983 - 1993; Walkhoff and Baumann, 1987; Bonjour and Delouche, 1989). For this model, the values used in the nominal case for boot stiffness parameters, K_0 and ν , were derived using curve fitting software on the “Normal” curve illustrated in Bonjour and Delouche (1989, Figure 3). See Figure 4.3. Although, this figure was actually illustrating the influence of locked versus free ankle movement on stiffness results, it provided a good resource for what could be considered “typical” curves. Additionally, this curve was selected simply due to ease of access to data points.

As stated in Chapter 3, only the forward flexing portion of the curve was considered, and the bending moment versus angular deflection relationship was approximated as a nonlinear equation of the form, $\tau = K_0 \cdot \theta^\nu$, where $\tau \equiv$ bending

moment [Nm] and $\theta \equiv$ forward angular deflection [deg]. The choice of this nonlinear function allows for flexibility of the model to accommodate greater nonlinear, or linear, responses of different boot designs.

The approximation was calculated by using the curve fitting feature of a mathematical software tool called ASYSTANT by Asyst Software Technologies of Rochester, New York (version 1.10). The Gauss-Newton method was selected as the choice for the curve fitting algorithm. Initial guesses were $K_o = 5.0$ and $\nu = 1.5$, with 3 iterations maximum per fit attempt. The approximation converged in 2 fit attempts.

From this curve fitting analysis, the best least-square fit values for the stiffness parameters were calculated to be:

$$K_o = 1.9524 \pm 0.2669 \text{ [Nm/deg]},$$

$$\nu = 1.6341 \pm 0.0503.$$

Figures 4.4 and 4.5 illustrate the output from the approximation run.

Using these approximated values for K_o and ν , two additional test values for each variable were chosen and plotted to understand the effect that increasing or decreasing either of these parameters had on the curve shape and slope. Since boot stiffness is due to a combination of these two variables, six additional test combinations were evaluated. As expected, greater values of K_o and/or ν produced steeper curves, thus indicating that stiffer boots would also have higher K_o and ν factors. Inversely, smaller values had gentler slopes, correlating with softer boots having lower K_o and ν values. Figure 4.6 illustrates these results from the various values and combinations.

The test values and combinations used are also listed in Table 4.1. These values were arbitrarily chosen and selected to be evenly distributed about the nominal case values.

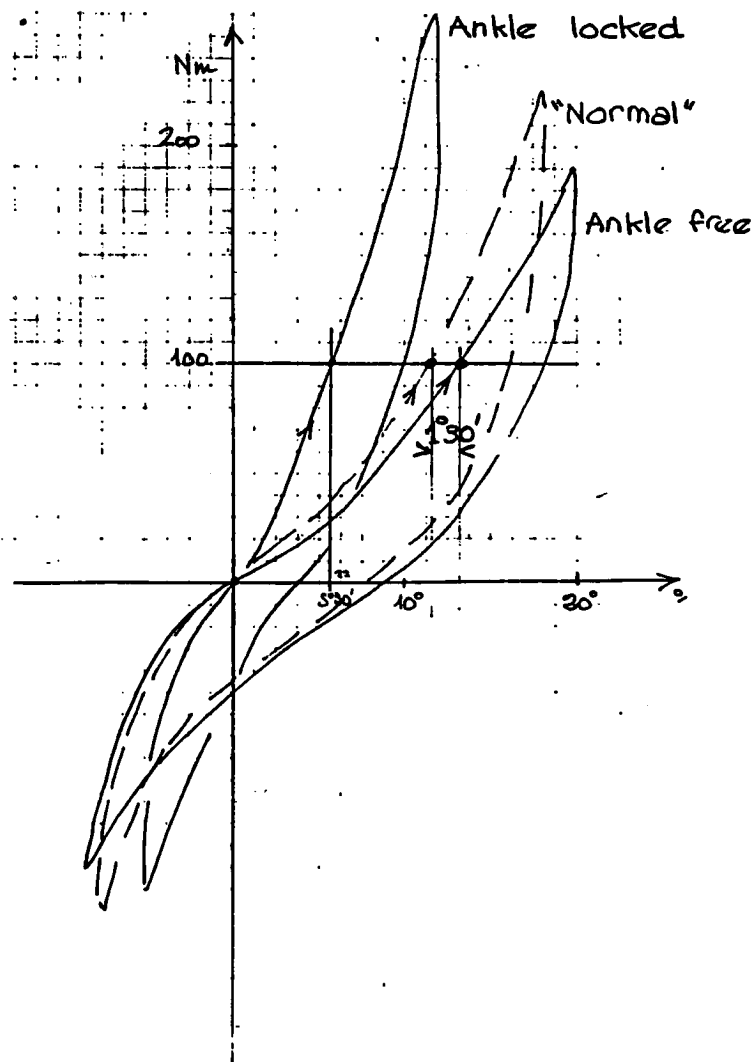


FIG. 3—Typical results with ankle free and locked. (The solid and dotted lines are representative of the scattering when testers try to follow the instructions.)

Figure 4.3 “Normal” curve was used for development of Nominal Test Case values for K_0 and v . Reprinted from Bonjour and Delouche (1989, p. 170)

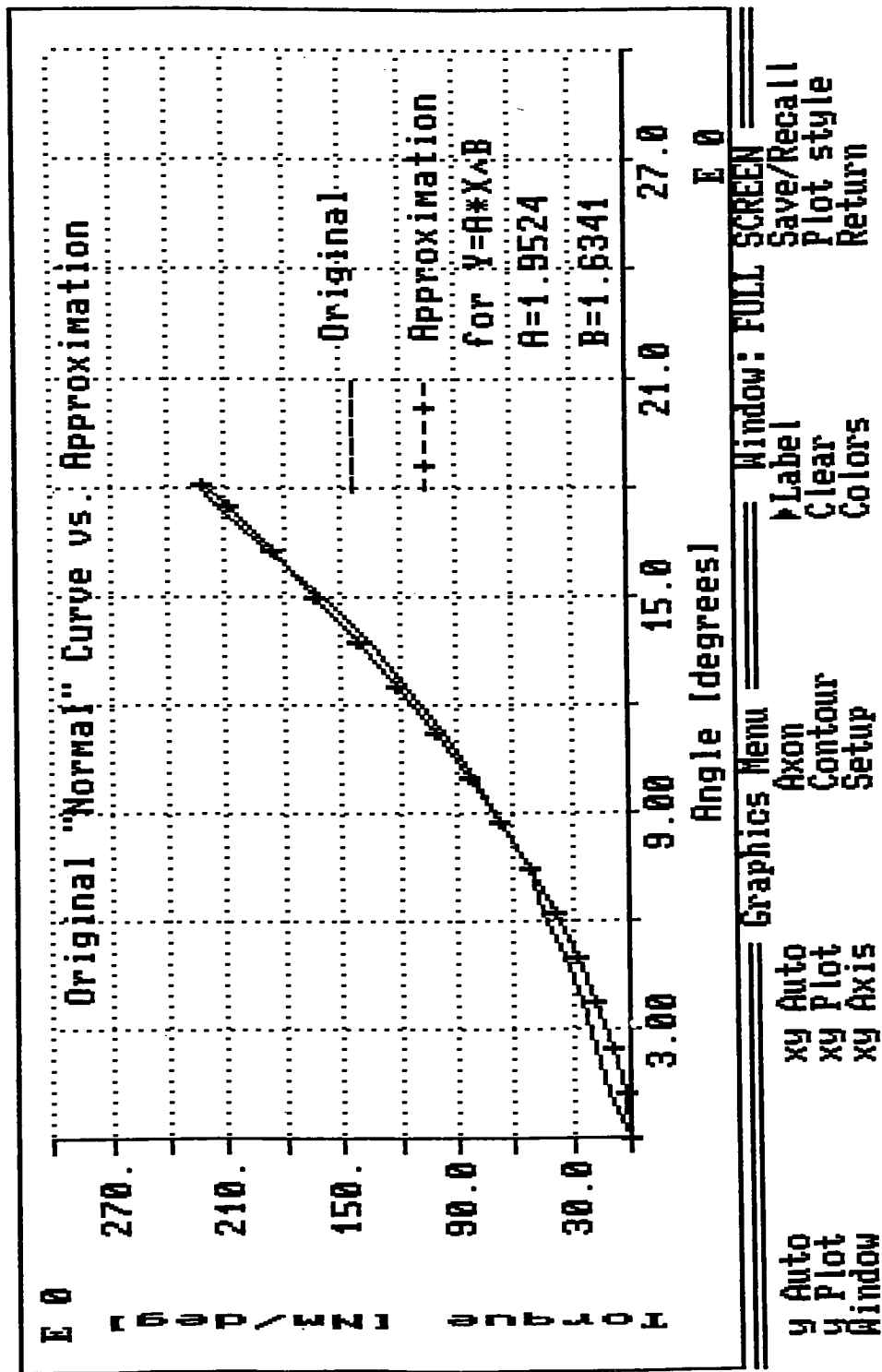


Figure 4.4 Screen Plot of Original Data vs. Approximation Curves for Bending Moment - Angular Deflection Relationship. Original data based on data points from "Normal" curve in Figure 4.3.

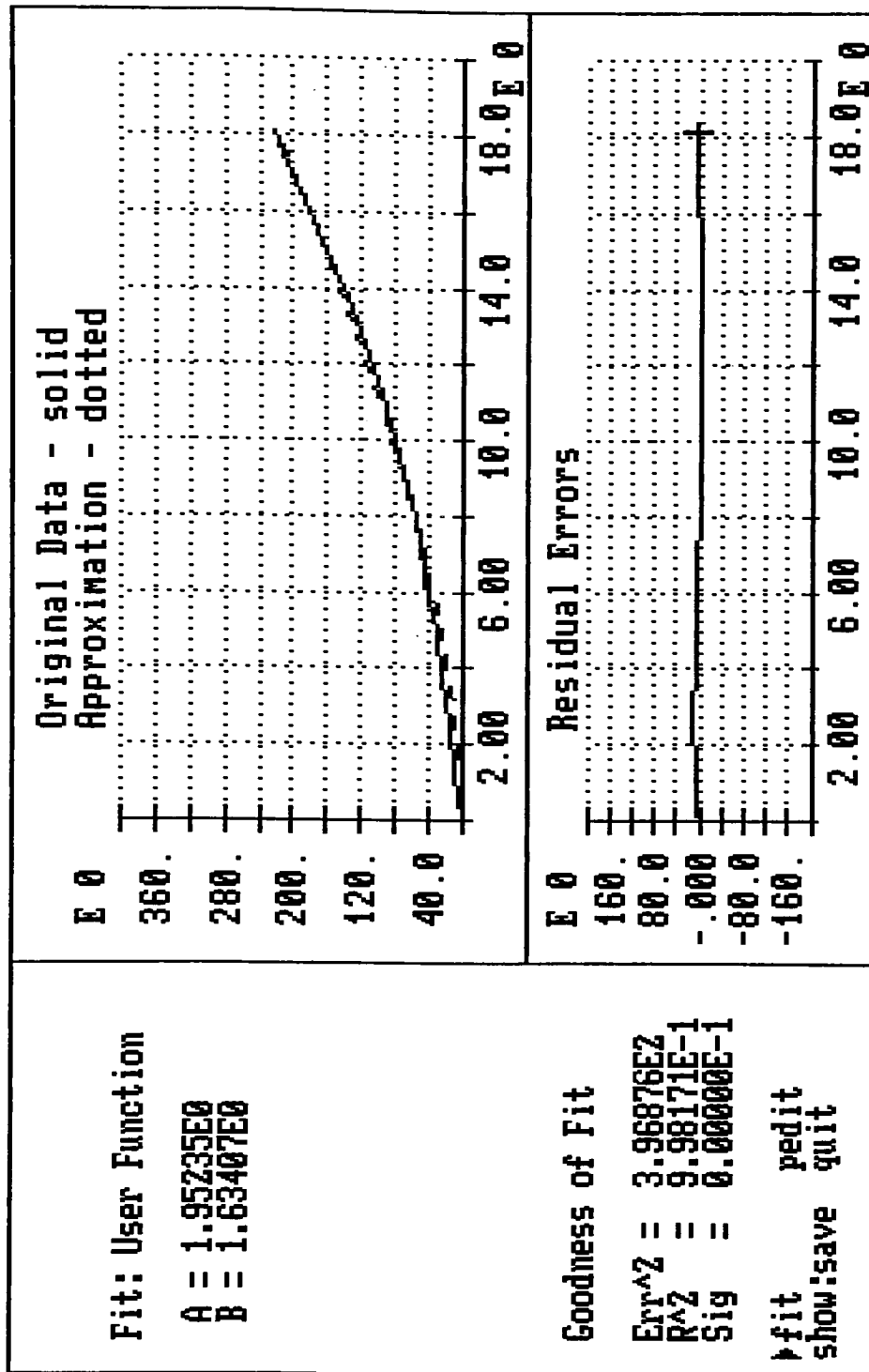


Figure 4.5 Screen Plot of Fit Results After Convergence. Curve fitting determined the coefficients for the best fit approximation of the nonlinear function $y = Ax^B$. A = K_0 and B = v .

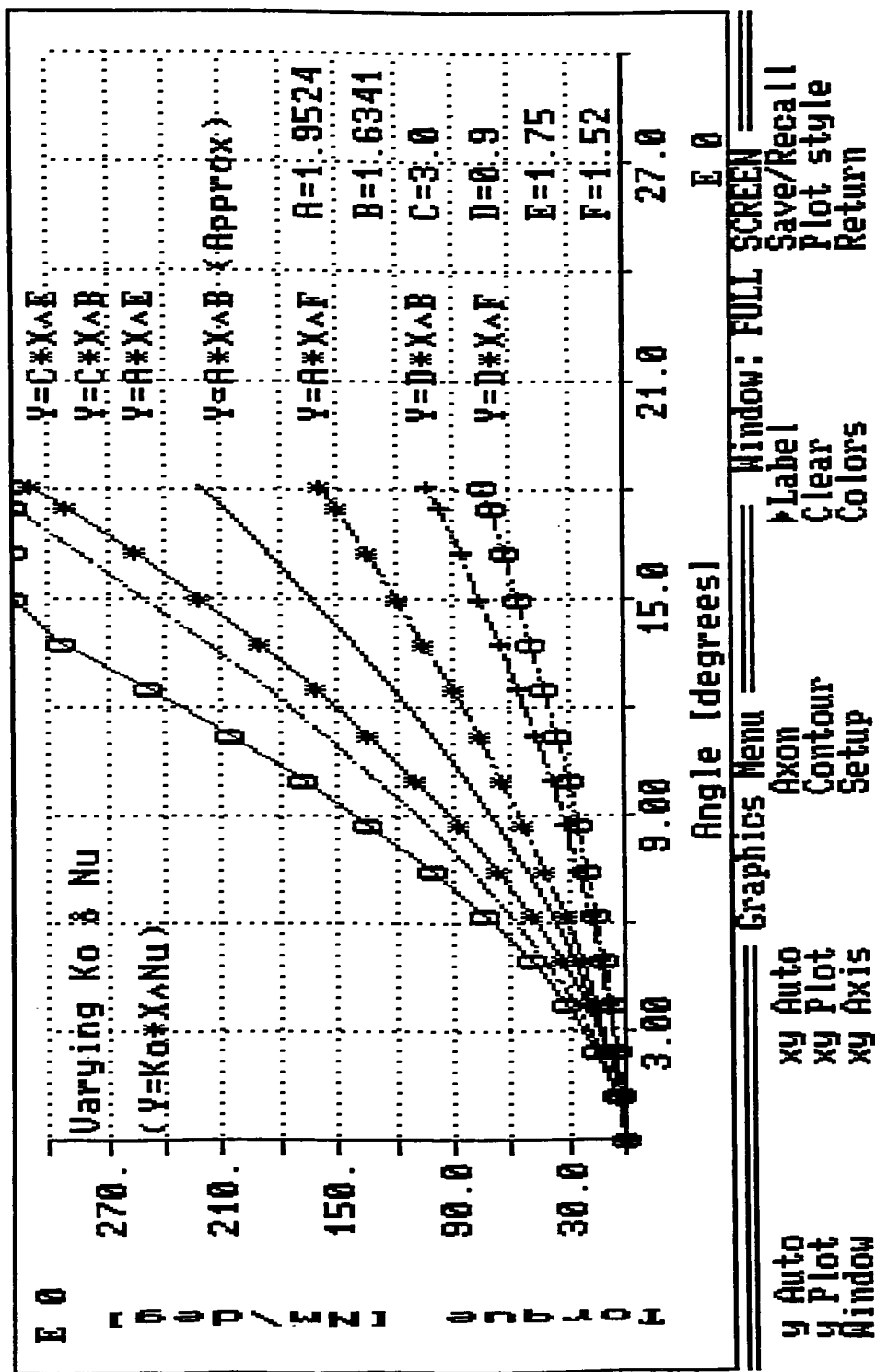


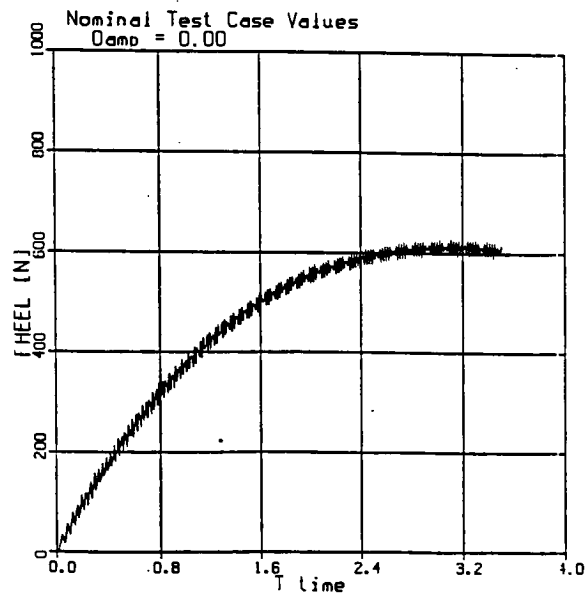
Figure 4.6 Screen Plot of Results from Varying K_0 and ν Test Values. $K_0 = 1.9524$ and $\nu = 1.6341$ are nominal test case coefficients. Curves illustrate that stiffer boots, with steeper curves, have higher K_0 and ν values. Whereas softer boots, with gentler slopes, have lower values.

Dissipation Factor

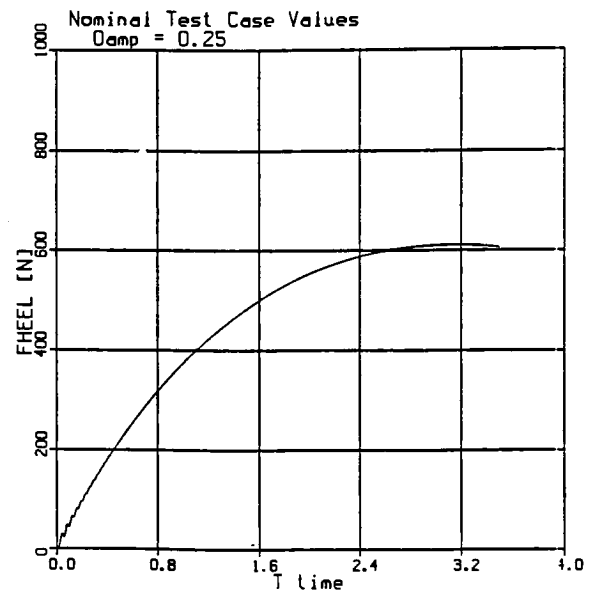
Although the original plan for this investigation did not include studying the influence of dissipation or damping, c , this value was also evaluated in the model analysis since it was already incorporated into the equations of motion. The hysteresis effect seen in the backward flexing or return portion of the moment-deflection curve illustrates one of the dissipative aspects of the boot; however, because the model was evaluating only the boot's activity during a forward flex, this portion of dissipative behavior was ignored. For this model, the property that variable c might be considered to represent could be the damping material properties of the inner boot and plastic shell during compression.

Inclusion of dissipation in this model was necessary to accommodate for the inherent vibrations and oscillations that would otherwise occur in this system. Without it, the model would simulate an undamped material that would vibrate. Running the computer simulation with $c = 0$ produced such an effect, where high frequency oscillations were observed. Figure 4.7(a) illustrates this effect. The nominal test case value for c was chosen as the condition when these oscillations were eliminated. This value was $c = 1.5$. Table 4.1 lists the other values that were attempted and Figures 4.7(a) -(d) illustrate the effects of modifying the dissipation. Notice that dissipation does not effect the model results for F_{HEEL} .

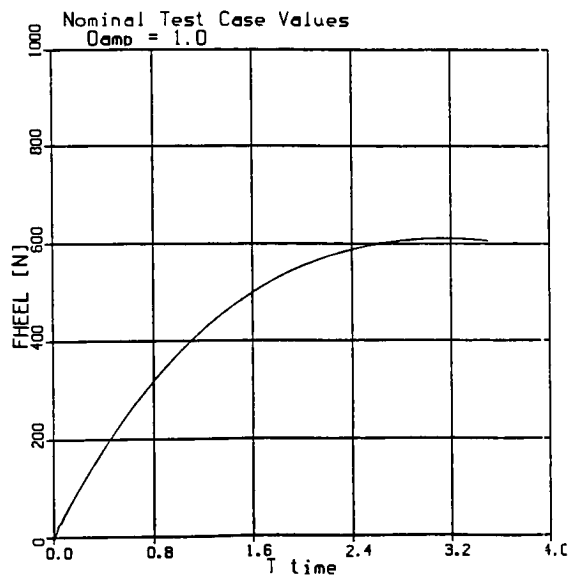
For the computer models, c was represented by the variable name "DAMP".



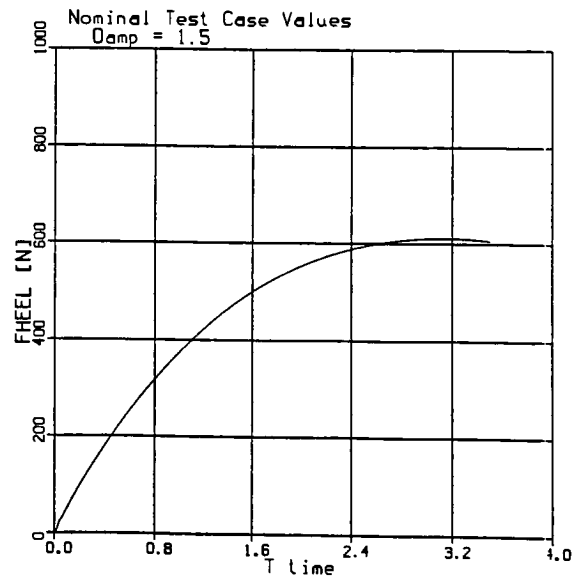
(a)



(b)



(c)



(d)

Figure 4.7 Plots illustrating effect of modifying dissipation factor, "DAMP". Damp = 1.5 was chosen as Nominal Test Case value since oscillations were eliminated at this point.

Table 4.1 Boot Parameters and Test Values. Note that Stiffness test values are based on a combination of K_o and ν . ϕ_o ("Phi") is given in both radians and degrees. The ACSL programs required angles to be given in radians.

Boot parameters and tested values							
Based on values used in ACSL programs							
	Stiffness=combo(K_o & ν)						
Damp [Nm-sec/deg]	K_o [Nm/deg]	ν	L1 [m]	L3 [m]	Phi [rad]	Phi [deg]	
0	0.9	1.52	0.31	0.12	0.227	13	
0.25	0.9	1.63	0.32	0.13	0.244	14	
1	1.95	1.52	0.33	0.14	0.262	15	
1.5	1.95	1.63	0.34	0.15	0.279	16	
	1.95	1.75	0.35	0.16	0.297	17	
	3	1.63					
	3	1.75					

Additional Analysis Constraints

Maximum Forward Lean Angle

The maximum forward lean angle is the value at which the boot shaft reached its hard stop and can no longer rotate forward with respect to the boot base. Recall that this point signified the transition from the first to the second condition. Maximum forward lean angle, which will be referred to as γ_{\max} , was defined to be the sum of initial lean angle, ϕ_o , and maximum relative shaft flex angle, $\alpha_{\max, \text{forward}}$, such that $\gamma_{\max} = \phi_o + \alpha_{\max, \text{forward}}$.

For the model analysis, $\gamma_{\max} = 30^\circ$ from the vertical. This value was selected based on Shealy and Miller's research (1989) which proposed that the maximum forward flexure of the ankle should not be greater than 30° in order to protect 93% of the population from injury due to excessive flexion of the ankle. (Note that for this model, $\gamma_{\max} = 30^\circ$ does not take into account the foot bed angle of the inner boot.)

This value was called "MAXLEAN" in the computer model.

Maximum Applied Force

During the actuation of the model, the force applied by the skier onto the boot was simulated by a sinusoidal function, $F(t) = f_o \sin(\frac{t}{2})$, for $0 \leq t \leq \pi$. Thus, at $t = \pi$, the maximum force, f_o , is applied.

$f_o = 1750\text{N}$ was selected. This value was chosen because the original intention was to evaluate the conditions while a skier was falling forward; however, no published data was found that specifically defined the range of maximum forces that could be experienced during such an action. In one reference (Quinn and Mote 1993), the authors calculated a maximum boot top force for normal skiing conditions to be $1298 \pm 22\text{N}$. Using this information, a value of f_o was chosen that might represent a typical falling force. This choice of 1750N turned out to be an increase of 35% of Quinn and Mote's value.

Future work in this area could include defining the force range during forward falls as well as representing the loading by a more typical forcing function.

Heel Force - Linear Spring Stiffness

The heel force in the model was simulated by the spring force generated by a linear spring attached to heel of the boot. This force was represented by the following relationship, $F_{HEEL} = k \cdot L_1 \sin \psi = k \cdot L_1 \psi$, for $\psi \ll 0$. For the model analysis, the spring stiffness, k , was chosen to be $k = 1.0 \times 10^6 \text{ N/m-deg}$. This value was selected after trial and error experiments which tried to choose a value that would ensure low values for ψ .

CHAPTER 5

COMPUTER SIMULATION MODELS

The time dependent, differential equations derived for the model were solved by computer simulation through programs written in the Advanced Continuous Simulation Language (ACSL), Version 6 Level 10D. Initially, a single program which evaluated only the first condition equations was used. Later, programs incorporating the stiffness discontinuity between the first and second conditions were developed. All of these programs are listed in Appendix D.

First Condition Program

This program, "1STONLY.CSL", only solved for the first condition equations (Equations 3.23, 3.24, 3.28 - 3.33). It did not base its termination on the maximum lean angle, rather it just continued to solve the equations until a selected termination time was achieved. This case could be physically interpreted as representing a boot that does not have a maximum forward lean angle or hard stop. Thus, the boot shaft would just continue to flex forward as more force is applied. In this case, the boot's flexing motion continues to absorb a portion of the input energy from the skier; therefore, the force experienced at the heel should be less than that which would be generated during the condition when the boot design reaches a hard stop and then acts as a single, rigid body.

The program was written such that the differential equation constants, i.e. boot characteristic parameters, were initialized to the nominal test case values defined in Chapter 4. While running the program, it was possible to individually vary these values in order to investigate the effects of each boot parameter on heel force.

Combined First and Second Programs

After developing the first condition only program and determining that it produced reasonable results, the next step was to develop a program that solved for the total system which incorporated both the first and second conditions. However, due to ACSL program language limitations, solution of both the first and second condition equations was not possible within the same program. Therefore, two separate programs were written, one for each condition. These programs were called “FIRST.CSL” and “SECOND.CSL”. FIRST.CSL was based on 1STONLY.CSL. After the first program met a termination criterion, final condition values were recorded and inputted into the second program to be used as initial conditions.

The termination criteria for the first program were either when $\gamma \geq \gamma_{\max}$ (maximum lean angle = 30°) or $t \geq t_{\max}$, whichever came first. The second program termination criterion was based on the combined times of the final condition time for the first and the runtime for the second, $(t_{1st,final} + t_{2nd,current}) \geq t_{\max}$. The choice of a maximum termination time of $t_{\max} = 3.5$ sec was an arbitrary selection that was greater than π . This value allowed for some opportunity to observe the model’s behavior beyond the point when the maximum force was applied. The same value for t_{\max} was also used in 1STONLY.CSL.

CHAPTER 6

RESULTS OF COMPUTER MODELS

First Condition Program

Recall that this program solved the differential equations of motion for the ski boot system when a forward flex hard stop condition was not considered. The equations were solved through a defined time span, $0 \leq t \leq t_{\max}$. The numerical results generated from this program are found in Appendix E.

Figure 6.1(a) illustrates the heel force response, F_{HEEL} , to the inputted skier force, F , as functions of time. The heel force generally followed the same function as the skier force but was 50% to 65% less. This result indicates that 50% to 65% of the input energy was not seen at the heel binding.

Figure 6.1(b) illustrates the magnitude of the heel force and skier force with respect to the change in angular deflection of the boot shaft, $\alpha (= \theta - \psi)$. Here again, the heel force was approximately 50% to 65% less than the skier force.

Effects Due to Boot Parameters

After investigating the behavior of the model in the nominal test case, the different boot parameters were varied in order to evaluate their influence on heel force. Specific statistical conclusions are not possible with the generated data during this investigation.

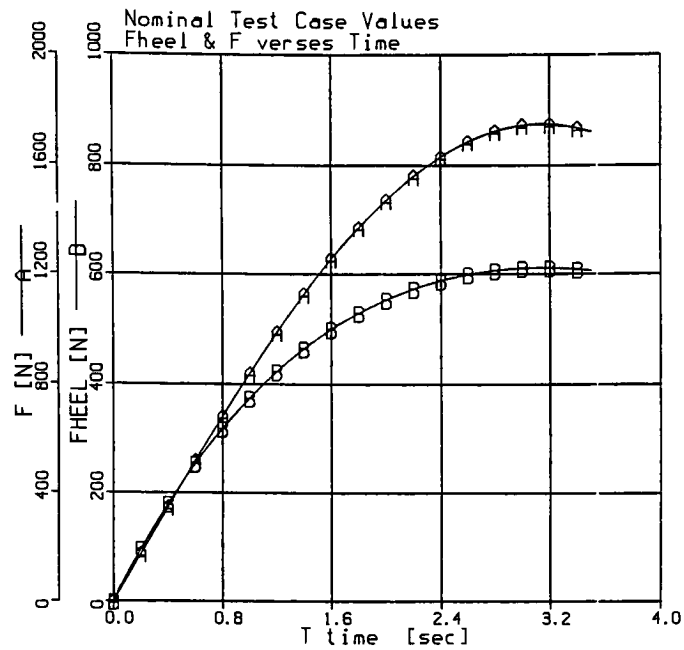
However, the model was able to indicate trends in the influence of each boot parameter on heel force.

Boot stiffness, which is characterized by both K_o and v , produced expected results in that the greater the boot stiffness, the greater the force experienced at the heel. With respect to the other evaluated boot parameters, boot stiffness appeared to have the most influence on affecting the heel force. These results are illustrated in Figure 6.2(a).

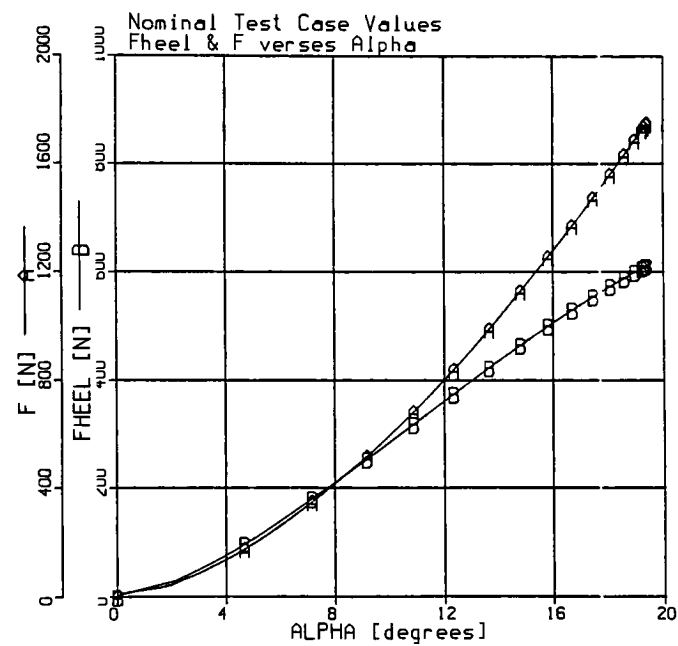
Boot sole length, L_1 , was varied within a range from 31 to 35 cm, where 33 cm was considered nominal. The results from the model indicated a negative trend, which meant that increasing the sole length caused the heel force to decrease. This result followed the trend that would naturally be expected. In comparison to the other parameters, sole length appeared to have the least influence on heel force. See Figure 6.2(b).

Functional boot height, L_3 , was also varied within a range from 12 to 16 cm; 14 cm was nominal. The model predicted a positive trend -- increasing functional boot height, increased heel force. This result also followed the expected. Figure 6.2(c) illustrates the results.

The initial forward lean angle of the unloaded boot, ϕ_o , was varied from 12° to 16° , with 14° being nominal. (The program actually required radians.) This parameter also displayed the expected negative trend with heel force. Figure 6.2(d) shows this trend.

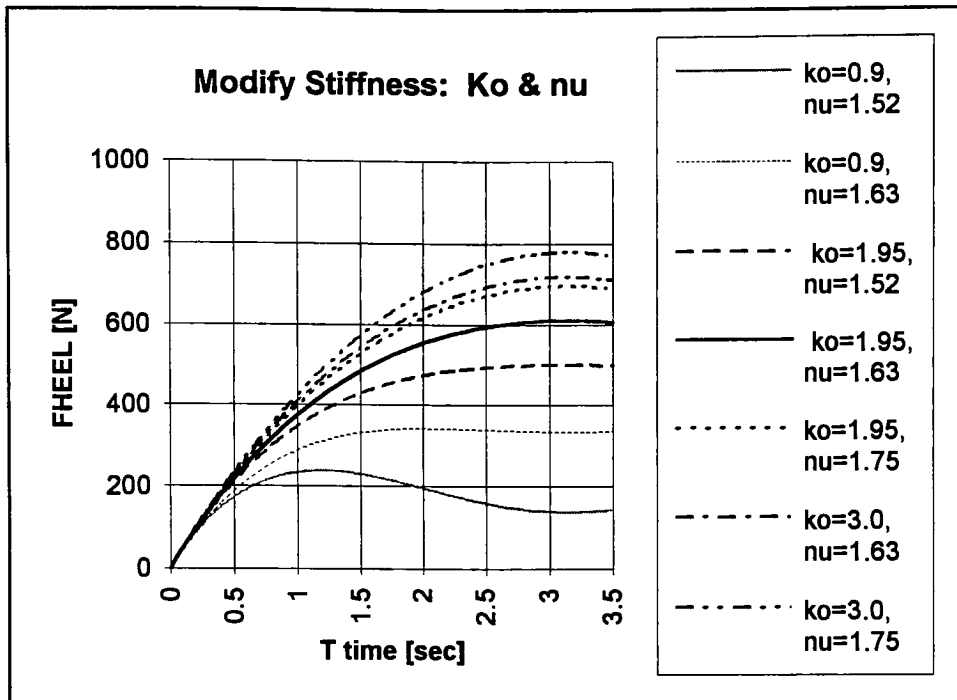


(a)



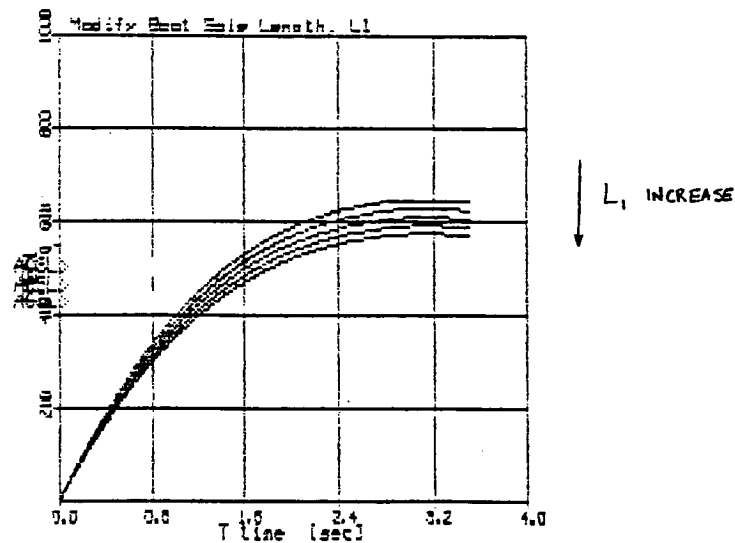
(b)

Figure 6.1 Plots comparing the inputted skier force, F , and resultant heel force, F_{HEEL} , as functions of time, t , and angular deflection of the boot, α .



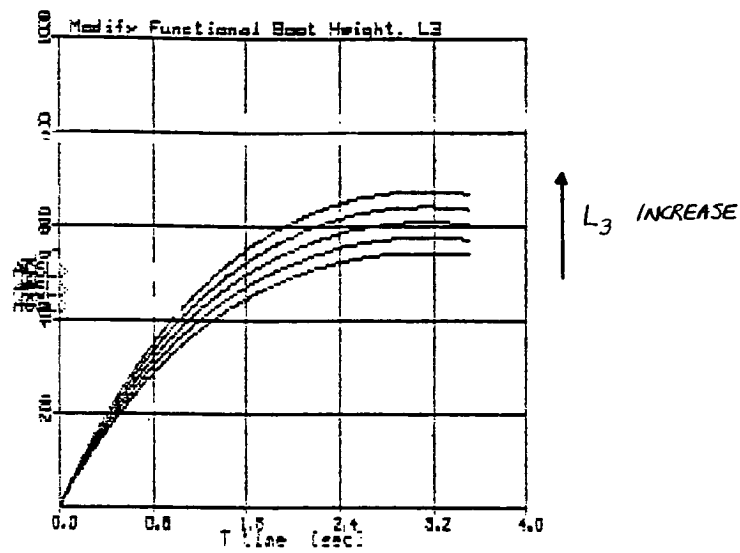
(a) graph generated by inputting ACSL data into MS Excel Chart

plot fheel



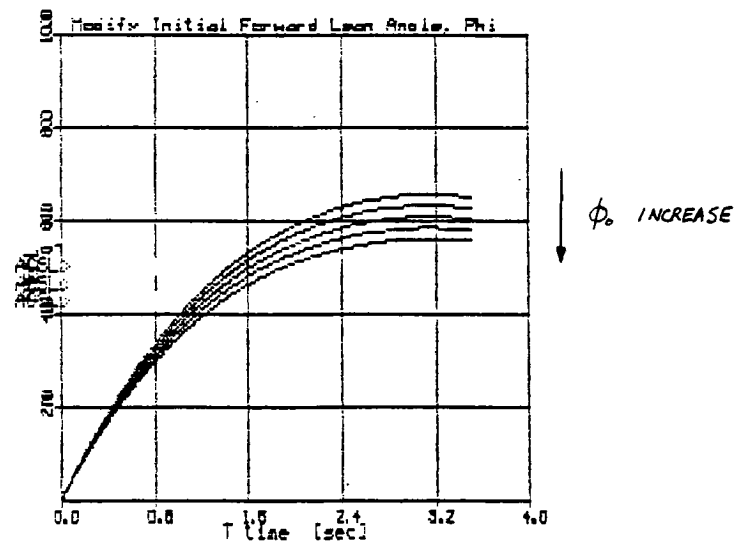
(b) graph generated during ACSL session

Figure 6.2 Plots illustrating the influence of the different characteristic boot properties on heel force, F_{HEEL} .



(c)

plot fheel



(d)

Figure 6.2 (con't) Plots illustrating the influence of the different characteristic boot properties on heel force, F_{HEEL} . Graphs were generated during ACSL session.

Combined First and Second Programs

These two programs evaluated the complete model which considered the case when a hard stop eventually limited the forward flex of the boot shaft. In a method similar to that used to evaluate 1STONLY.CSL results, the nominal test case was first solved; then the multiple test values of each boot parameter were also solved.

To start, FIRST.CSL was executed to solve the first condition equations. If the first program terminated due to reaching the hard stop, then the final conditions were inputted as initial conditions into the second program. The second condition equations were subsequently solved in SECOND.CSL. The data generated for both programs are found in Appendix E.

Since the model was solved using two different programs, and therefore, two different ACSL execution sessions, it was not possible to plot the results using the ACSL plotting feature. Instead, the data from both programs were combined onto a PC-based Microsoft Excel spreadsheet, Version 4.0a. Graphs were generated from these transferred data.

Figure 6.3 compares the results from the first condition only program and the combined programs. As expected, this graph showed that the heel force was the same for both of the first condition programs during the time period when the boot shaft flexed forward from its initial position until it reached the hard stop. Beyond that point, the curves began to deviate from each other since the second condition model was applicable in the combined programs.

For the combined programs, the computed heel force after the hard stop was greater than the value computed for the single program. These results, which were due to the second condition model, correlated with the assumption that the boot can now be considered to behave like a solid, rigid body. In this case, less of the input force energy was absorbed by the boot and more was transferred to the heel. Therefore, the heel force was greater. In contrast, during the 1STONLY.CSL program when the boot shaft continued to flex forward unbounded, the flexing action of the shaft absorbed more of the input energy and transferred less to the heel. Thus, the heel force was less.

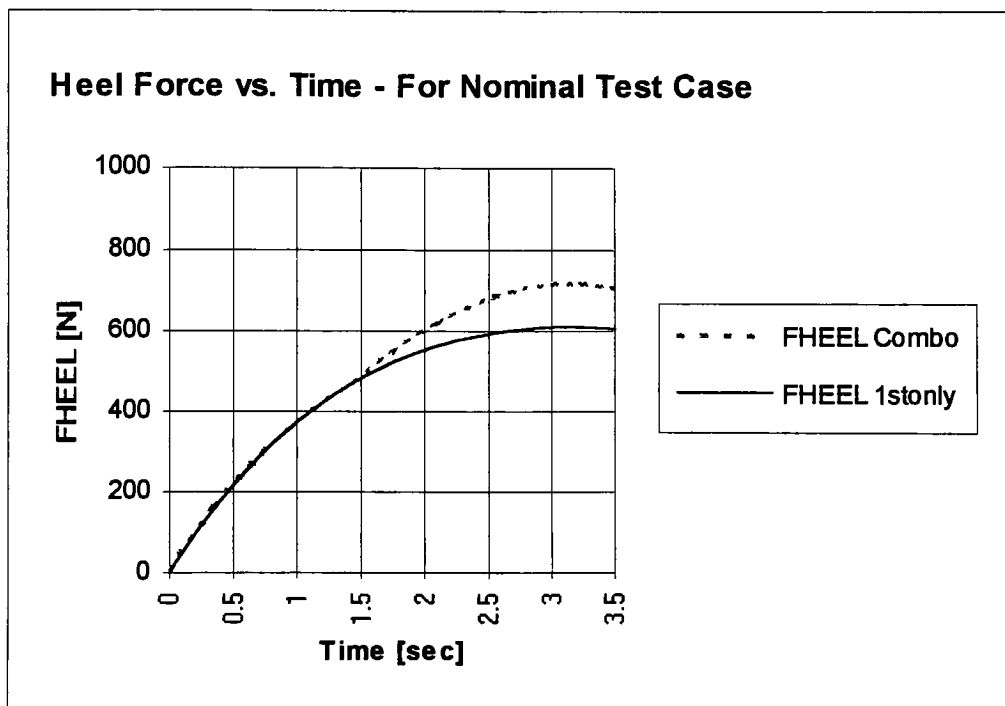


Figure 6.3 Comparison of results between 1STONLY.CSL and combination of FIRST.CSL and SECOND.CSL as functions of time, t . The graph represents the nominal test case data. The boot shaft reached its maximum forward lean, $\gamma_{\max} = 30^\circ$ @ $t = 1.44$ sec.

Figure 6.4 shows the response of the heel force to the input skier force. The heel force calculated during the first condition displayed a non-linear correspondence to the input force. This effect might be attributed to the energy loss experienced due to the flexing of the boot shaft. The second condition result had a linear correspondence, as might be expected for a rigid body where input energies are directly transferred. The force equation developed for the static model of the second condition also corroborated this relationship. The equation describing this relationship is in Appendix B.

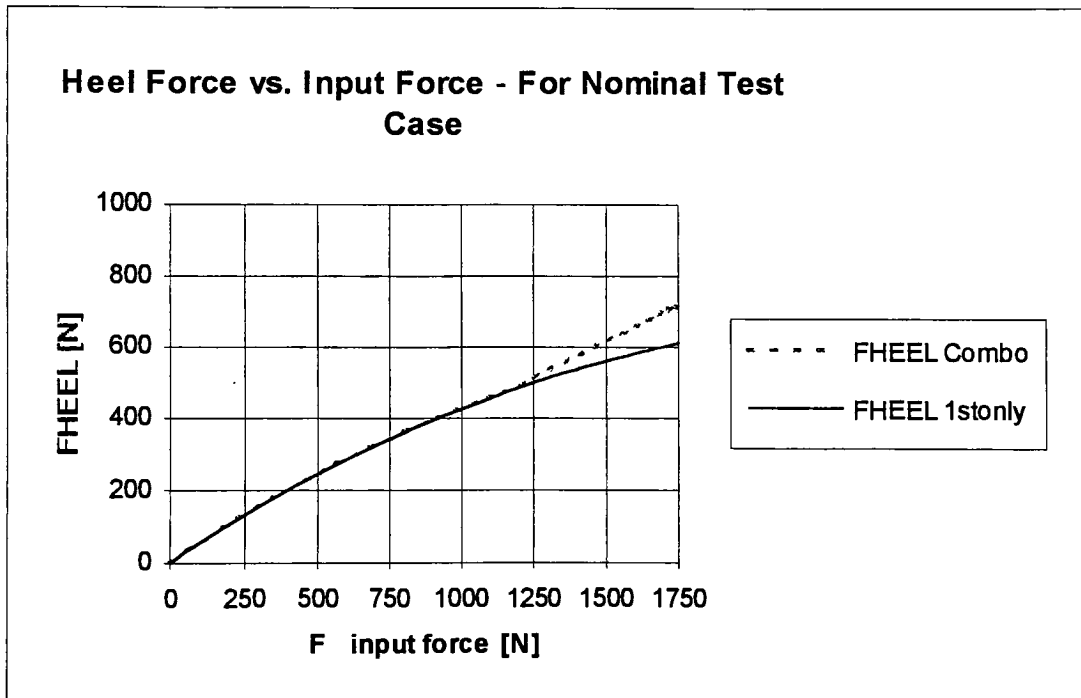


Figure 6.4 Comparison of results between 1STONLY.CSL and combination of FIRST.CSL and SECOND.CSL as functions of input skier force, F.

Effects Due to Boot Parameters

The response of the heel force to the four boot parameters produced some very interesting, and initially unexpected, results during the second condition. This was especially true for boot stiffness and initial lean angle.

Boot Stiffness

The first condition results were of course the same as mentioned previously in the section under the first condition only results. The influence of boot stiffness showed a positive trend with respect to heel force, which meant that greater stiffness caused greater heel force.

However, when the second condition model was applied, the final results were quite different. Figure 6.5(a) shows that if given enough time, or applied force, the heel force for the different stiffnesses will eventually converge to the same value. This effect was different from that observed when the first condition model was allowed to continue unbounded. In that case, the model calculated distinctly different solutions and curves for each stiffness as time progressed. Recall Figure 6.2(a).

The explanation for this convergence was because the equations of motion for the second condition model were not dependent on the boot stiffness variables. Therefore, as the model equations continued to integrate over time, the effect from boot stiffness became less a contributing factor to the final result.

This graph also illustrated the effect of boot stiffness on rate of forward flexure. The lower valued stiffnesses could be envisioned as representing softer boots which flex

quite easily and, therefore, would reach the hard stop quickly. The bottom curves on the graph demonstrated such an effect, where the first condition curves ended after only a short time, and the second condition curves then continued for the remainder of the sampling time. The top curve, which represented the greatest stiffness, $K_o = 3.0$ and $v = 1.75$, illustrated the effect of having a boot that was so stiff that it never flexed to an angle near, or theoretically beyond, the maximum lean angle. Thus, the second condition model did not apply to this case and the curve did not converge to the same value as the other curves.

Boot Sole Length

The results for the effect of boot sole length, L_1 , followed the same negative trend as observed in the first condition only solutions, in which greater lengths caused lower forces. The curves for the different test values remained distinct because sole length contributes to the force calculations even in the second condition.

The main change, due to the combined model results, was that the heel forces generated during the second condition were greater than in the previous solution.

These results also showed that the rate at which the shaft flexed was independent of sole length because the solutions for all of the test values met the requirements for the first to second condition transition at the same time. This transition occurred at $t = 1.44$ sec.

Figure 6.5(b) illustrates these results.

Functional Boot Height

Figure 6.5(c) shows the results for the functional boot height, L_3 , as also remaining distinctly separate. These results continued to follow the positive trend previously observed.

These results indicated that boot height affected the shaft flexural rate. Longer shafts created greater lever arms and increased the moment about the shaft and base pivot point.

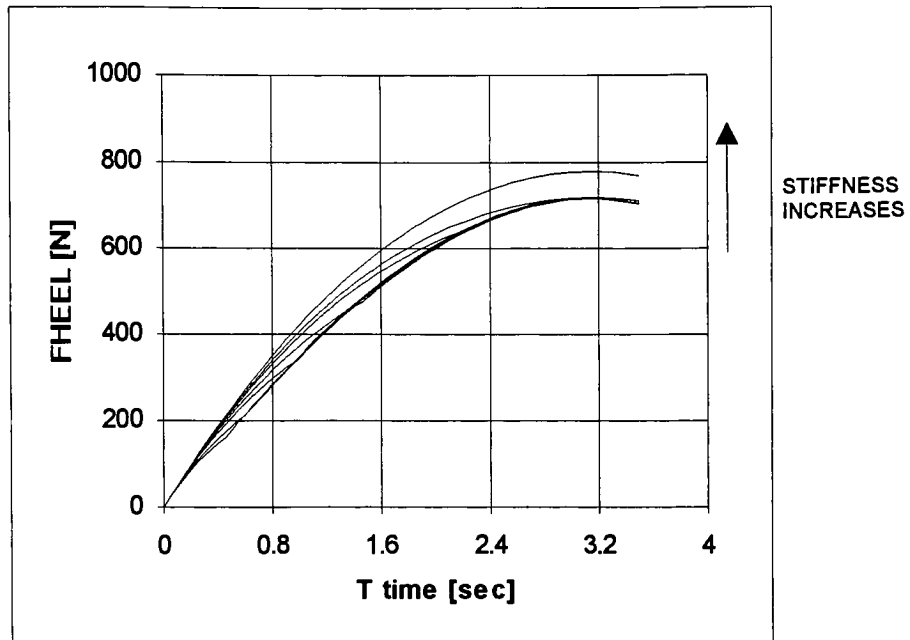
Interestingly, all of the test values generated nearly the same heel force at the transition point between conditions. This value was approximately $472 \text{ N} \pm 2\text{N}$.

Of additional interest, for skiing situations that would satisfy the second condition requirements, these results now indicated that functional boot height, rather than boot stiffness, was the most influential parameter in affecting heel force.

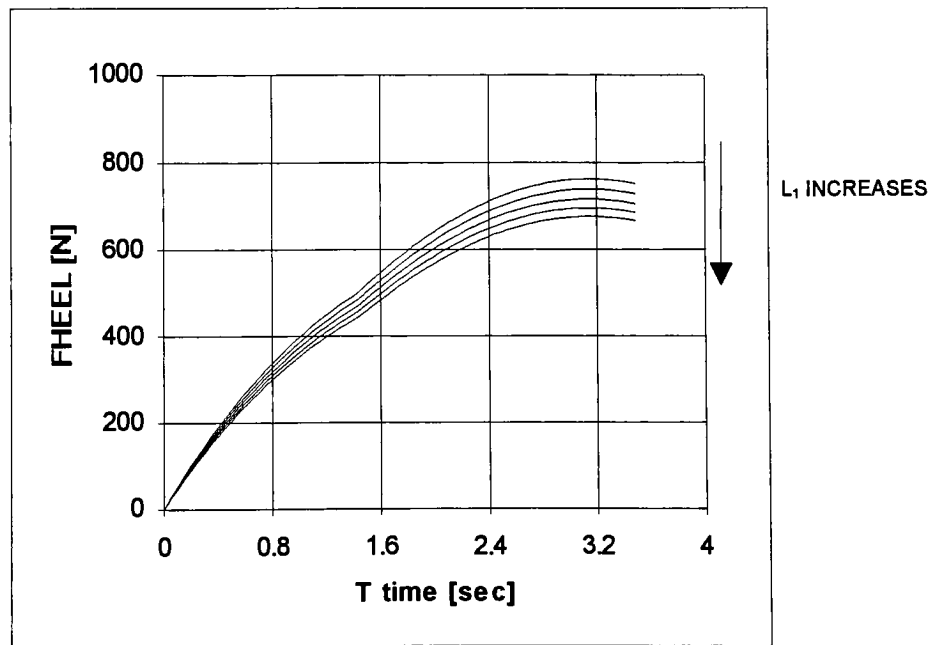
Initial Forward Lean Angle

During the first condition portion of the solution, the results for initial forward lean angle, ϕ_0 , displayed the same negative trend as before. However, during the second condition solution, the results displayed similar effects as boot stiffness. The solutions converged over time. This convergence was a result of the equations of motion being independent from ϕ_0 during the second condition model. See Figure 6.5(d).

This graph also illustrated that boots with smaller values of ϕ_0 (top curves) took longer to reach the maximum lean angle than boots with larger values (bottom curves). This effect is intuitively obvious.

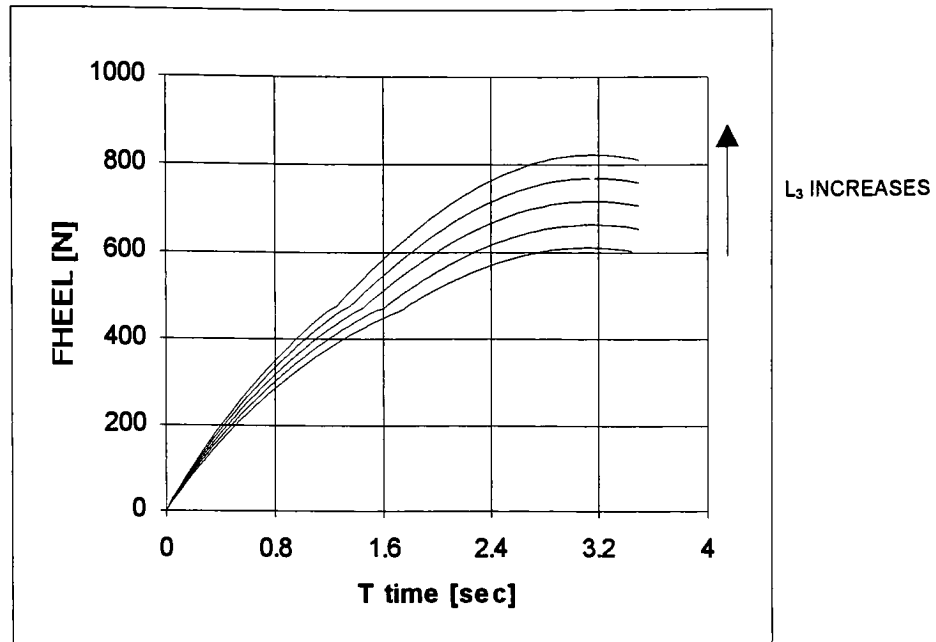


(a) Modify Boot Stiffness, K_o and v

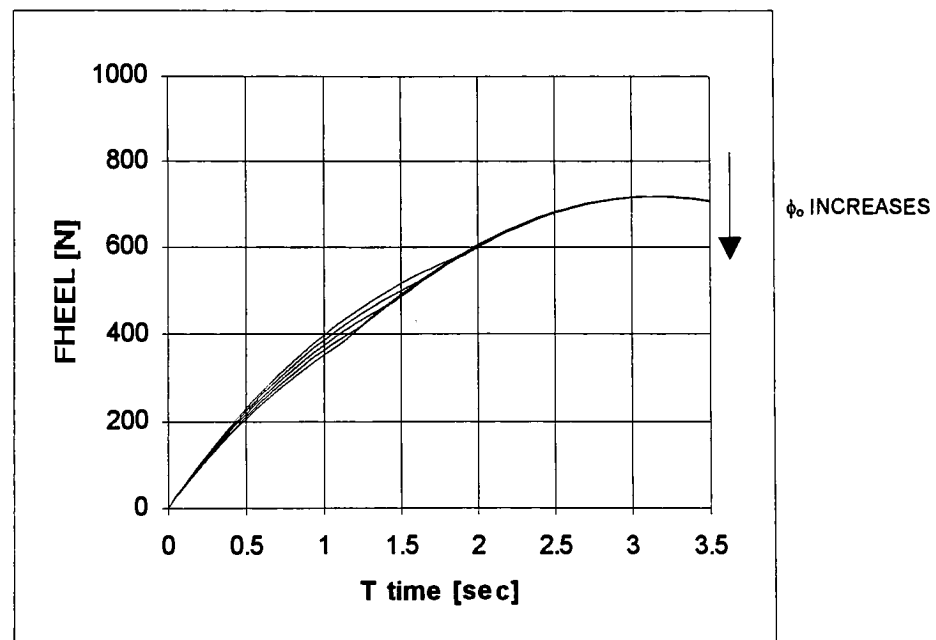


(b) Modify Boot Sole Length, L_1

Figure 6.5 Plots illustrating the influence of the different characteristic boot properties on heel force, F_{HEEL} , for complete model including second condition.



(c) Modify Functional Boot Height, L_3 (The sharp delineation between the first and second condition curves is an effect of the graphing procedure.)



(d) Modify Initial Forward Lean Angle, ϕ_0

Figure 6.5 (con't) Plots illustrating the influence of the different characteristic boot properties on heel force, F_{HEEL} , for complete model including second condition.

CHAPTER 7

CONCLUSIONS AND FUTURE RESEARCH

Conclusions

The primary objective of this investigation was to determine the influence of certain alpine ski boot characteristics on heel retention forces. These boot characteristics were boot stiffness, sole length, functional boot height, and initial forward lean angle.

In order to evaluate these effects, a dynamic model representing a ski boot under a forward leaning load was successfully developed such that it was able to calculate a vertical heel force.

This model considered the stiffness discontinuity which occurred if the input force caused the boot shaft to flex forward until it reached the boot's safety hard stop. To accommodate this discontinuity, the model evaluated two different conditions. The first condition pertained while the boot shaft flexed forward from the unloaded condition until it reached the hard stop. The second condition occurred if the input force continued after the hard stop was reached.

The results for the two conditions were quite interesting, yet within expectation. For the first condition, boot stiffness and functional boot height produced positive trends with respect to heel force. This meant that greater values for these parameters caused greater heel forces. The inverse was true for boot sole length and initial forward lean angle. Negative trends were noted -- greater values caused lower heel forces.

Assuming that the test values used with the model were within a reasonable range, the results implied that boot stiffness could significantly effect the heel force during the first condition. In comparison, the other boot parameters appeared to have only a modest influence on this force experienced at the heel of the boot.

The second condition solution produced different results, especially for boot stiffness and initial forward lean angle. Since both of these parameters do not effect the equations of motion during this situation, the heel force solutions tended to converge to the same value for different stiffness or lean angle values. Because of these results, functional boot height appeared, instead, to be the most influential on affecting heel force.

The heel forces generated during the second condition were found to be greater than those during the first, given the same input force. This result was because the boot could now be assumed to behave like a rigid body. Thus, the input energy was transmitted directly to the heel, rather than partially absorbed by the flexing motion of the shaft.

The model was based on the equations of motion for the boot. The chosen method for determining these equations of motion was Lagrangian mechanics. This method produced multiple dependent differential equations that required simultaneous solution.

Although this model was a simple, low order design, it appeared to produce reasonable conclusions on the general trends of the system. Simple models may be a very useful tool during development opportunities. These models can be less cumbersome since there are fewer variables and constants to consider. They allow for the “big picture” to show through.

Future Research

There are numerous opportunities for future work that can be conducted as follow-up research to this topic. One of the areas that has already been mentioned is modifying the forcing function to either an impulse force or some other non-sinusoidal function. Experimental forward fall data could be generated and used to develop these new forcing functions.

Another area that was mentioned is inclusion in the model of other forces and moments, both external and internal to the boot. External forces at the boot toe or ball of the foot could be added if the model were to not pivot freely about the toe. Lateral forces and moments could be considered if the model were expanded beyond the restrictions of the sagittal, x-y, plane. Work in this area could assist in the prediction of binding release.

Experimental research could be conducted with an emphasis on determining that the model correctly represented the physical world.

The model could be further refined. More sophisticated calculations of the moments of inertia could be added. Studying the influence of increasing the maximum forward lean angle could be done. A statistical evaluation of each boot parameter could be done to understand the statistical significance of each parameter with respect to heel force.

The differential equations for the system were solved by computer programs written in ACSL. This language was cumbersome and had numerous restrictions, but it

was successful at providing results. If this model were to be computer simulated again in the future, a more versatile language or software application tool could be used.

A finite element model (FEM) of the boot system could be developed and the results from that model could be compared with those generated from this model. The FEM model could in turn be modified to produce more sophisticated results and incorporate material property characteristics.

These are just a few of the potential topics that could be explored further. As was stated at the beginning of this paper, ski research has been occurring for quite sometime and it will continue to supply topics of research in the future due to the search for increased fundamental quantitative knowledge.

REFERENCE LIST

- American Society for Testing and Materials, **Standard Practice for the Selection of Release Torque Values for Alpine Ski Bindings**, (ASTM Standard No. F939-85), American Society for Testing and Materials, Philadelphia, 1985, pp. 515 -516.
- Asang, E. and Hauser, W., **Design of Ski Boots and Its Influence on Binding Settings**, *Ski Trauma and Skiing Safety IV*, W. Hauser, J. Karlsson, and M. Magi, Eds., TÜEV, Munich, 1982, pp. 37 - 43.
- Bonjour, F. and Delouche, G., **Problems Encountered in Flex Measurements on Alpine Ski Boots**, *Skiing Trauma and Safety: Seventh International Symposium, ASTM STP 1022*, Robert J. Johnson, C. D. Mote, Jr., and Marc-Hervé Binet, Eds., American Society for Testing and Materials, Philadelphia, 1989, pp. 167 - 177.
- Ekeland, A., Holtmoen, A., and Lystad, H., **Lower Extremity Equipment - Related Injuries in Alpine Recreational Skiers**, *The American Journal of Sports Medicine*, Vol. 21, No. 2, 1993, pp. 201 - 205.
- Freeman, J. R., Weaver, J. K., Oden, R. R., and Kirk, R. E., **Changing Patterns in Tibial Fractures Resulting from Skiing**, *Clinical Orthopaedics and Related Research*, No. 216, March, 1987, pp. 19 - 23.
- Glenne, B. and VonAllmen, B., **Basic Mechanics of Alpine Skiing**, *Ski Trauma and Skiing Safety III*, R. J. Johnson, W. Hauser, J. Karlsson, and M. K. Lamont, Eds., TÜV, Munich, 1982, pp. 50 - 57.
- Hall, B. L., Schaff, P. S., and Nelson, R. C., **Dynamic Displacement and Pressure Distribution in Alpine Ski Boots**, *Skiing Trauma and Safety: Eighth International Symposium, ASTM STP 1104*, C. D. Mote, Jr. and Robert J. Johnson, Eds., American Society for Testing and Materials, Philadelphia, 1991, pp. 186 - 199.
- Hauser, W., Asang, E., and Schaff, P., **Influence of Ski Boot Design on Skiing Safety and Skiing Performance**, *Skiing Trauma and Safety: Fifth International Symposium, ASTM STP 860*, R. J. Johnson and C. D. Mote, Jr., Eds., American Society for Testing and Materials, Philadelphia, 1985, pp. 159 - 164.

- Hull, M. L. and Mote, C. D., Jr., **Computer Analysis of Leg Loading in Alpine Skiing, *Ski Trauma and Skiing Safety III***, R. J. Johnson, W. Hauser, J. Karlsson, and M. K. Lamont, Eds., TÜV, Munich, 1982, pp. 58 - 64.
- International Association of Safety in Skiing, **Skischuhe fuer Erwachsene ab Groesse 36, Anforderungen und Prefung [Adult Ski Boots Greater Than Size 36, Requirements and Tests, (IAS Specification No. 150)]**, TÜV, Munich, May 1980.
- Johnson, R. J., Ettlinger, C. F., and Shealy, J. E., **Skier Injury Trends -- 1972 - 1990, *Skiing Trauma and Safety: Ninth International Symposium, ASTM STP 1182***, Robert J. Johnson, C. D. Mote, Jr., and John Zelcer, Eds., American Society for Testing and Materials, Philadelphia, 1993, pp. 11 - 22.
- Kuo, C. Y., Louie, J. K., and Mote, C. D., Jr., **Control of Torsion and Bending of the Lower Extremity During Skiing, *Skiing Trauma and Safety: Fifth International Symposium, ASTM STP 860***, R. J. Johnson and C. D. Mote, Jr., Eds., American Society for Testing and Materials, Philadelphia, 1985, pp. 91 -109.
- International Organization for Standardization / Technical Committee 83 / Subcommittee 3 / Working Group 14 (ISO / TC83 / SC3 / WG14), unpublished meeting minutes and correspondences, September 13, 1983 to August 26, 1993.
- Lyle, C. and Hubbard, M., **Optimal Ski Boot Stiffness for the Prevention of Boot-Top Fracture, *Skiing Trauma and Safety: Fifth International Symposium, ASTM STP 860***, R. J. Johnson and C. D. Mote, Jr., Eds., American Society for Testing and Materials, Philadelphia, 1985, pp. 173 - 181.
- Mote, C. D., Jr., and Hull, M. L., **Laboratory and Field Research on Ski Bindings, *Skiing Safety II, International Series in Sport Sciences***, J. M. Figueras, Ed., University Park Press, Baltimore, Vol. 5, 1978, pp. 244 - 270.
- Mote, C. D., Jr., **The Forces of Skiing and Their Implication to Injury, *International Journal of Sport Biomechanics***, No. 3, 1987, pp. 309 - 325.
- Quinn, T. P. and Mote, C. D., Jr., **Prediction of the Loading Along the Leg During Snow Skiing, *Skiing Trauma and Safety: Ninth International Symposium, ASTM STP 1182***, Robert J. Johnson, C. D. Mote, Jr., and John Zelcer, Eds., American Society for Testing and Materials, Philadelphia, 1993, pp. 128 - 149.
- Raskulinecz, G. and Bahniuk, E., **Simulation of an Alpine Skier by the Use of an Anthropometric Dummy, *Ski Trauma and Skiing Safety III***, R. J. Johnson, W. Hauser, J. Karlsson, and M. K. Lamont, Eds., TÜV, Munich, 1982, pp. 29 -35.

- Schaff, P., Schattner, R., and Hauser, W., **Biomechanical Inquiries on Ski Boots and Resulting Practical Requirements**, *Skiing Trauma and Safety: Sixth International Symposium, ASTM STP 938*, C. D. Mote, Jr. and R. J. Johnson, Eds., American Society for Testing and Materials, Philadelphia, 1987, pp. 154 - 175.
- Schaff, P. S. and Hauser, W., **Influence of Ski Boot Construction on Knee Load - A Biomechanical Investigation on Safety and Performance Aspects of Ski Boots**, *Skiing Trauma and Safety: Ninth International Symposium, ASTM STP 1182*, Robert J. Johnson, C. D. Mote, Jr., and John Zelcer, Eds., American Society for Testing and Materials, Philadelphia, 1993, pp. 75 - 88.
- Schattner, R., Hauser, W., and Asang, E., **Basic Mechanics of Boot / Skier Interaction**, *Skiing Trauma and Safety: Fifth International Symposium, ASTM STP 860*, R. J. Johnson and C. D. Mote, Jr., Eds., American Society for Testing and Materials, Philadelphia, 1985, pp. 151 - 158.
- Shealy, J. E. and Ettlinger, C. F., **The In-Boot Fracture**, *Skiing Trauma and Safety: Sixth International Symposium, ASTM STP 938*, C. D. Mote, Jr. and R. J. Johnson, Eds., American Society for Testing and Materials, Philadelphia, 1987, pp. 113 - 126.
- Shealy, J. E. and Miller, D. A., **Dorsiflexion of the Human Ankle as It Relates to Ski Boot Design in Downhill Skiing**, *Skiing Trauma and Safety: Seventh International Symposium, ASTM STP 1022*, Robert J. Johnson, C. D. Mote, Jr., and Marc-Hervé Binet, Eds., American Society for Testing and Materials, Philadelphia, 1989, pp. 146 - 152.
- Shealy, J. E., **Comparison of Downhill Ski Injury Patterns -- 1978 - 81 vs. 1988 - 90**, *Skiing Trauma and Safety: Ninth International Symposium, ASTM STP 1182*, Robert J. Johnson, C. D. Mote, Jr., and John Zelcer, Eds., American Society for Testing and Materials, Philadelphia, 1993, pp. 23 - 32.
- Walkhoff, K. and Bauman, C. W., **Alpine Ski Boot Hysteresis Characteristics Interpreted for Skier Target Groups Within the Current Standards**, *Skiing Trauma and Safety: Sixth International Symposium, ASTM STP 938*, C. D. Mote, Jr. and R. J. Johnson, Eds., American Society for Testing and Materials, Philadelphia, 1987, pp. 127 - 144.
- Wylie, C. R. and Barrett, L. C., *Advanced Engineering Mathematics*, 5th ed., McGraw-Hill Book Company, New York, 1982.

Yee, A. G. and Mote, C. D., Jr., **Skiing Forces and Moments at the Knee and Boot Top: Boot Stiffness Effects and Modeling**, *Skiing Trauma and Safety: Ninth International Symposium, ASTM STP 1182*, Robert J. Johnson, C. D. Mote, Jr., and John Zelcer, Eds., American Society for Testing and Materials, Philadelphia, 1993, pp. 111 - 127.

APPENDIX A

BACKGROUND WORK ON SKIER FORCE

In the initial plan for this investigation, the boot loading scenario was intended to be based on a skier falling in a forward motion similar to the situation encountered when a skier hits the uphill side of a mogul and falls forward. The Principle of the Conservation of Angular Momentum was going to be used to approximate this impulse force. However, while doing the theory development, it was realized that actual force and time measurements were necessary to provide a first approximation to use to simulate this impulse force, and this information was not available from the current literature.

Therefore, in order to continue with the model development, this activity was suspended and the sinusoidal forcing function approach was chosen. Future research efforts could be directed to this topic of modeling the impulse force during a forward fall.

The preliminary work done during this investigation is attached for future reference.

Principle of Conservation of Angular Momentum:

The Principle of the Conservation of Angular Momentum is illustrated in Figure A.1. This shows that if a body which has a total angular momenta, $\sum (H_r)_i$, is acted upon

by an external, angular impulse, $\int_{t_1}^{t_2} \sum \mathbf{M}_P dt$, then the body will experience a new total angular momenta, $\sum (\mathbf{H}_P)_2$, which is the sum of the original plus the angular impulse.

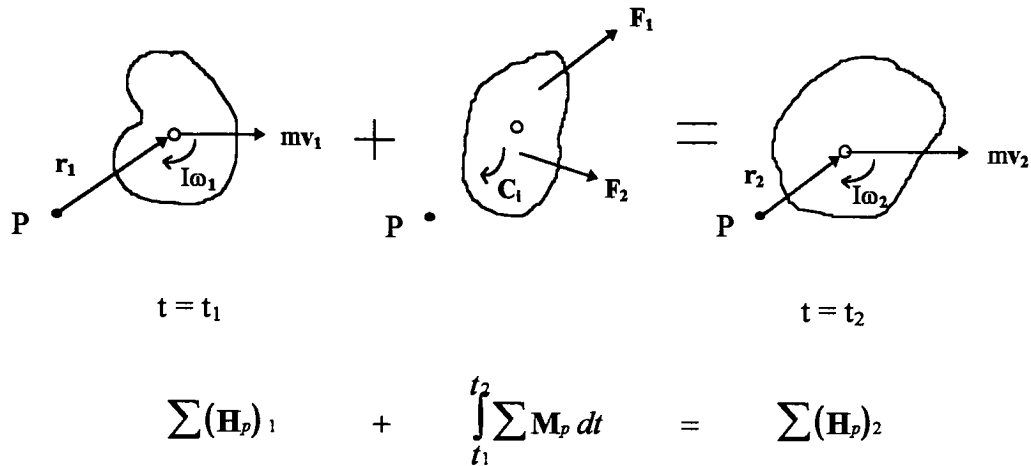


Figure A.1. Body acted upon by an impulse.

$$\text{Angular Momentum} = \mathbf{H}_P = I\vec{\omega} + (\mathbf{r} \times m\mathbf{v}) \quad \text{A.1}$$

$$\text{Angular Impulse} = \int_{t_1}^{t_2} \sum \mathbf{M}_P dt = \int_{t_1}^{t_2} \sum (\mathbf{r}_i \times \mathbf{F}_i) dt + \int_{t_1}^{t_2} \sum \mathbf{C}_i dt \quad \text{A.2}$$

Equation (A.1) is the definition of Angular Momentum for a body with respect to point P. It is due to the rotational inertia, $I\vec{\omega}$, and the moment of linear momentum, $\mathbf{r} \times m\mathbf{v}$.

Equation (A.2) says that the Angular Impulse is the integral of the sum of the external moments about point P, which can be broken down to be the moments of any external forces plus any external couples.

Simple Case

Now, apply this theory to a simple case: a rigid body moving along a frictionless surface hits a short obstruction. The free body diagrams of the system illustrate how the initial condition plus the external impulse become the final rotational motion.

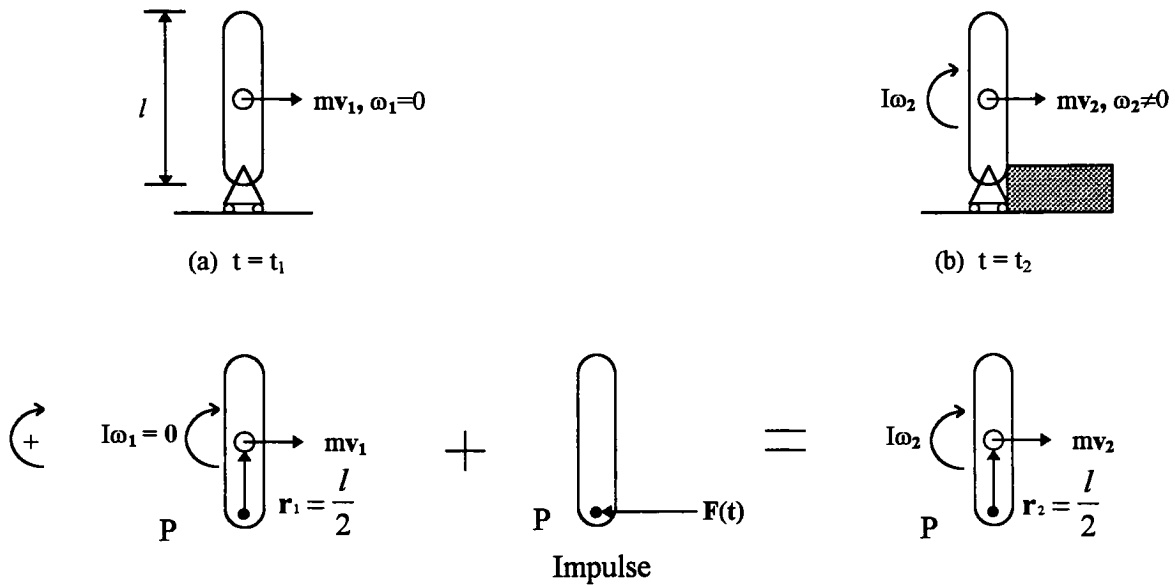


Figure A.2. Simple rigid body model.

Summing the angular momenta of each condition about P, the following relationships arise:

$$\left(0\hat{\mathbf{k}} + \frac{l}{2}mv_1\hat{\mathbf{k}} \right) + (0\hat{\mathbf{k}}) = \left(I\omega_2\hat{\mathbf{k}} + \frac{l}{2}mv_2\hat{\mathbf{k}} \right)$$

Since only the $\hat{\mathbf{k}}$ component remains, the equation becomes:

$$\frac{l}{2}mv_1 = I\omega_2 + \frac{l}{2}mv_2 \quad \text{A.3}$$

And using Kinematics, we know that $v = r\omega$ (or $\omega = \frac{v}{r}$).

Therefore, $v_2 = \frac{l}{2}\omega_2$,

or $\omega_2 = \frac{2}{l}v_2$.

A.4

Thus, plugging Equation A.4 into Equation A.3 gives,

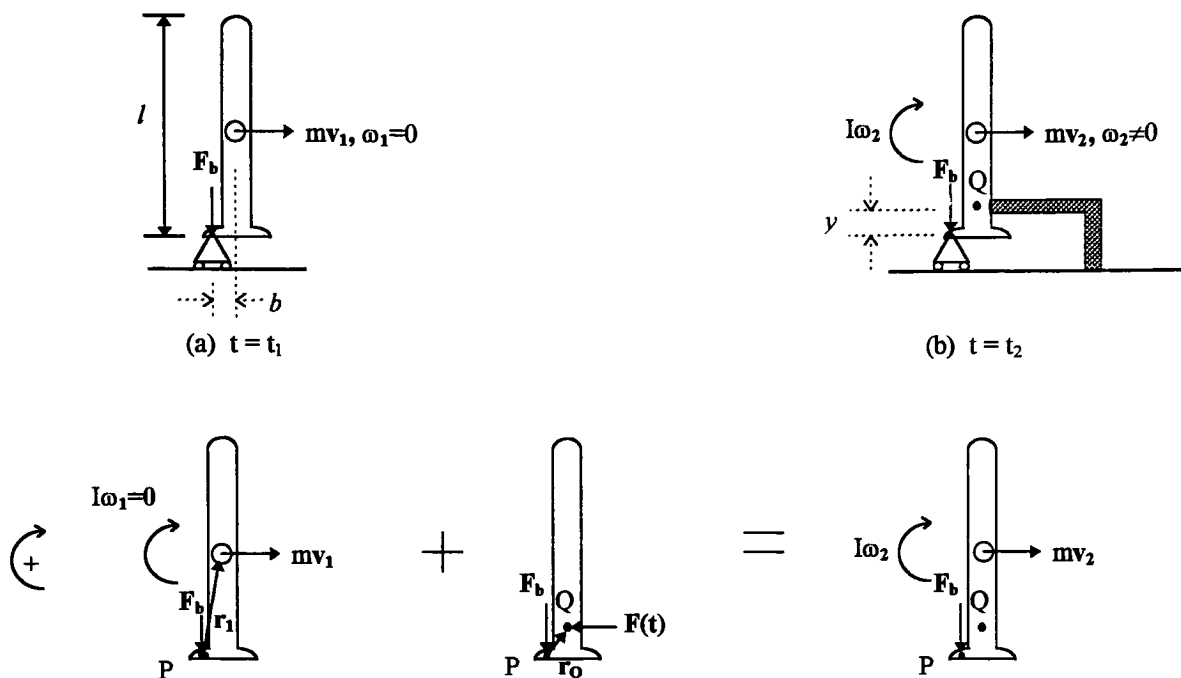
$$\begin{aligned}\frac{l}{2}mv_1 &= I\left(\frac{2}{l}v_2\right) + \frac{l}{2}mv_2 \\ \frac{l}{2}mv_1 &= v_2\left(\frac{2I}{l} + \frac{ml}{2}\right)\end{aligned}$$

A.5

Simplified Skier Case

Next, apply this principle to an example similar to the condition of a simplified skier who is simulated as a slender, rigid body. Instead of hitting a short obstacle directly in line with P, the body impacts the object at a distance y above P. In this case, the point P is not located along the vertical axis of the center of gravity. Additionally, a force, F_b , is directed vertically downward, to simulate the rear binding force. See Figure A.3.

(remainder of page is blank)

Figure A.3. Skier Model hitting obstacle at y .

Again summing the angular momenta effects about P before and after the impact, gives the following:

$$\left(0\hat{\mathbf{k}} + \frac{l}{2}mv_1\hat{\mathbf{k}}\right) + \left[-\int_{t_1}^{t_2} yF(t)dt\right]\hat{\mathbf{k}} = \left(I\omega_2\hat{\mathbf{k}} + \frac{l}{2}mv_2\hat{\mathbf{k}}\right) \quad \text{A.6}$$

$$\frac{l}{2}mv_1 - \int_{t_1}^{t_2} [yF(t)]dt = I\omega_2 + \frac{l}{2}mv_2$$

$\int_{t_1}^{t_2} F(t)dt$ can be found by using the Principle of Linear Momentum.

$$mv_1 - \int_{t_1}^{t_2} F(t)dt = mv_2$$

$$-\int_{t_1}^{t_2} F(t)dt = m(v_2 - v_1) \quad \text{A.7}$$

Using Equations A.4, $\omega_2 = \frac{2}{l}v_2$, and A.7, we can solve for v_2 by substituting back into Equation A.6. Thus, the following is derived:

$$\frac{l}{2}mv_1 + my(v_2 - v_1) = I\frac{2}{l}v_2 + \frac{l}{2}mv_2 \quad \text{A.8}$$

Once v_2 is found, it can be substituted back into Equation A.6 (or A.7) to find $F(t)$.

Average Skier Example

Using the skier model defined by Raskulinecz and Bahniuk (1979), the following values could be assigned to a 75th percentile male in a seated position, tipped forward.

$$\frac{l}{2} \equiv \text{distance from center of mass to ground} = 0.794 \text{ m}$$

$$m = 80.1 \text{ kg} + 4.9 \text{ kg for clothing} = 85.0 \text{ kg}$$

$$I = 8.06 \text{ kg-m}^2 \text{ (mean value, mass moment about any axis in horizontal plane)}$$

Additionally, the following values were also assumed,

$$v_1 = 15 \text{ mph} = 6.70 \text{ m/s}$$

$$y = L_3 \equiv \text{functional boot height} (= 0.135 \text{ m for Nordica N955, size 28.5})$$

Therefore, putting these values into Equation A.8,

$$\begin{aligned} & (0.794 \text{ m})(85 \text{ kg})(6.7 \text{ m/s}) + (85 \text{ kg})(0.135 \text{ m})(v_2 - 6.7 \text{ m/s}) \\ &= \frac{8.06 \text{ kg-m}^2}{0.794 \text{ m}}v_2 + (0.794 \text{ m})(85 \text{ kg})v_2 \end{aligned}$$

$$\therefore v_2 = 5.67 \text{ m/s} = 12.7 \text{ mph}$$

APPENDIX B

STATIC MODEL AT CONDITION OF MAXIMUM APPLIED LOAD

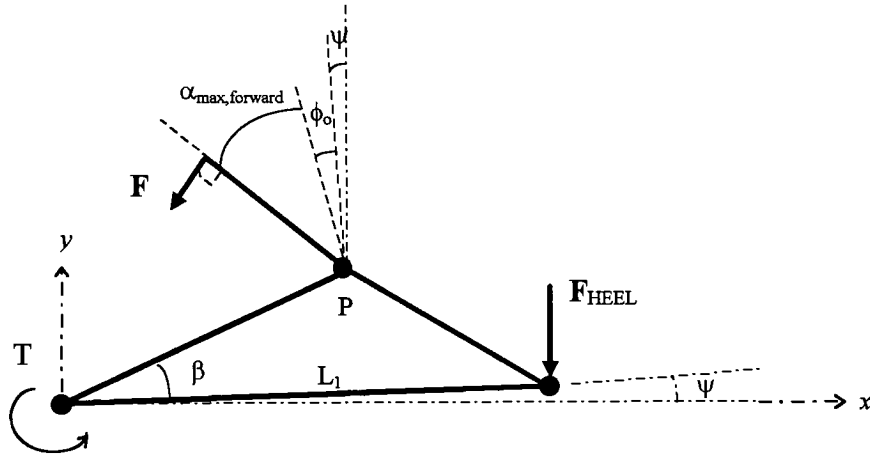


Figure B.1 Free Body Diagram of Model at Condition of Maximum Applied Load. Shaft has reached $\alpha_{\max, \text{forward}}$.

Figure B.1 illustrates the free body diagram for a static model of the boot at the condition when the maximum applied skier's force is reached. It is assumed that the boot shaft has already rotated to the hard stop at $\alpha_{\max, \text{forward}}$. Therefore, this situation is the same as the last iteration in the second condition of the dynamic model when $t = t_{\max}$, $F = F(t_{\max})$, $\psi = \psi(t_{\max})$, and $F_{\text{HEEL}} = F_{\text{HEEL}}(t_{\max})$.

Calculation of the heel force using the static model can be used as a reference to compare against the final results of the dynamic model. In this static model, the heel force is determined by summing the moments about point T.

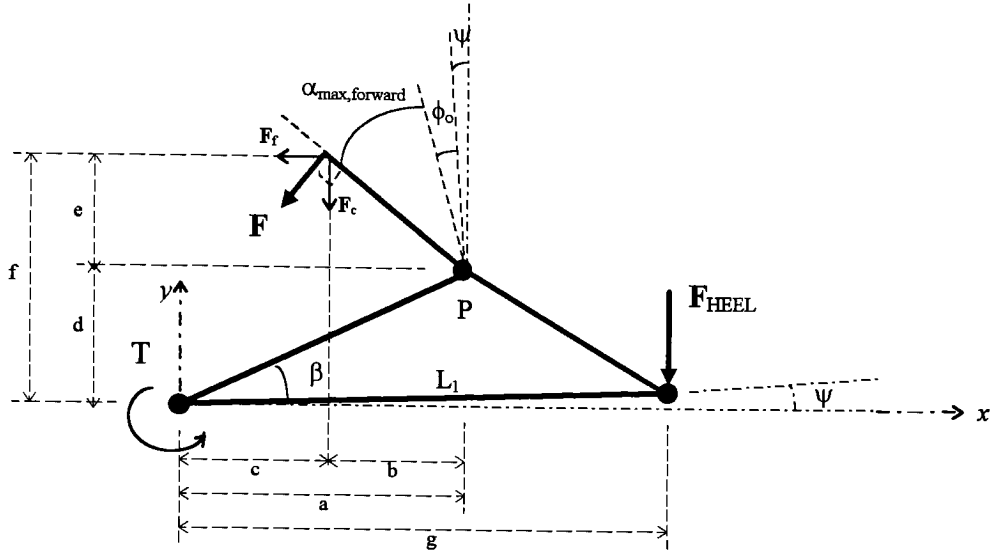


Figure B.2

$$\Sigma \mathbf{M}_T = 0 = -\mathbf{F}_c \cdot c + \mathbf{F}_f \cdot f - \mathbf{F}_{\text{HEEL}} \cdot g$$

$$\begin{array}{lll} \text{where} & \mathbf{F}_c = \mathbf{F} \sin(\alpha_{\max} + \phi_o + \psi) & \mathbf{F}_f = \mathbf{F} \cos(\alpha_{\max} + \phi_o + \psi) \\ & a = L_2 \cos(\beta + \psi) & d = L_2 \sin(\beta + \psi) \\ & b = L_3 \sin(\alpha_{\max} + \phi_o + \psi) & e = L_3 \cos(\alpha_{\max} + \phi_o + \psi) \\ & c = a - b & f = d + e \end{array}$$

$$g = L_1 \cos \psi$$

$$\begin{aligned} \Sigma \mathbf{M}_T = 0 &= -(\mathbf{F} \sin(\alpha_{\max} + \phi_o + \psi) \cdot (L_2 \cos(\beta + \psi) - L_3 \sin(\alpha_{\max} + \phi_o + \psi))) \\ &+ (\mathbf{F} \cos(\alpha_{\max} + \phi_o + \psi) \cdot (L_2 \sin(\beta + \psi) + L_3 \cos(\alpha_{\max} + \phi_o + \psi))) \\ &- \mathbf{F}_{\text{HEEL}} \cdot (L_1 \cos \psi) \\ &= \mathbf{F} L_3 - \mathbf{F} L_2 \sin(\alpha_{\max} + \phi_o - \beta) - \mathbf{F}_{\text{HEEL}} \cdot (L_1 \cos \psi) \end{aligned}$$

Therefore,

$$\mathbf{F}_{\text{HEEL}} = \mathbf{F} \left[\frac{L_3 - L_2 \sin(\alpha_{\max} + \phi_o - \beta)}{L_1 \cos \psi} \right]$$

where $\mathbf{F} = \mathbf{F}(t_{\max})$ and $\psi = \psi(t_{\max})$.

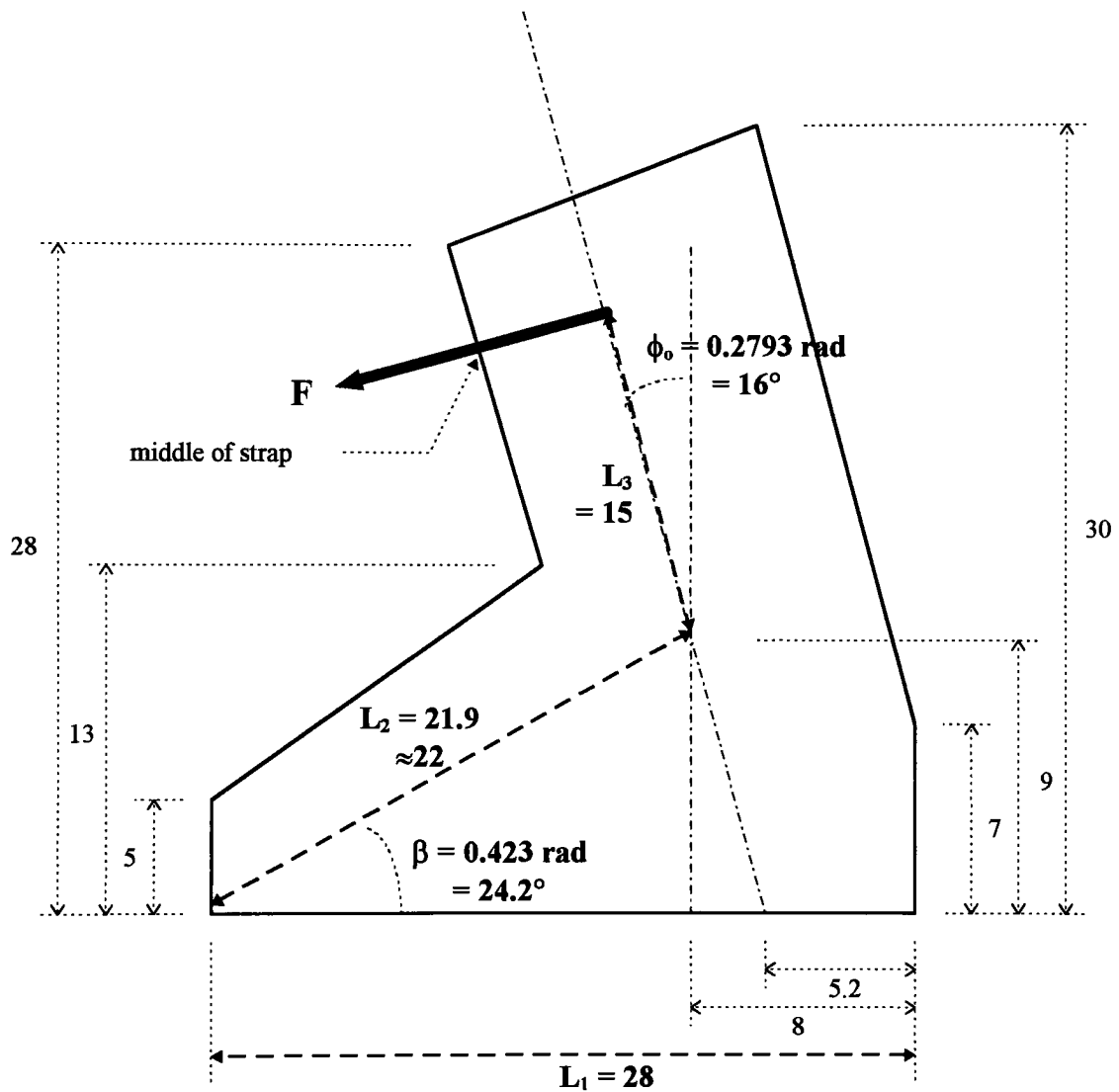
APPENDIX C

COMPARISON BOOT DATA:

DOLOMITE 65C JUNIOR RACING, FRONT ENTRY

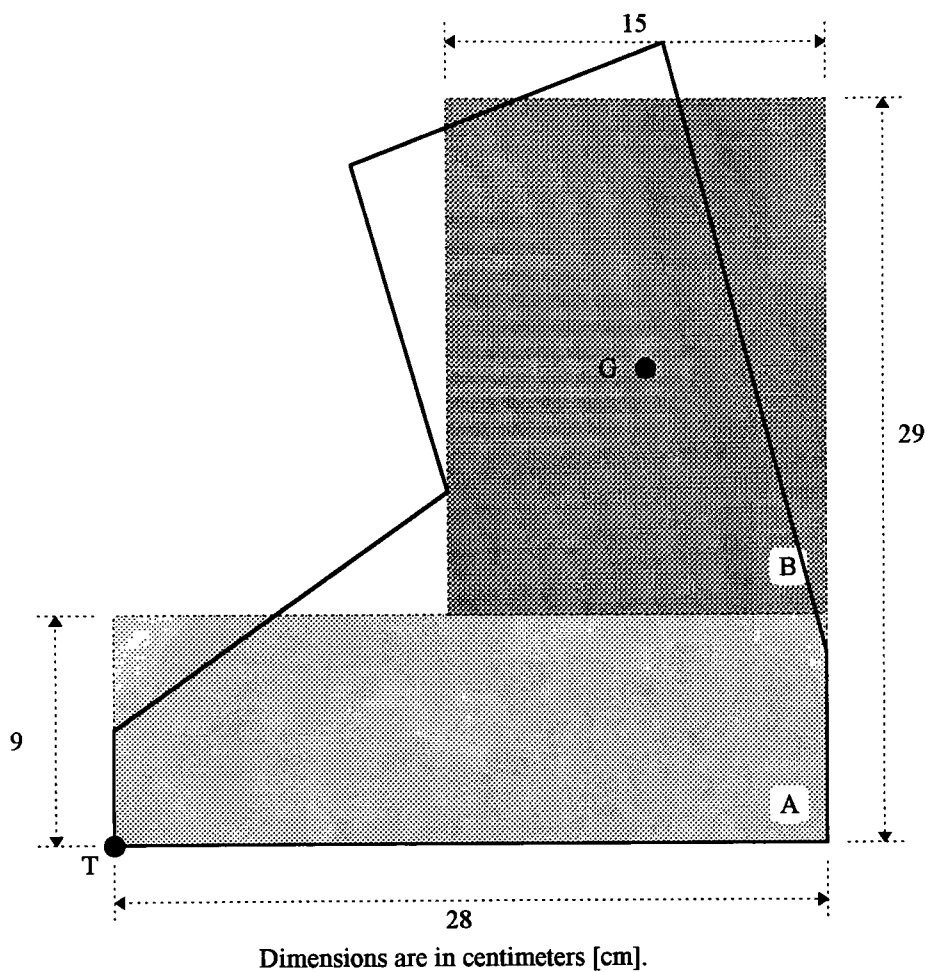
TRAPPEUR CARBON, FRONT ENTRY

ALSO INCLUDES DERIVATION OF MASS MOMENTS OF INERTIA VALUES



Dimensions are in centimeters [cm] unless noted.

Figure C.1 Dimensional Data for Dolomite 65C Junior Racing, Front Entry, size 23.5
 $L_1 = 28\text{cm}$, $L_2 = 22\text{cm}$, $L_3 = 15\text{cm}$, $\beta = 0.423\text{ rad}$, $\phi_0 = 0.2793\text{ rad}$.



Base (A):

$$\text{Area}_A = 252 \text{ cm}^2$$

$$m_A = 0.795 \text{ kg}$$

$$J_T = J_{o,A} = 0.023 \text{ kg-m}^2$$

Shaft (B):

$$\text{Area}_B = 300 \text{ cm}^2$$

$$m_B = 0.947 \text{ kg}$$

$$I_G = I_{G,B} = 0.005 \text{ kg-m}^2$$

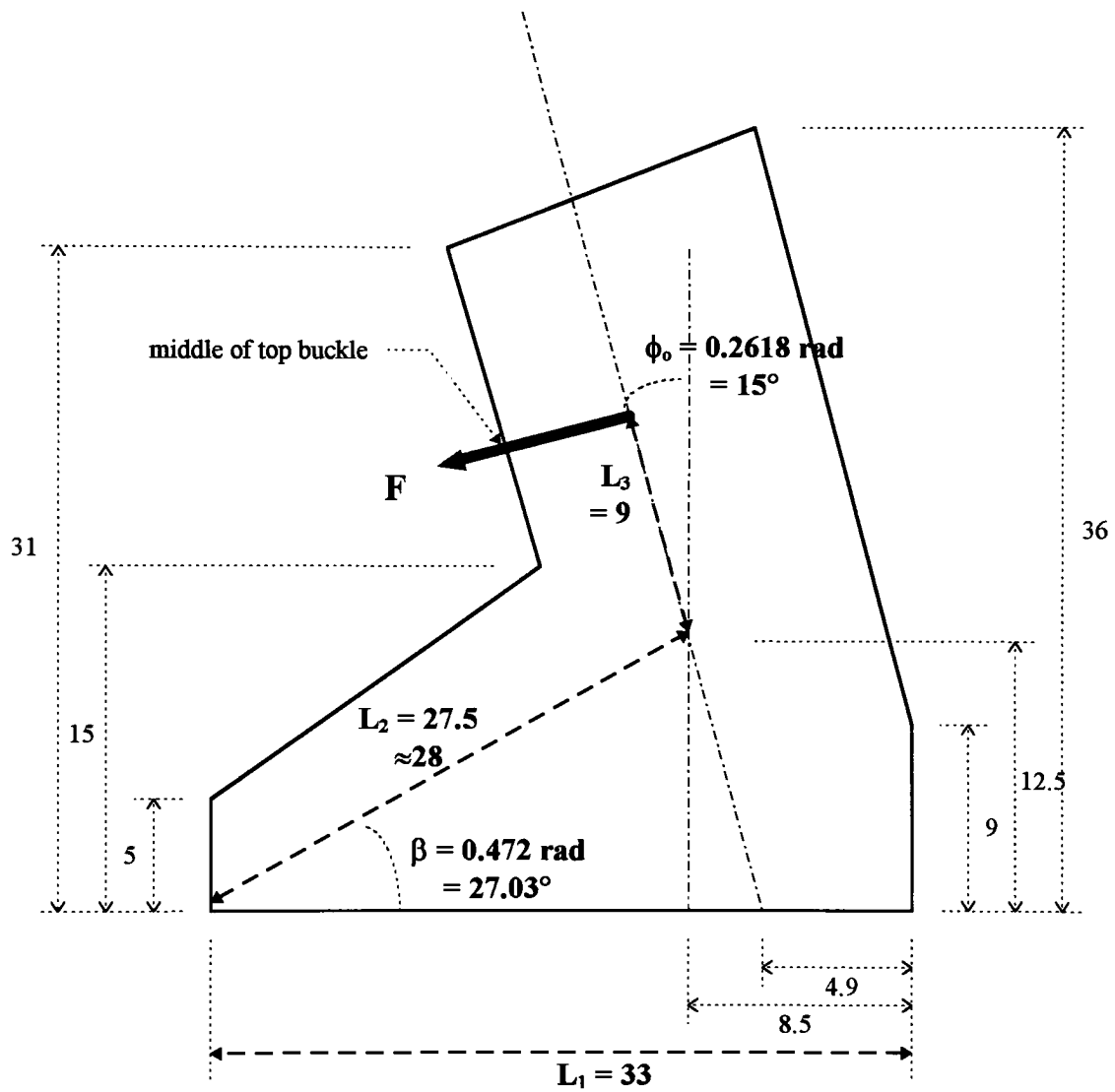
Total Boot (A+B):

$$\text{Area}_{TOT} = 552 \text{ cm}^2$$

$$m = 1.742 \text{ kg}$$

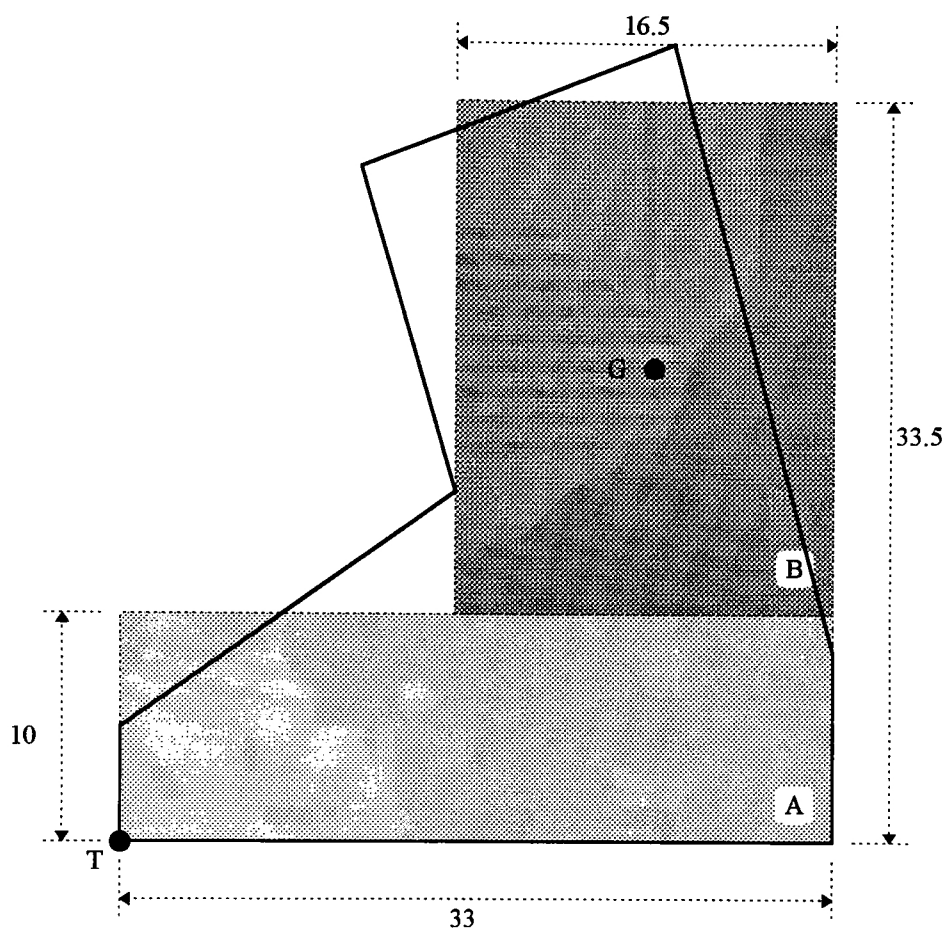
$$J_{TOT} = 0.074 \text{ kg-m}^2$$

Figure C.2 Inertial Data for Dolomite 65C Junior Racing, Front Entry, size 23.5.
Calculations based on boot base (A) and shaft (B) represented as simple rectangles.



Dimensions are in centimeters [cm] unless noted.

Figure C.3 Dimensional Data for Trappeur Carbon, Front Entry, unknown size.
 $L_1 = 33\text{cm}$, $L_2 = 28\text{cm}$, $L_3 = 9\text{cm}$, $\beta = 0.472 \text{ rad}$, $\phi_0 = 0.2618 \text{ rad}$.



Dimensions are in centimeters [cm].

Base (A):

$$\text{Area}_A = 330 \text{ cm}^2$$

$$m_A = 1.024 \text{ kg}$$

$$J_T = J_{o,A} = 0.041 \text{ kg-m}^2$$

Shaft (B):

$$\text{Area}_B = 387.75 \text{ cm}^2$$

$$m_B = 1.204 \text{ kg}$$

$$I_G = I_{G,B} = 0.008 \text{ kg-m}^2$$

Total Boot (A+B):

$$\text{Area}_{TOT} = 717.75 \text{ cm}^2$$

$$m = 2.228 \text{ kg}$$

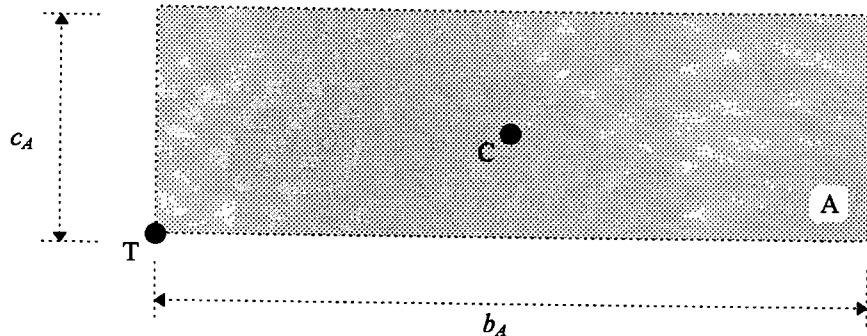
$$J_{TOT} = 0.143 \text{ kg-m}^2$$

Figure C.4 Inertial Data for Trapeur Carbon, Front Entry, unknown size.
Calculations based on boot base (A) and shaft (B) represented as simple rectangles.

Derivation of Mass Moments of Inertia Values

Boot Base (A):

Figure C.5
Simplified boot
base used to
approximate
mass moment of
inertia about
point T, J_T .



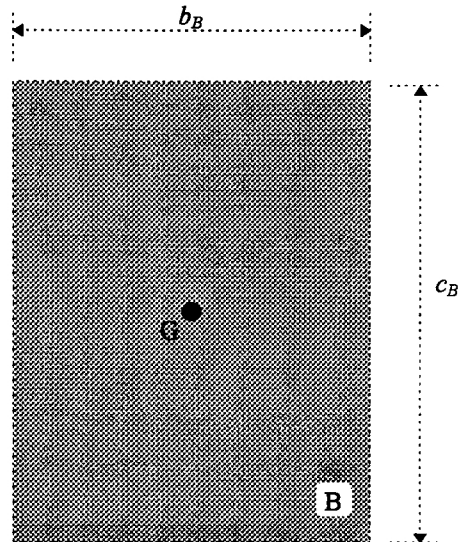
The mass moment of inertia of the base (A) about point T, J_T , is derived by using the parallel axis theorem. Thus the moment of inertia for the base is:

$$\begin{aligned}
 J_T &= I_C + m_A (\overline{CT})^2 \\
 &= \frac{m_A}{12} (b_A^2 + c_A^2) + m_A \left(\left(\frac{b_A}{2} \right)^2 + \left(\frac{c_A}{2} \right)^2 \right) \\
 &= \frac{m_A}{3} (b_A^2 + c_A^2)
 \end{aligned}$$

$$\therefore \quad \underline{J_T = \frac{m_A}{3} (b_A^2 + c_A^2)}$$

Boot Shaft (B):

Figure C.6
Simplified boot
shaft used to
approximate
mass moment of
inertia about
point G, I_G .



Point G is also the location of the center of mass, C, for the simplified boot shaft. Therefore,

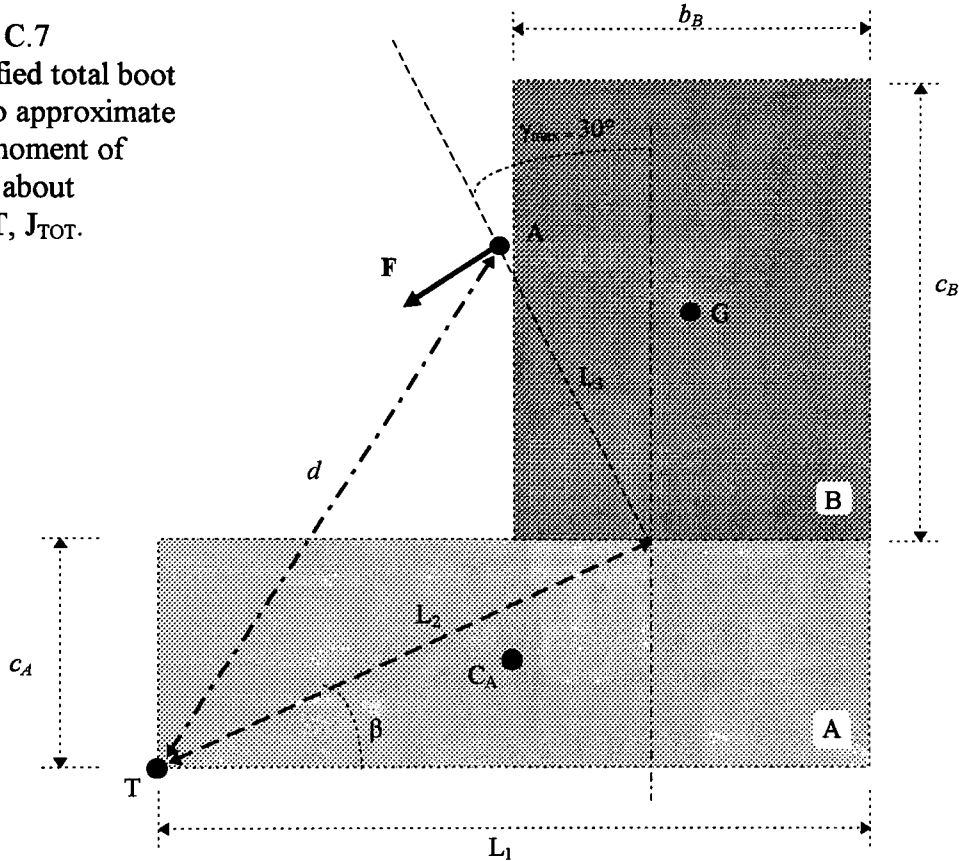
$$I_G = I_C$$

$$= \frac{m_B}{12} (b_B^2 + c_B^2)$$

$$\therefore \quad \underline{I_G = \frac{m_B}{12} (b_B^2 + c_B^2)}$$

Total Boot (A+B):

Figure C.7
Simplified total boot
used to approximate
mass moment of
inertia about
point T, J_{TOT} .



The moment of inertia for the total boot about point T, J_{TOT} , was derived from the combination of the moment of inertia for the base about T, J_T , and the moment for the shaft, I_G , about point T modified by the parallel axis theorem. The parallel axis theorem was adjusted for the case when the shaft had reached the maximum forward lean angle, $\gamma_{max} = 30^\circ$. The distance, d , used was $d = \overline{AT}$, where A was the point of application of the input force, F .

$$\mathbf{d} = \left(L_2 \cos \beta - \frac{L_3}{2} \sin(\gamma_{max}) \right) \hat{i} + \left(L_2 \sin \beta - \frac{L_3}{2} \cos(\gamma_{max}) \right) \hat{j}$$

$$J_{TOT} = J_T + (I_G + m_B d^2)$$

$$\therefore \quad \underline{J_{TOT} = J_T + \left[I_G + m_B (L_2^2 - L_2 L_3 \sin(\gamma_{max} - \beta)) \right]}$$

APPENDIX D

ACSL PROGRAMS

“1STONLY.CSL”

solves only first condition equations, timed termination

“FIRST.CSL”

solves only first condition equations, termination based on lean angle,
used with “Second.csl”

“SECOND.CSL”

solves second condition equations using input from “First.csl”, timed termination

PROGRAM 1STONLY

```

" ---- Solve equations of motion for the model ----"
" ---- using only the first condition -----"
" ---- Constants are based on Nominal Test Case Values ----"

" ---- Constant values for Nordica N955 boot parameters ----"

    CONSTANT L1 =.33, L2 =.26, L3 = .14
    CONSTANT Mshaft = 1.18, IG =.008, JT =.039
    CONSTANT beta = .505, phi = .2618

" ---- Assumed values for boot stiffness, damping, heel retention ---"
" ---- spring stiffness, and maximum force at t=(Pi/2) ----"

    CONSTANT K0 = 1.95, nu = 1.63, damp=1.5
    CONSTANT k = 1E+06
    CONSTANT f0 = 1750.

" ---- Computing constants ----"

    CONSTANT TSTP = 3.5 , R2D = 57.3

"----- force F -----"
    F = f0*sin(t/2)
"-----"

    A = IG + ( Mshaft*L3**2)/4.
    D = JT + Mshaft*L2**2
    C = cos( q1-q2 + phi - beta )
    S = sin( q1-q2 + phi - beta )
    B = ( ( Mshaft*L2*L3 )/2.) * S
    det = A*D - B*B

    prod = ( D*B*p1**2 + (A*D+B**2)*p1*p2 + A*B*p2**2 )/det**2

    momt = K0*(R2D**nu)*( abs(q1-q2)**nu )*sign(1.,q1-q2)

    q1dot = ( D*p1 + B*p2 )/det
    q2dot = ( A*p2 + B*p1 )/det
    p1dot = -( Mshaft*L2*L3*prod*C )/2. - momt + F*L3 ...
            -damp*(q1dot-q2dot)
    p2dot = ( Mshaft*L2*L3*prod*C )/2. -k*(L1**2)*q2 + ...
            momt - F*L2*S + damp*(q1dot-q2dot)

    q1 = integ(q1dot,0)
    q2 = integ(q2dot,0)
    p1 = integ(p1dot,0)
    p2 = integ(p2dot,0)

    fheel = k*(L1)*q2
    theta = 57.3*q1
    psi = 57.3*q2
    alpha = (q1-q2)*57.3

"-----TERMINATION CONDITION"
    TERMT(T.GE.TSTP)
"-----COMMUNICATION INTERVAL IN SECS"
    CINTERVAL CINT = 0.01

END

```

D-II

PROGRAM FIRST

```

" ---- Solve equations of motion for the model ----"      D-III
" ---- using only the first condition -----"
" ---- Terminate solution when either the shaft hits the hard ----"
" ---- stop (at alpha+phi='maxlean' angle), or time reaches ----"
" ---- the maximum run time, TSTP. ----"
" ---- Terminal conditions will be used as input values for ----"
" ---- solution of the second condition, program SECOND.CSL ----"

" ---- Constant values for Nordica N955 boot parameters -----"

      CONSTANT  L1 = .33, L2 = .26, L3 = .14
      CONSTANT  Mshaft = 1.18, IG = .008, JT = .039
      CONSTANT  beta = .505, phi = .2618

" ---- Assumed values for boot stiffness, damping, heel retention ----"
" ---- spring stiffness, maximum force at t=(Pi/2), and maximum ----"
" ---- forward lean angle (maxlean = 30 deg) ----"

      CONSTANT  K0 = 1.95, nu = 1.63, damp = 1.5
      CONSTANT  k = 1E+06
      CONSTANT  f0 = 1750.0, maxlean = 0.5236

" ---- Computing constants ----"
" ---- (R2D=radians to degrees conversion factor) ----"
      CONSTANT  TSTP = 3.5 , R2D = 57.3

      DYNAMIC
      DERIVATIVE

"----- force F -----"
      F = f0*sin(t/2)
"-----"

      A = IG + ( Mshaft*L3**2)/4.
      D = JT + Mshaft*L2**2
      C = cos( q1-q2 + phi - beta )
      S = sin( q1-q2 + phi - beta )
      B = ( ( Mshaft*L2*L3 )/2.) * S
      det = A*D - B*B

      prod = ( D*B*p1**2 + (A*D+B**2)*p1*p2 + A*B*p2**2 )/det**2

      momt =  K0*(R2D**nu)*( abs(q1-q2)**nu )*sign(1.,q1-q2)

      q1dot = ( D*p1 + B*p2 )/det
      q2dot = ( A*p2 + B*p1 )/det
      p1dot = -( Mshaft*L2*L3*prod*C )/2. - momt + F*L3 ...
              -damp*(q1dot-q2dot)
      p2dot = ( Mshaft*L2*L3*prod*C )/2. -k*(L1**2)*q2 + ...
              momt - F*L2*S + damp*(q1dot-q2dot)

      q1 = integ(q1dot,0)
      q2 = integ(q2dot,0)
      p1 = integ(p1dot,0)
      p2 = integ(p2dot,0)

```

fheel = k*(L1)*q2

theta = 57.3*q1

psi = 57.3*q2

D-IV

alphanad = q1 - q2

alpha = alphanad * 57.3

END \$ "of derivative"

"-----TERMINATION CONDITION"

TERMT (((alphanad+phi).GE.maxlean) .OR. (T.GE.TSTP))

"-----COMMUNICATION INTERVAL IN SECS"

CINTERVAL CINT = 0.01

END \$ "of dynamic"

END \$ "of program"

PROGRAM SECOND

```

" -- Only solve for second condition:      ----"
" -- Input terminal condition values from  ----"
" -- 1st condition program, FIRST.CSL      ----"
                                                    D-V

" ---- Constant values for Nordica N955 boot parameters-----"

    CONSTANT  L1 =.33, L2 = .26, L3 = .14
    CONSTANT  Jtot = .127
    CONSTANT  beta = .505, phi = .2618

    CONSTANT  k = 1E+06, K0 = 1.95, nu = 1.63, damp = 1.5
    CONSTANT  f0 = 1750, maxlean = 0.5236

    CONSTANT  TSTP = 3.5, R2D = 57.3

"----- Initialize input values from 1st condition program ----"
"----- actual values generated from termination of 1st con.  --"
"----- will be entered during execution of program          ----"
        q2 = 0.0
        p2 = 0.0
        t1Cmax = 0.0
" -----"

    DYNAMIC
    DERIVATIVE

"----- force F modified to account for time at -----"
"----- termination of 1st condition -----"

        F = f0*sin((t+t1Cmax)/2)
"-----"

        S = sin( maxlean - beta )

        pdot = (F*L3)-(F*L2*S) - (k*(L1**2)*q) - damp*qdot
        qdot = p / Jtot

        p = integ(pdot,p2)
        q = integ(qdot,q2)

        fheel = k*L1*q
        psi = 57.3*q

        runtime = t + t1Cmax

    END $ "of dervative"
"-----TERMINATION CONDITION"
        TERMT( runtime .GE. TSTP )
"-----COMMUNICATION INTERVAL IN SECS"
        CINTERVAL CINT = 0.01

    END $ "of dynamic"
    END $ "of program"

```

APPENDIX E

ACSL PROGRAM RESULTS - NUMERICAL DATA

.

“1STONLY.CSL”

solves only first condition equations, timed termination

“FIRST.CSL”

solves only first condition equations, termination based on lean angle,
used with “Second.csl”

“SECOND.CSL”

solves second condition equations using input from “First.csl”, timed termination

Nominal Test Case							L1=0.31						
T	FHEEL	F	Q2	P2	ALPHA		T	FHEEL	F	Q2	P2	ALPHA	
0	0	0	0	0	0	0	0	0	0	0	0	0	0
0.05	27.4848	43.7454	8.33E-05	0.0020643	1.9745	0.05	29.2686	43.7454	9.44E-05	0.00205606	1.97458	0.05	29.2686
0.1	50.279	87.4635	1.52E-04	0.00149844	3.01512	0.1	53.5141	87.4635	1.73E-04	0.00152189	3.01514	0.1	53.5141
0.15	73.6717	131.127	2.23E-04	0.00124332	3.90145	0.15	78.4111	131.127	2.53E-04	0.00126754	3.90145	0.15	78.4111
0.2	96.2986	174.708	2.92E-04	0.00104624	4.67469	0.2	102.515	174.708	3.31E-04	0.00106917	4.67469	0.2	102.515
0.25	118.183	218.181	3.58E-04	9.02E-04	5.37107	0.25	125.809	218.181	4.05E-04	9.24E-04	5.37107	0.25	125.809
0.3	139.386	261.517	4.22E-04	7.92E-04	6.0119	0.3	148.358	261.517	4.79E-04	8.12E-04	6.0119	0.3	148.358
0.35	159.885	304.689	4.85E-04	7.02E-04	6.60962	0.35	170.2	304.689	5.49E-04	7.22E-04	6.60961	0.35	170.2
0.4	179.766	347.671	5.45E-04	6.27E-04	7.17231	0.4	191.363	347.671	6.17E-04	6.45E-04	7.17231	0.4	191.363
0.45	199.029	390.436	6.03E-04	5.62E-04	7.7056	0.45	211.87	390.436	6.83E-04	5.81E-04	7.7056	0.45	211.87
0.5	217.695	432.957	6.60E-04	5.05E-04	8.21357	0.5	231.739	432.957	7.48E-04	5.24E-04	8.21357	0.5	231.739
0.55	235.777	475.207	7.14E-04	4.55E-04	8.69932	0.55	260.989	475.207	8.10E-04	4.73E-04	8.69932	0.55	260.989
0.6	253.291	517.16	7.68E-04	4.11E-04	9.16522	0.6	269.532	517.16	8.70E-04	4.27E-04	9.16522	0.6	269.532
0.65	270.247	558.79	8.19E-04	3.70E-04	9.61316	0.65	287.683	558.79	9.28E-04	3.86E-04	9.61316	0.65	287.683
0.7	286.66	600.071	8.69E-04	3.33E-04	10.0447	0.7	305.154	600.071	9.84E-04	3.49E-04	10.0447	0.7	305.154
0.75	302.538	640.977	9.17E-04	2.99E-04	10.451	0.75	322.057	640.977	0.0103889	3.15E-04	10.451	0.75	322.057
0.8	317.893	681.482	9.63E-04	2.69E-04	10.8632	0.8	338.402	681.482	0.0109162	2.83E-04	10.8632	0.8	338.402
0.85	332.735	721.561	0.00100829	2.40E-04	11.2521	0.85	354.201	721.561	0.0114259	2.54E-04	11.2521	0.85	354.201
0.9	347.073	761.19	0.00105174	2.14E-04	11.6284	0.9	369.455	761.19	0.0119182	2.27E-04	11.6284	0.9	369.455
0.95	360.916	800.342	0.00109369	1.90E-04	11.9929	0.95	384.201	800.342	0.0123936	2.03E-04	11.9929	0.95	384.201
1	374.275	838.995	0.00113417	1.67E-04	12.3459	1	398.422	838.995	0.0128523	1.80E-04	12.3459	1	398.422
1.05	387.159	877.123	0.00117321	1.45E-04	12.688	1.05	412.137	877.123	0.0132947	1.59E-04	12.688	1.05	412.137
1.1	399.576	914.703	0.00121084	1.27E-04	13.0196	1.1	425.355	914.703	0.0137211	1.39E-04	13.0196	1.1	425.355
1.15	411.537	951.711	0.00124708	1.09E-04	13.3411	1.15	438.087	951.711	0.0141319	1.21E-04	13.3411	1.15	438.087
1.2	423.049	988.124	0.00128197	9.27E-05	13.6526	1.2	450.343	988.124	0.0145272	1.04E-04	13.6526	1.2	450.343
1.25	434.123	1023.92	0.00131552	7.74E-05	13.9546	1.25	452.131	1023.92	0.0149074	8.78E-05	13.9545	1.25	452.131
1.3	444.767	1069.08	0.00134778	6.33E-05	14.2472	1.3	473.451	1069.08	0.015273	7.32E-05	14.2472	1.3	473.451
1.35	454.99	1093.57	0.00137876	5.02E-05	14.5307	1.35	484.344	1093.57	0.015624	5.97E-05	14.5307	1.35	484.344
1.4	464.802	1127.38	0.00140849	3.82E-05	14.8052	1.4	494.789	1127.38	0.0159609	4.74E-05	14.8052	1.4	494.789
1.45	474.212	1160.49	0.001437	2.72E-05	15.071	1.45	504.806	1160.49	0.0162841	3.60E-05	15.071	1.45	504.806
1.5	483.227	1192.87	0.00146433	1.72E-05	15.328	1.5	514.403	1192.87	0.0165937	2.56E-05	15.328	1.5	514.403
1.55	491.859	1224.5	0.00149048	7.97E-06	15.5766	1.55	523.592	1224.5	0.0168901	1.62E-05	15.5766	1.55	523.592
1.6	500.115	1255.37	0.0015155	-1.67E-07	15.8168	1.6	532.381	1255.37	0.0171736	7.39E-06	15.8168	1.6	532.381
1.65	508.004	1285.45	0.00153941	-7.91E-05	16.0487	1.65	540.779	1285.45	0.0174445	-5.31E-07	16.0487	1.65	540.779
1.7	515.536	1314.74	0.00156223	-1.45E-05	16.2724	1.7	548.795	1314.74	0.0177031	-7.61E-06	16.2724	1.7	548.795
1.75	522.717	1343.2	0.00158399	-2.05E-05	16.4879	1.75	556.441	1343.2	0.0179497	-1.39E-05	16.4879	1.75	556.441
1.8	529.559	1370.82	0.00160472	-2.58E-05	16.6955	1.8	563.724	1370.82	0.0181846	-1.95E-05	16.6955	1.8	563.724
1.85	536.068	1397.59	0.00162445	-3.05E-05	16.895	1.85	570.653	1397.59	0.0184082	-2.45E-05	16.895	1.85	570.653
1.9	542.253	1423.48	0.00164319	-3.44E-05	17.0867	1.9	577.237	1423.48	0.0186205	-2.86E-05	17.0867	1.9	577.237
1.95	548.122	1448.48	0.00166098	-3.77E-05	17.2705	1.95	583.485	1448.48	0.0188221	-3.23E-05	17.2705	1.95	583.485
2	553.683	1472.57	0.00167783	-4.05E-05	17.4464	2	589.405	1472.57	0.0190131	-3.54E-05	17.4464	2	589.405
2.05	558.944	1495.75	0.00169377	-4.27E-05	17.6147	2.05	595.004	1495.75	0.0191937	-3.78E-05	17.6147	2.05	595.004
2.1	563.912	1517.99	0.00170882	-4.43E-05	17.7752	2.1	600.293	1517.99	0.0193643	-3.97E-05	17.7752	2.1	600.293
2.15	568.595	1539.28	0.00172302	-4.54E-05	17.928	2.15	605.278	1539.28	0.0195251	-4.11E-05	17.928	2.15	605.278
2.2	572.999	1559.61	0.00173636	-4.61E-05	18.0731	2.2	609.957	1559.61	0.0196974	-4.22E-05	18.0731	2.2	609.957
2.25	577.133	1578.97	0.00174889	-4.64E-05	18.2107	2.25	614.367	1578.97	0.0198183	-4.26E-05	18.2107	2.25	614.367
2.3	581.002	1597.34	0.00176061	-4.60E-05	18.3406	2.3	618.485	1597.34	0.0199511	-4.26E-06	18.3406	2.3	618.485
2.35	584.612	1614.71	0.00177155	-4.55E-05	18.4629	2.35	622.329	1614.71	0.0200751	-4.21E-05	18.4629	2.35	622.329
2.4	587.969	1631.07	0.00178173	-4.44E-05	18.5777	2.4	625.903	1631.07	0.0201904	-4.14E-05	18.5777	2.4	625.903
2.45	591.08	1646.41	0.00179115	-4.30E-05	18.6849	2.45	629.215	1646.41	0.0202973	-4.02E-05	18.6849	2.45	629.215
2.5	593.95	1660.72	0.00179985	-4.14E-05	18.7846	2.5	632.269	1660.72	0.0203958	-3.88E-05	18.7846	2.5	632.269
2.55	596.584	1674	0.00180783	-3.92E-05	18.8768	2.55	635.073	1674	0.0204862	-3.69E-05	18.8768	2.55	635.073
2.6	598.985	1686.23	0.00181511	-3.70E-05	18.9515	2.6	637.629	1686.23	0.0205687	-3.47E-05	18.9515	2.6	637.629
2.65	601.16	1697.4	0.0018217	-3.44E-05	19.0387	2.65	639.945	1697.4	0.0206434	-3.24E-05	19.0387	2.65	639.945
2.7	603.112	1707.52	0.00182761	-3.16E-05	19.1084	2.7	642.023	1707.52	0.0207104	-2.98E-05	19.1084	2.7	642.023
2.75	604.844	1716.56	0.00183286	-2.86E-05	19.1707	2.75	643.866	1716.56	0.0207699	-2.70E-05	19.1707	2.75	643.866
2.8	606.36	1724.54	0.00183746	-2.53E-05	19.2255	2.8	645.48	1724.54	0.0208219	-2.41E-05	19.2255	2.8	645.48
2.85	607.663	1731.43	0.0018414	-2.20E-05	19.2728	2.85	646.867	1731.43	0.0208667	-2.09E-05	19.2728	2.85	646.867
2.9	608.756	1737.25	0.00184471	-1.84E-05	19.3127	2.9	648.03	1737.25	0.0209042	-1.76E-05	19.3127	2.9	648.03
2.95	609.639	1741.98	0.00184739	-1.48E-05	19.3451	2.95	648.97	1741.98	0.0209345	-1.40E-05	19.3451	2.95	648.97
3	610.316	1745.62	0.00184944	-1.10E-05	19.3701	3	649.691	1745.62	0.0209578	-1.04E-06	19.3701	3	649.691
3.05	610.788	1748.17	0.00185087	-7.25E-06	19.3876	3.05	650.194	1748.17	0.020974	-6.91E-06	19.3876	3.05	650.194
3.1	611.055	1749.62	0.00185168	-3.38E-06	19.3977	3.1	650.478	1749.62	0.0209831	-3.20E-06	19.3977	3.1	650.478
3.15	611.118	1749.98	0.00185187	4.22E-07	19.4004	3.15	650.545	1749.98	0.0209853	4.08E-07	19.4004	3.15	650.545
3.2	610.977	1749.25	0.00185145	4.45E-06	19.3956	3.2	650.395	1749.25	0.0209805	4.11E-06	19.3956	3.2	650.395
3.25	610.532	1747.43	0.0018504	8.14E-06	19.3834	3.25	650.028	1747.43	0.0209686	7.73E-06	19.3834	3.25	650.028
3.3	610.083	1744.51	0.00184874	1.20E-05	19.3637	3.3	649.443	1744.51	0.0209498	1.13E-05	19.3537	3.3	649.443
3.35	609.327	1740.51	0.00184645	1.57E-05	19.3366	3.35	648.639	1740.51	0.0209238	1.48E-05	19.3366	3.35	648.639
3.4	608.365	1735.41	0.00184353	1.93E-05	19.302	3.4	647.614	1735.41	0.0208908	1.83E-05	19.3021	3.4	647.614
3.45	607.193	1729.23	0.00183998	2.27E-05	19.2601	3.45	646.367	1729.23	0.0208505	2.16E-05	19.2601	3.45	646.367
3.5	605.81	1721.98	0.00183579	2.61E-05	19.2106	3.5	644.895	1721.98	0.0208031	2.48E-05	19.2105	3.5	644.895

L1=0.32						L1=0.34					
T	FHEEL	F	Q2	P2	ALPHA	T	FHEEL	F	Q2	P2	ALPHA
0	0	0	0	0	0	0	0	0	0	0	0
0.05	28.3192	43.7454	8.85E-05	0.00206022	1.97454	0.05	26.7062	43.7454	7.85E-05	0.00205117	1.97445
0.1	51.8696	87.4635	1.62E-04	0.00151643	3.01512	0.1	48.8104	87.4635	1.44E-04	0.00149622	3.01511
0.15	75.9661	131.127	2.37E-04	0.00125128	3.90145	0.15	71.4962	131.127	2.10E-04	0.00123437	3.90145
0.2	99.3089	174.708	3.10E-04	0.0010573	4.67469	0.2	93.4664	174.708	2.75E-04	0.00103615	4.67469
0.25	121.877	218.181	3.81E-04	9.12E-04	5.37107	0.25	114.706	218.181	3.37E-04	8.93E-04	5.37107
0.3	143.72	261.517	4.49E-04	8.02E-04	6.0119	0.3	135.267	261.517	3.98E-04	7.83E-04	6.0119
0.35	164.882	304.689	5.15E-04	7.12E-04	6.60962	0.35	156.183	304.689	4.56E-04	6.94E-04	6.60961
0.4	185.383	347.671	5.79E-04	6.36E-04	7.17231	0.4	174.478	347.671	5.13E-04	6.19E-04	7.17231
0.45	205.249	390.436	6.41E-04	5.71E-04	7.7056	0.45	193.176	390.436	5.68E-04	5.54E-04	7.7056
0.5	224.498	432.957	7.02E-04	5.14E-04	8.21357	0.5	211.292	432.957	6.21E-04	4.98E-04	8.21357
0.55	243.145	475.207	7.60E-04	4.64E-04	8.69932	0.55	228.842	475.207	6.73E-04	4.48E-04	8.69932
0.6	261.206	517.16	8.16E-04	4.19E-04	9.16522	0.6	245.841	517.16	7.23E-04	4.03E-04	9.16522
0.65	278.693	568.79	8.71E-04	3.78E-04	9.61316	0.65	262.299	568.79	7.71E-04	3.63E-04	9.61316
0.7	295.618	600.071	9.24E-04	3.41E-04	10.0447	0.7	278.229	600.071	8.18E-04	3.26E-04	10.0447
0.75	311.992	640.977	9.75E-04	3.07E-04	10.461	0.75	293.64	640.977	8.64E-04	2.93E-04	10.461
0.8	327.827	681.482	0.00102446	2.76E-04	10.8632	0.8	308.543	681.482	9.07E-04	2.62E-04	10.8632
0.85	343.133	721.561	0.00107229	2.47E-04	11.2521	0.85	322.948	721.561	9.50E-04	2.34E-04	11.2521
0.9	357.919	761.19	0.0011185	2.20E-04	11.6284	0.9	336.864	761.19	9.91E-04	2.08E-04	11.6284
0.95	372.195	800.342	0.00116311	1.96E-04	11.9929	0.95	350.301	800.342	0.0010303	1.84E-04	11.9929
1	385.971	838.995	0.00120616	1.73E-04	12.3459	1	363.267	838.995	0.00106843	1.62E-04	12.3459
1.05	399.258	877.123	0.00124768	1.52E-04	12.688	1.05	375.772	877.123	0.00110521	1.41E-04	12.688
1.1	412.063	914.703	0.0012877	1.33E-04	13.0196	1.1	387.824	914.703	0.00114066	1.22E-04	13.0196
1.15	424.397	951.711	0.00132624	1.15E-04	13.3411	1.15	399.433	951.711	0.0011748	1.04E-04	13.3411
1.2	436.27	988.124	0.00136334	9.78E-05	13.6526	1.2	410.606	988.124	0.00120767	8.80E-05	13.6526
1.25	447.689	1023.92	0.00139903	8.23E-05	13.9546	1.25	421.355	1023.92	0.00123928	7.29E-05	13.9546
1.3	458.666	1059.08	0.00143333	6.81E-05	14.2472	1.3	431.685	1059.08	0.00126966	5.89E-05	14.2472
1.35	469.209	1093.57	0.00146628	5.47E-05	14.5307	1.35	441.608	1093.57	0.00129885	4.61E-05	14.5307
1.4	479.327	1127.38	0.0014979	4.26E-05	14.8052	1.4	451.131	1127.38	0.00132686	3.43E-05	14.8052
1.45	489.031	1160.49	0.00152822	3.15E-05	15.071	1.45	460.264	1160.49	0.00135372	2.34E-05	15.071
1.5	498.329	1192.87	0.00156728	2.12E-05	15.328	1.5	469.015	1192.87	0.00137946	1.35E-05	15.328
1.55	507.23	1224.5	0.00158509	1.18E-05	15.5766	1.55	477.393	1224.5	0.0014041	4.47E-06	15.5766
1.6	515.743	1255.37	0.0016117	3.39E-06	15.8168	1.6	485.406	1255.37	0.00142766	-3.64E-06	15.8168
1.65	523.88	1285.46	0.00163712	-4.32E-06	16.0487	1.65	493.063	1285.46	0.00145018	-1.11E-05	16.0487
1.7	531.646	1314.74	0.00166139	-1.13E-06	16.2724	1.7	500.373	1314.74	0.00147168	-1.77E-05	16.2724
1.75	539.052	1343.2	0.00168454	-1.74E-05	16.4879	1.75	507.344	1343.2	0.00149219	-2.35E-05	16.4879
1.8	546.108	1370.82	0.00170659	-2.28E-05	16.6955	1.8	513.984	1370.82	0.00151172	-2.86E-05	16.6955
1.85	552.82	1397.59	0.00172756	-2.77E-05	16.895	1.85	520.301	1397.59	0.0015303	-3.30E-05	16.895
1.9	559.198	1423.48	0.00174749	-3.16E-05	17.0867	1.9	526.304	1423.48	0.00154795	-3.68E-05	17.0867
1.95	565.251	1448.48	0.00176641	-3.53E-05	17.2705	1.95	532	1448.48	0.00156471	-4.01E-05	17.2705
2	570.985	1472.57	0.00178433	-3.81E-05	17.4464	2	537.398	1472.57	0.00158058	-4.28E-05	17.4464
2.05	576.411	1495.75	0.00180128	-4.04E-05	17.6147	2.05	542.504	1495.75	0.0015956	-4.47E-05	17.6147
2.1	581.534	1517.99	0.00181729	-4.21E-05	17.7752	2.1	547.326	1517.99	0.00160978	-4.63E-05	17.7752
2.15	586.363	1539.28	0.00183239	-4.35E-05	17.928	2.15	551.871	1539.28	0.00162315	-4.73E-05	17.928
2.2	590.906	1559.61	0.00184658	-4.41E-05	18.0731	2.2	556.147	1559.61	0.00163573	-4.79E-05	18.0731
2.25	595.168	1578.97	0.0018599	-4.48E-05	18.2107	2.25	560.159	1578.97	0.00164753	-4.79E-05	18.2107
2.3	599.158	1597.34	0.00187237	-4.43E-05	18.3406	2.3	563.913	1597.34	0.00165857	-4.76E-05	18.3406
2.35	602.881	1614.71	0.001884	-4.38E-05	18.4629	2.35	567.417	1614.71	0.00166887	-4.69E-05	18.4629
2.4	606.343	1631.07	0.00189482	-4.30E-05	18.5777	2.4	570.676	1631.07	0.00167846	-4.57E-05	18.5777
2.45	609.552	1646.41	0.00190485	-4.17E-05	18.6649	2.45	573.696	1646.41	0.00168734	-4.41E-05	18.6649
2.5	612.511	1660.72	0.0019141	-4.01E-05	18.7846	2.5	576.481	1660.72	0.00169553	-4.23E-05	18.7846
2.65	615.226	1674	0.00192258	-3.82E-05	18.8768	2.55	579.037	1674	0.00170305	-4.04E-05	18.8768
2.6	617.704	1686.23	0.00193032	-3.59E-05	18.9615	2.6	581.368	1686.23	0.00170991	-3.79E-05	18.9615
2.65	619.947	1697.4	0.00193733	-3.34E-05	19.0387	2.65	583.479	1697.4	0.00171612	-3.53E-05	19.0387
2.7	621.959	1707.52	0.00194362	-3.08E-05	19.1084	2.7	585.374	1707.52	0.00172169	-3.23E-05	19.1084
2.75	623.745	1716.56	0.0019492	-2.78E-05	19.1707	2.75	587.055	1716.56	0.00172663	-2.92E-05	19.1707
2.8	625.309	1724.64	0.00195409	-2.46E-05	19.2255	2.8	588.526	1724.64	0.00173096	-2.59E-05	19.2255
2.85	626.653	1731.43	0.00195829	-2.14E-05	19.2728	2.85	589.791	1731.43	0.00173468	-2.24E-05	19.2728
2.9	627.779	1737.25	0.00196181	-1.79E-05	19.3127	2.9	590.851	1737.25	0.00173778	-1.88E-05	19.3127
2.95	628.69	1741.98	0.00196466	-1.44E-05	19.3451	2.95	591.709	1741.98	0.00174032	-1.50E-05	19.3451
3	629.389	1745.62	0.00196684	-1.07E-05	19.3701	3	592.365	1745.62	0.00174225	-1.13E-05	19.3701
3.05	629.875	1748.17	0.00196836	-7.14E-06	19.3876	3.05	592.823	1748.17	0.0017436	-7.43E-06	19.3876
3.1	530.15	1749.62	0.00196922	-3.28E-06	19.3977	3.1	593.082	1749.62	0.00174436	-3.38E-06	19.3977
3.15	630.215	1749.98	0.00196942	3.34E-07	19.4004	3.15	593.144	1749.98	0.00174454	4.89E-07	19.4004
3.2	630.07	1749.25	0.00196897	4.34E-06	19.3956	3.2	593.007	1749.25	0.00174414	4.48E-06	19.3956
3.25	629.715	1747.43	0.00196786	7.92E-06	19.3834	3.25	592.673	1747.43	0.00174315	8.35E-06	19.3834
3.3	629.148	1744.51	0.00196609	1.16E-05	19.3637	3.3	592.139	1744.51	0.00174159	1.23E-05	19.3637
3.35	628.369	1740.51	0.00196365	1.52E-05	19.3366	3.35	591.406	1740.51	0.00173943	1.60E-05	19.3366
3.4	627.376	1735.41	0.00196055	1.88E-05	19.3021	3.4	590.472	1735.41	0.00173668	1.97E-05	19.3021
3.45	626.168	1729.23	0.00195678	2.24E-05	19.2601	3.45	589.334	1729.23	0.00173334	2.33E-05	19.2601
3.5	624.741	1721.98	0.00195232	2.52E-05	19.2106	3.5	587.992	1721.98	0.00172939	2.67E-05	19.2106

L1=0.35						L3=0.12					
T	FHEEL	F	Q2	P2	ALPHA	T	FHEEL	F	Q2	P2	ALPHA
0	0	0	0	0	0	0	0	0	0	0	0
0.05	25.9296	43.7454	7.41E-05	0.00203515	1.97442	0.05	24.432	43.7454	7.40E-05	0.00173682	1.76853
0.1	47.4127	87.4635	1.35E-04	0.00148046	3.0151	0.1	45.261	87.4635	1.37E-04	0.00123648	2.73636
0.15	69.4544	131.127	1.98E-04	0.00122279	3.90145	0.15	56.3541	131.127	2.01E-04	0.00102097	3.54617
0.2	90.7967	174.708	2.59E-04	0.0010271	4.67469	0.2	86.7088	174.708	2.63E-04	8.67E-04	4.25024
0.25	111.428	218.181	3.18E-04	8.85E-04	5.37107	0.25	106.398	218.181	3.22E-04	7.65E-04	4.88423
0.3	131.402	261.517	3.75E-04	7.75E-04	6.0119	0.3	125.451	261.517	3.80E-04	6.70E-04	5.46754
0.35	150.749	304.689	4.31E-04	6.86E-04	6.60961	0.35	143.899	304.689	4.35E-04	6.00E-04	6.01154
0.4	169.493	347.671	4.84E-04	6.11E-04	7.17231	0.4	161.769	347.671	4.90E-04	5.42E-04	6.52362
0.45	187.656	390.436	5.35E-04	5.47E-04	7.7056	0.45	179.08	390.436	5.43E-04	4.92E-04	7.00893
0.5	205.265	432.957	5.86E-04	4.91E-04	8.21357	0.5	195.847	432.957	5.93E-04	4.48E-04	7.47118
0.55	222.304	475.207	6.35E-04	4.41E-04	8.69932	0.55	212.087	475.207	6.43E-04	4.09E-04	7.91319
0.6	238.817	517.16	6.82E-04	3.97E-04	9.16522	0.6	227.81	517.16	6.90E-04	3.73E-04	8.33713
0.65	254.805	558.79	7.28E-04	3.57E-04	9.61316	0.65	243.029	558.79	7.35E-04	3.42E-04	8.74472
0.7	270.279	600.071	7.72E-04	3.20E-04	10.0447	0.7	257.755	600.071	7.81E-04	3.13E-04	9.13735
0.75	285.25	640.977	8.15E-04	2.87E-04	10.461	0.75	271.997	640.977	8.24E-04	2.86E-04	9.51617
0.8	299.728	681.482	8.56E-04	2.56E-04	10.8632	0.8	285.765	681.482	8.56E-04	2.62E-04	9.88211
0.85	313.721	721.561	8.96E-04	2.28E-04	11.2521	0.85	299.068	721.561	9.06E-04	2.39E-04	10.235
0.9	327.24	761.19	9.35E-04	2.03E-04	11.6284	0.9	311.915	761.19	9.45E-04	2.18E-04	10.5784
0.95	340.293	800.342	9.72E-04	1.79E-04	11.9929	0.95	324.316	800.342	9.83E-04	1.99E-04	10.91
1	352.888	838.995	0.00100825	1.57E-04	12.3459	1	336.277	838.995	0.00101902	1.81E-04	11.2312
1.05	365.036	877.123	0.00104296	1.35E-04	12.688	1.05	347.808	877.123	0.00105396	1.64E-04	11.5425
1.1	376.744	914.703	0.00107641	1.17E-04	13.0196	1.1	358.918	914.703	0.00108763	1.49E-04	11.8442
1.15	388.02	951.711	0.00110863	9.98E-05	13.3411	1.15	369.614	951.711	0.00112004	1.34E-04	12.1366
1.2	398.875	988.124	0.00113964	8.37E-05	13.6526	1.2	379.906	988.124	0.00115123	1.20E-04	12.4201
1.25	409.316	1023.92	0.00116947	6.88E-05	13.9546	1.25	369.801	1023.92	0.00118121	1.08E-04	12.6949
1.3	419.352	1059.08	0.00119815	5.50E-05	14.2472	1.3	399.308	1059.08	0.00121002	9.60E-05	12.9611
1.35	428.991	1093.57	0.00122569	4.23E-05	14.5307	1.35	408.435	1093.57	0.00123768	8.48E-05	13.219
1.4	438.242	1127.35	0.00125212	3.06E-05	14.8052	1.4	417.192	1127.35	0.00126422	7.46E-05	13.4688
1.45	447.114	1160.49	0.00127747	1.99E-05	15.071	1.45	425.585	1160.49	0.00128965	6.52E-05	13.7106
1.5	455.615	1192.87	0.00130176	1.02E-05	15.328	1.5	433.623	1192.87	0.00131401	5.64E-05	13.9445
1.55	463.753	1224.5	0.00132501	1.28E-05	15.5756	1.55	441.315	1224.5	0.00133732	4.82E-05	14.1706
1.6	471.537	1265.37	0.00134725	-6.81E-05	15.8168	1.6	448.669	1265.37	0.0013596	4.08E-05	14.3691
1.65	478.975	1285.46	0.0013685	-1.40E-05	16.0487	1.65	455.692	1285.46	0.00138089	3.38E-05	14.6001
1.7	486.076	1314.74	0.00138879	-2.04E-05	16.2724	1.7	462.394	1314.74	0.00140119	2.75E-05	14.8036
1.75	492.848	1343.2	0.00140814	-2.61E-05	16.4879	1.75	468.781	1343.2	0.00142055	2.18E-05	14.9998
1.8	499.298	1370.82	0.00142657	-3.11E-05	16.6955	1.8	474.863	1370.82	0.00143898	1.56E-05	15.1888
1.85	506.435	1397.59	0.0014441	-3.55E-05	16.895	1.85	480.646	1397.59	0.0014565	1.18E-05	15.3702
1.9	511.267	1423.48	0.00146076	-3.93E-05	17.0867	1.9	486.138	1423.48	0.00147315	7.56E-05	15.5445
1.95	516.8	1448.48	0.00147657	-4.23E-05	17.2706	1.95	491.347	1448.48	0.00148893	3.74E-05	15.7118
2	522.044	1472.57	0.00149155	-4.48E-05	17.4464	2	496.28	1472.57	0.00150388	3.91E-07	15.8719
2.05	527.004	1495.75	0.00150573	-4.65E-05	17.6147	2.05	500.945	1495.75	0.00151802	-2.59E-05	16.0249
2.1	531.688	1517.99	0.00151911	-4.80E-05	17.7752	2.1	505.348	1517.99	0.00153135	-5.11E-05	16.171
2.15	536.104	1539.28	0.00153172	-4.90E-05	17.928	2.15	509.496	1539.28	0.00154393	-7.31E-05	16.31
2.2	540.257	1559.61	0.00154359	-4.95E-05	18.0731	2.2	513.395	1559.61	0.00155574	-9.07E-05	16.4421
2.25	544.154	1578.97	0.00155473	-4.94E-05	18.2107	2.25	517.053	1578.97	0.00156683	-1.06E-05	16.5672
2.3	547.802	1597.34	0.00156515	-4.90E-05	18.3406	2.3	520.474	1597.34	0.0015772	-1.17E-05	16.6854
2.35	551.206	1614.71	0.00157487	-4.82E-05	18.4629	2.35	523.656	1614.71	0.00158687	-1.26E-05	16.7967
2.4	554.371	1631.07	0.00158392	-4.70E-05	18.5777	2.4	526.633	1631.07	0.00159586	-1.31E-05	16.9011
2.45	557.304	1646.41	0.0015923	-4.54E-05	18.6849	2.45	529.35	1646.41	0.00160418	-1.35E-05	16.9987
2.5	560.01	1660.72	0.00160003	-4.35E-05	18.7846	2.5	531.914	1660.72	0.00161186	-1.35E-05	17.0894
2.55	562.493	1674	0.00160712	-4.13E-05	18.8768	2.55	534.235	1674	0.0016189	-1.34E-05	17.1733
2.6	564.768	1686.23	0.00161359	-3.88E-05	18.9615	2.6	536.357	1686.23	0.00162632	-1.29E-05	17.2504
2.65	566.808	1697.4	0.00161945	-3.61E-05	19.0387	2.65	538.275	1697.4	0.00163114	-1.24E-05	17.3206
2.7	568.646	1707.52	0.00162471	-3.31E-05	19.1084	2.7	539.995	1707.52	0.00163635	-1.16E-05	17.384
2.75	570.282	1716.56	0.00162935	-2.98E-05	19.1707	2.75	541.522	1716.56	0.00164098	-1.08E-05	17.4407
2.8	571.711	1724.54	0.00163346	-2.64E-05	19.2255	2.8	542.858	1724.54	0.00164502	-9.68E-05	17.4905
2.85	572.94	1731.43	0.00163697	-2.28E-05	19.2728	2.85	544.006	1731.43	0.0016485	-8.44E-05	17.5336
2.9	573.969	1737.25	0.00163991	-1.91E-05	19.3127	2.9	544.967	1737.25	0.00165141	-7.22E-05	17.5699
2.95	574.803	1741.98	0.00164229	-1.53E-05	19.3451	2.95	545.745	1741.98	0.00165377	-5.87E-05	17.5994
3	575.441	1745.62	0.00164412	-1.15E-05	19.3701	3	546.341	1745.62	0.00165558	-4.35E-05	17.6221
3.05	575.888	1748.17	0.00164539	-7.59E-05	19.3876	3.05	546.755	1748.17	0.00165683	-2.93E-05	17.6381
3.1	576.137	1749.62	0.00164611	-3.58E-05	19.3977	3.1	546.99	1749.62	0.00165756	-1.37E-05	17.5473
3.15	576.197	1749.98	0.00164628	4.56E-07	19.4004	3.15	547.046	1749.98	0.00165771	9.89E-08	17.6497
3.2	576.064	1749.25	0.0016459	4.54E-05	19.3956	3.2	546.921	1749.25	0.00165734	1.78E-05	17.6454
3.25	575.739	1747.43	0.00164497	8.47E-05	19.3834	3.25	546.617	1747.43	0.00165642	3.15E-05	17.6343
3.3	575.221	1744.51	0.00164349	1.24E-05	19.3637	3.3	546.133	1744.51	0.00165495	4.72E-05	17.6164
3.35	574.509	1740.51	0.00154145	1.64E-05	19.3366	3.35	545.467	1740.51	0.00165293	6.09E-05	17.6918
3.4	573.601	1735.41	0.00163886	2.01E-05	19.302	3.4	544.619	1735.41	0.00165036	7.50E-05	17.5603
3.45	572.496	1729.23	0.0016357	2.38E-05	19.2601	3.45	543.687	1729.23	0.00164723	8.70E-05	17.5221
3.5	571.192	1721.98	0.00163198	2.72E-05	19.2106	3.5	542.357	1721.98	0.00164354	9.86E-05	17.4772

L3=0.13						L3=0.15					
T	FHEEL	F	Q2	P2	ALPHA	T	FHEEL	F	Q2	P2	ALPHA
0	0	0	0	0	0	0	0	0	0	0	0
0.05	25.9319	43.7454	7.86E-05	0.00189642	1.87208	0.05	29.0988	43.7454	8.82E-05	0.00224535	2.07612
0.1	47.7631	87.4635	1.45E-04	0.00135768	2.87755	0.1	52.8141	87.4635	1.60E-04	0.00162863	3.14963
0.15	70.0088	131.127	2.12E-04	0.00113145	3.72645	0.15	77.3413	131.127	2.34E-04	0.00135558	4.07171
0.2	91.4963	174.708	2.77E-04	9.55E-04	4.46561	0.2	101.114	174.708	3.05E-04	0.00113693	4.87809
0.25	112.28	218.181	3.40E-04	8.29E-04	5.13126	0.25	124.105	218.181	3.76E-04	9.75E-04	5.60437
0.3	132.394	261.517	4.01E-04	7.32E-04	5.74376	0.3	146.364	261.517	4.44E-04	8.52E-04	6.27275
0.35	151.874	304.689	4.60E-04	6.52E-04	6.31502	0.35	167.928	304.689	5.09E-04	7.51E-04	6.8962
0.4	170.745	347.671	5.17E-04	5.85E-04	6.85278	0.4	188.826	347.671	5.72E-04	6.68E-04	7.48313
0.46	189.028	390.436	5.73E-04	5.28E-04	7.36244	0.45	209.08	390.436	6.34E-04	5.94E-04	8.03941
0.5	205.739	432.957	6.26E-04	4.78E-04	7.84789	0.5	228.708	432.957	6.93E-04	5.30E-04	8.56929
0.55	223.895	475.207	6.78E-04	4.33E-04	8.3121	0.55	247.727	475.207	7.51E-04	4.74E-04	9.07599
0.6	240.508	517.16	7.29E-04	3.94E-04	8.75733	0.6	268.15	517.16	8.07E-04	4.24E-04	9.562
0.65	255.59	558.79	7.78E-04	3.68E-04	9.1854	0.65	283.992	558.79	8.61E-04	3.79E-04	10.0293
0.7	272.153	600.071	8.25E-04	3.25E-04	9.59776	0.7	301.265	600.071	9.13E-04	3.35E-04	10.4794
0.75	287.207	640.977	8.70E-04	2.95E-04	9.99561	0.75	317.979	640.977	9.64E-04	3.00E-04	10.9137
0.8	301.762	681.482	9.14E-04	2.67E-04	10.3799	0.8	334.145	681.482	0.00101255	2.68E-04	11.3333
0.85	315.828	721.551	9.57E-04	2.42E-04	10.7516	0.85	349.775	721.551	0.00105992	2.34E-04	11.739
0.9	329.414	761.19	9.98E-04	2.18E-04	11.1112	0.9	364.877	761.19	0.00110569	2.05E-04	12.1316
0.95	342.528	800.342	0.00103797	1.96E-04	11.4595	0.95	379.462	800.342	0.00114989	1.78E-04	12.5117
1	355.182	838.995	0.00107631	1.76E-04	11.7969	1	393.54	838.995	0.00119255	1.54E-04	12.88
1.05	357.352	877.123	0.00111328	1.68E-04	12.1235	1.05	407.12	877.123	0.0012337	1.31E-04	13.2369
1.1	379.135	914.703	0.0011489	1.40E-04	12.4407	1.1	420.212	914.703	0.00127337	1.09E-04	13.6829
1.15	390.459	951.711	0.00118321	1.24E-04	12.7478	1.15	432.825	951.711	0.00131159	8.99E-05	13.9182
1.2	401.353	988.124	0.00121622	1.09E-04	13.0456	1.2	444.969	988.124	0.00134839	7.19E-05	14.2432
1.25	411.83	1023.92	0.00124797	9.47E-05	13.3341	1.25	456.653	1023.92	0.0013838	5.52E-05	14.5682
1.3	421.898	1059.08	0.00127848	8.19E-05	13.6137	1.3	467.887	1059.08	0.00141784	3.99E-05	14.8635
1.35	431.566	1093.57	0.00130778	6.98E-05	13.8846	1.35	478.68	1093.57	0.00145054	2.59E-05	15.1592
1.4	440.843	1127.35	0.00133589	5.87E-05	14.147	1.4	489.041	1127.35	0.00148194	1.30E-05	15.4456
1.45	449.735	1160.49	0.00136284	4.84E-05	14.4009	1.45	498.98	1160.49	0.00151206	1.40E-06	15.7228
1.5	458.256	1192.87	0.00138865	3.90E-05	14.6466	1.5	508.507	1192.87	0.00154093	-9.39E-05	15.991
1.55	466.409	1224.5	0.00141336	3.03E-05	14.8841	1.55	517.63	1224.5	0.00156858	-1.89E-05	16.2503
1.6	474.207	1255.37	0.00143699	2.24E-05	15.1135	1.6	526.368	1255.37	0.00159503	-2.76E-05	16.5008
1.65	481.656	1285.46	0.00145956	1.52E-05	15.3352	1.65	534.702	1285.46	0.00162031	-3.53E-05	16.7427
1.7	488.765	1314.74	0.00146111	8.52E-05	15.5489	1.7	542.689	1314.74	0.00164445	-4.21E-05	16.9761
1.75	495.542	1343.2	0.00150164	2.72E-05	15.7549	1.75	550.269	1343.2	0.00168748	-4.82E-05	17.201
1.8	501.996	1370.82	0.0015212	-2.67E-05	15.9532	1.8	557.511	1370.82	0.00168943	-5.33E-05	17.4174
1.85	508.135	1397.59	0.0015398	-7.34E-05	16.1439	1.85	564.403	1397.59	0.00171031	-5.77E-05	17.6256
1.9	513.967	1423.48	0.00155746	-1.15E-05	16.3271	1.9	570.954	1423.48	0.00173016	-6.13E-05	17.8256
1.95	519.499	1448.48	0.00157424	-1.51E-05	16.5027	1.95	577.172	1448.48	0.00174901	-6.43E-05	18.0173
2	524.74	1472.57	0.00159012	-1.82E-05	16.6709	2	583.066	1472.57	0.00176687	-6.68E-05	18.2009
2.05	529.696	1495.75	0.00160514	-2.08E-05	16.8316	2.05	588.644	1495.75	0.00178377	-6.81E-05	18.3764
2.1	534.375	1517.99	0.00161932	-2.30E-05	16.985	2.1	593.912	1517.99	0.00179973	-6.92E-05	18.5438
2.15	538.784	1539.28	0.00163268	-2.46E-05	17.131	2.15	598.88	1539.28	0.00181479	-6.96E-05	18.7032
2.2	542.93	1559.61	0.00164524	-2.60E-05	17.2697	2.2	603.554	1559.61	0.00182895	-6.95E-05	18.8546
2.25	546.82	1578.97	0.00165703	-2.69E-05	17.4011	2.25	607.941	1578.97	0.00184225	-6.89E-05	18.9981
2.3	550.46	1597.34	0.00166805	-2.75E-05	17.5253	2.3	612.049	1597.34	0.00185469	-6.76E-05	19.1336
2.35	553.856	1614.71	0.00167835	-2.77E-05	17.6422	2.35	615.883	1614.71	0.00186631	-6.61E-05	19.2613
2.4	557.013	1631.07	0.00168792	-2.74E-05	17.7519	2.4	619.45	1631.07	0.00187712	-6.39E-05	19.351
2.45	559.937	1646.41	0.00169678	-2.70E-05	17.8544	2.46	622.755	1646.41	0.00188714	-6.15E-05	19.4928
2.5	562.635	1660.72	0.00170495	-2.64E-05	17.9496	2.5	625.806	1680.72	0.00189638	-5.86E-05	19.5969
2.55	566.11	1674	0.00171245	-2.52E-05	18.0377	2.55	628.605	1674	0.00190487	-5.55E-05	19.693
2.6	567.366	1686.23	0.00171929	-2.41E-05	18.1187	2.6	631.16	1686.23	0.00191261	-5.18E-05	19.7814
2.65	569.409	1697.4	0.00172548	-2.25E-05	18.1924	2.65	633.473	1697.4	0.00191961	-4.81E-05	19.8619
2.7	571.242	1707.52	0.00173104	-2.08E-05	18.2591	2.7	635.549	1707.52	0.00192591	-4.40E-05	19.9346
2.75	572.868	1716.55	0.00173597	-1.89E-05	18.3186	2.75	637.392	1716.55	0.00193149	-3.95E-05	19.9996
2.8	574.292	1724.54	0.00174028	-1.69E-05	18.3709	2.8	639.006	1724.54	0.00193638	-3.51E-05	20.0567
2.85	575.515	1731.43	0.00174398	-1.47E-05	18.4161	2.85	640.393	1731.43	0.00194058	-3.03E-05	20.1051
2.9	576.54	1737.25	0.00174709	-1.23E-05	18.4542	2.9	641.555	1737.25	0.00194411	-2.53E-05	20.1477
2.95	577.369	1741.98	0.0017496	-1.00E-05	18.4852	2.95	642.496	1741.98	0.00194696	-2.04E-05	20.1815
3	578.005	1745.62	0.00175153	-7.37E-05	18.5091	3	643.217	1745.62	0.00194914	-1.51E-05	20.2076
3.05	578.447	1748.17	0.00175287	-4.93E-05	18.5259	3.05	643.719	1748.17	0.00195066	-9.92E-05	20.2268
3.1	578.697	1749.62	0.00175353	-2.22E-05	18.5355	3.1	644.004	1749.62	0.00195153	-4.61E-05	20.2364
3.15	578.756	1749.98	0.00175381	3.34E-07	18.5381	3.15	644.071	1749.98	0.00195173	6.69E-07	20.2391
3.2	578.624	1749.25	0.00175341	2.89E-05	18.5335	3.2	843.922	1749.25	0.00195128	6.05E-05	20.2342
3.25	578.3	1747.43	0.00175243	5.68E-05	18.5218	3.25	643.555	1747.43	0.00195017	1.13E-05	20.2214
3.3	577.784	1744.51	0.00175086	8.04E-05	18.5031	3.3	642.97	1744.51	0.00194839	1.65E-05	20.2009
3.35	577.075	1740.51	0.00174871	1.05E-05	18.4772	3.35	642.168	1740.51	0.00194596	2.16E-05	20.1726
3.4	576.171	1735.41	0.00174597	1.30E-05	18.4442	3.4	641.142	1735.41	0.00194285	2.68E-05	20.1366
3.45	575.071	1729.23	0.00174264	1.51E-05	18.404	3.45	639.895	1729.23	0.00193908	3.15E-05	20.0927
3.5	573.772	1721.98	0.0017357	1.73E-05	18.3568	3.5	638.423	1721.98	0.00193461	3.53E-05	20.0411

L3=0.16						PHI=0.2269					
T	FHEEL	F	Q2	P2	ALPHA	T	FHEEL	F	Q2	P2	ALPHA
0	0	0	0	0	0	0	0	0	0	0	0
0.05	30.7808	43.7454	9.33E-05	0.00244576	2.17722	0.05	28.7335	43.7454	8.71E-05	0.00239012	1.97454
0.1	56.3757	87.4635	1.68E-04	0.00175931	3.28159	0.1	52.6361	87.4635	1.60E-04	0.00174899	3.01513
0.15	81.0174	131.127	2.46E-04	0.001467	4.2377	0.15	77.2111	131.127	2.34E-04	0.00146327	3.90145
0.2	105.941	174.708	3.21E-04	0.00122803	5.07631	0.2	101.028	174.708	3.06E-04	0.00124425	4.67489
0.25	130.044	218.181	3.94E-04	0.00104769	5.63175	0.25	124.099	218.181	3.76E-04	0.00108376	5.37107
0.3	153.384	261.517	4.65E-04	9.10E-04	6.52698	0.3	146.471	261.517	4.44E-04	9.61E-04	6.0119
0.35	176.001	304.689	5.33E-04	7.98E-04	7.1755	0.35	168.175	304.689	5.10E-04	8.62E-04	6.60962
0.4	197.924	347.671	6.00E-04	7.04E-04	7.78605	0.4	189.238	347.671	5.73E-04	7.78E-04	7.17231
0.45	219.175	390.436	6.64E-04	6.23E-04	8.36474	0.45	209.68	390.436	6.35E-04	7.07E-04	7.7056
0.5	239.774	432.957	7.27E-04	5.52E-04	8.91597	0.5	229.518	432.957	6.96E-04	6.44E-04	8.21357
0.55	259.737	475.207	7.87E-04	4.90E-04	9.44309	0.55	248.766	475.207	7.54E-04	5.88E-04	8.69932
0.6	279.08	517.16	8.46E-04	4.34E-04	9.94868	0.6	267.436	517.16	8.10E-04	5.39E-04	9.16522
0.65	297.817	558.79	9.02E-04	3.84E-04	10.4348	0.65	285.546	558.79	8.65E-04	4.94E-04	9.61316
0.7	315.959	600.071	9.57E-04	3.38E-04	10.9031	0.7	303.099	600.071	9.18E-04	4.53E-04	10.0447
0.75	333.519	640.977	0.00101066	2.97E-04	11.3549	0.75	320.109	640.977	9.70E-04	4.15E-04	10.461
0.8	350.508	681.482	0.00106214	2.59E-04	11.7914	0.8	336.584	681.482	0.00101995	3.81E-04	10.8632
0.85	366.936	721.561	0.00111193	2.24E-04	12.2134	0.85	352.534	721.561	0.00106828	3.49E-04	11.2521
0.9	382.814	761.19	0.00116004	1.92E-04	12.6219	0.9	367.957	761.19	0.00111505	3.19E-04	11.6284
0.95	398.152	800.342	0.00120652	1.62E-04	13.0174	0.95	382.893	800.342	0.00116028	2.92E-04	11.9929
1	412.96	838.995	0.0012514	1.35E-04	13.4005	1	397.321	838.995	0.001204	2.66E-04	12.3459
1.05	427.249	877.123	0.00129469	1.10E-04	13.7718	1.05	411.257	877.123	0.00124623	2.43E-04	12.688
1.1	441.027	914.703	0.00133645	8.69E-05	14.1317	1.1	424.713	914.703	0.00128701	2.20E-04	13.0195
1.15	454.306	951.711	0.00137668	6.57E-05	14.4806	1.15	437.694	951.711	0.00132636	2.00E-04	13.3411
1.2	467.094	988.124	0.00141544	4.61E-05	14.8187	1.2	450.212	988.124	0.00136428	1.81E-04	13.6526
1.25	479.401	1023.92	0.00145273	2.81E-05	15.1464	1.25	462.272	1023.92	0.00140082	1.63E-04	13.9546
1.3	491.237	1069.08	0.0014886	1.17E-05	15.464	1.3	473.885	1069.08	0.00143601	1.46E-04	14.2472
1.35	502.612	1093.57	0.00152307	-3.41E-06	15.7717	1.35	485.058	1093.57	0.00146987	1.30E-04	14.5307
1.4	513.536	1127.38	0.00155617	-1.71E-05	16.0696	1.4	495.8	1127.38	0.00150242	1.16E-04	14.8052
1.45	524.018	1160.49	0.00156793	-2.95E-05	16.358	1.45	505.12	1160.49	0.0015337	1.03E-04	15.071
1.5	534.068	1192.87	0.00161839	-4.07E-05	16.637	1.5	516.025	1192.87	0.00156371	8.99E-05	15.328
1.55	543.695	1224.5	0.00164756	-5.07E-05	16.9068	1.55	525.526	1224.5	0.0015925	7.85E-05	15.5766
1.6	562.908	1255.37	0.00167546	-5.95E-05	17.1674	1.6	534.628	1255.37	0.00162009	6.78E-05	15.8168
1.65	561.718	1285.46	0.00170218	-6.75E-05	17.4191	1.65	543.342	1285.46	0.00164649	5.60E-05	16.0487
1.7	570.134	1314.74	0.00172768	-7.42E-05	17.6619	1.7	561.675	1314.74	0.00167174	4.89E-05	16.2724
1.75	578.164	1343.2	0.00175201	-8.02E-05	17.8958	1.75	559.636	1343.2	0.00169587	4.06E-05	16.4879
1.8	585.818	1370.82	0.00177521	-8.51E-05	18.1211	1.8	567.233	1370.82	0.00171889	3.30E-05	16.6955
1.85	593.105	1397.59	0.00179729	-8.93E-05	18.3376	1.85	574.473	1397.59	0.00174083	2.61E-05	16.895
1.9	600.034	1423.48	0.00181829	-9.24E-05	18.5456	1.9	561.365	1423.48	0.00176171	1.99E-05	17.0867
1.95	606.614	1448.48	0.00183822	-9.49E-05	18.7451	1.95	567.915	1448.48	0.00178156	1.43E-05	17.2706
2	612.851	1472.57	0.00185713	-9.65E-05	18.9361	2	594.133	1472.57	0.0018004	9.33E-06	17.4464
2.05	618.757	1495.75	0.00187602	-9.75E-05	19.1187	2.05	600.025	1495.75	0.00181826	4.99E-06	17.6147
2.1	624.336	1517.99	0.00189193	-9.76E-05	19.2929	2.1	605.599	1517.99	0.00183515	1.06E-06	17.7752
2.15	629.599	1639.28	0.00190788	-9.74E-05	19.4587	2.15	610.861	1639.28	0.00185109	-2.27E-06	17.928
2.2	634.553	1559.61	0.00192289	-9.62E-05	19.6162	2.2	615.818	1559.61	0.00186611	-5.13E-06	18.0731
2.25	639.203	1578.97	0.00193698	-9.46E-05	19.7655	2.25	620.477	1578.97	0.00188023	-7.57E-06	18.2107
2.3	643.559	1597.34	0.00195018	-9.23E-05	19.9065	2.3	624.844	1597.34	0.00189347	-9.51E-06	18.3406
2.35	647.626	1614.71	0.0019625	-8.96E-05	20.0393	2.35	628.925	1614.71	0.00190583	-1.11E-05	18.4629
2.4	651.41	1631.07	0.00197397	-8.63E-05	20.1838	2.4	632.726	1631.07	0.00191735	-1.23E-05	18.5777
2.45	654.919	1646.41	0.0019846	-8.26E-05	20.2602	2.45	636.253	1646.41	0.00192804	-1.29E-05	18.6849
2.5	658.157	1660.72	0.00199442	-7.85E-05	20.3884	2.5	639.51	1660.72	0.00193791	-1.34E-05	18.7646
2.55	661.13	1674	0.00200342	-7.39E-05	20.4885	2.55	642.602	1674	0.00194698	-1.37E-05	18.8768
2.6	663.842	1686.23	0.00201164	-6.89E-05	20.5804	2.6	645.235	1686.23	0.00195526	-1.35E-05	18.9615
2.65	666.3	1697.4	0.00201909	-6.36E-05	20.6642	2.65	647.712	1697.4	0.00196276	-1.30E-05	19.0387
2.7	668.506	1707.52	0.00202578	-5.79E-05	20.7398	2.7	649.936	1707.52	0.0019695	-1.24E-05	19.1084
2.75	670.485	1716.56	0.00203171	-5.23E-05	20.8074	2.75	651.913	1716.56	0.00197549	-1.17E-05	19.1707
2.8	672.18	1724.54	0.00203691	-4.60E-05	20.8668	2.8	653.645	1724.54	0.00198074	-1.05E-05	19.2256
2.85	673.654	1731.43	0.00204138	-3.99E-05	20.9182	2.85	655.134	1731.43	0.00198525	-9.38E-06	19.2728
2.9	674.891	1737.25	0.00204512	-3.31E-05	20.9614	2.9	655.383	1737.25	0.00198904	-7.87E-06	19.3127
2.95	675.891	1741.98	0.00204815	-2.65E-05	20.9966	2.95	657.394	1741.98	0.0019921	-6.56E-06	19.3451
3	676.658	1745.62	0.00205048	-2.00E-05	21.0237	3	658.169	1745.62	0.00199445	-4.84E-06	19.3701
3.05	677.192	1748.17	0.0020521	-1.29E-05	21.0427	3.05	658.71	1748.17	0.00199609	-3.22E-06	19.3876
3.1	677.495	1749.62	0.00205301	-5.94E-06	21.0537	3.1	659.016	1749.62	0.00199702	-1.54E-06	19.3977
3.15	677.567	1749.98	0.00205323	8.65E-07	21.0566	3.15	659.069	1749.98	0.00199724	1.18E-07	19.4004
3.2	677.408	1749.25	0.00205275	7.91E-06	21.0514	3.2	658.929	1749.25	0.00199575	1.90E-06	19.3956
3.25	677.018	1747.43	0.00205157	1.48E-05	21.0381	3.25	658.534	1747.43	0.00199556	3.63E-06	19.3834
3.3	676.397	1744.51	0.00204969	2.16E-05	21.0168	3.3	657.906	1744.51	0.00199365	5.13E-06	19.3637
3.35	675.542	1740.51	0.0020471	2.84E-05	20.9873	3.35	657.043	1740.51	0.00199104	6.75E-06	19.3366
3.4	674.463	1735.41	0.0020438	3.50E-05	20.9498	3.4	655.943	1735.41	0.0019877	8.15E-06	19.3021
3.45	673.128	1729.23	0.00203978	4.14E-05	20.9042	3.45	654.804	1729.23	0.00198365	9.48E-06	19.2601
3.5	671.564	1721.98	0.00203504	4.77E-05	20.8505	3.5	653.025	1721.98	0.00197886	1.06E-05	19.2106

PHI=0.2443						PHI=0.2793					
T	FHEEL	F	Q2	P2	ALPHA	T	FHEEL	F	Q2	P2	ALPHA
0	0	0	0	0	0	0	0	0	0	0	0
0.05	28.1121	43.7454	8.52E-05	0.00222801	1.97452	0.05	26.8553	43.7454	8.14E-05	0.00189995	1.97447
0.1	51.4625	87.4635	1.56E-04	0.00162426	3.01513	0.1	49.0916	87.4635	1.49E-04	0.00137227	3.01511
0.15	75.4496	131.127	2.29E-04	0.00135377	3.90145	0.15	71.8881	131.127	2.18E-04	0.00113255	3.90145
0.2	96.6735	174.708	2.99E-04	0.00114569	4.67469	0.2	93.9168	174.708	2.85E-04	9.47E-04	4.67469
0.25	121.153	218.181	3.67E-04	9.93E-04	5.37107	0.25	115.204	218.181	3.49E-04	8.11E-04	5.37107
0.3	142.934	261.517	4.33E-04	8.77E-04	6.0119	0.3	135.79	261.517	4.11E-04	7.07E-04	6.0119
0.35	184.047	304.689	4.97E-04	7.82E-04	6.60962	0.35	155.713	304.689	4.72E-04	6.22E-04	6.60961
0.4	184.521	347.671	5.59E-04	7.03E-04	7.17231	0.4	175	347.671	5.30E-04	5.51E-04	7.17231
0.45	204.376	390.436	6.19E-04	6.35E-04	7.7056	0.45	193.673	390.436	5.87E-04	4.90E-04	7.7056
0.5	223.629	432.957	6.78E-04	5.75E-04	8.21357	0.5	211.75	432.957	6.42E-04	4.38E-04	8.21357
0.55	242.297	475.207	7.34E-04	5.22E-04	8.69932	0.55	229.247	475.207	6.95E-04	3.89E-04	8.69932
0.6	260.391	517.16	7.89E-04	4.75E-04	9.16522	0.6	245.18	517.16	7.45E-04	3.45E-04	9.15522
0.65	277.925	558.79	8.42E-04	4.32E-04	9.61316	0.65	262.56	558.79	7.96E-04	3.08E-04	9.61316
0.7	294.909	600.071	8.94E-04	3.93E-04	10.0447	0.7	278.4	600.071	8.44E-04	2.73E-04	10.0447
0.75	311.355	640.977	9.44E-04	3.57E-04	10.481	0.75	293.712	640.977	8.90E-04	2.41E-04	10.461
0.8	327.271	681.482	9.92E-04	3.25E-04	10.8632	0.8	308.506	681.482	9.35E-04	2.12E-04	10.8632
0.85	342.668	721.561	0.00103839	2.95E-04	11.2521	0.85	322.793	721.561	9.78E-04	1.86E-04	11.2521
0.9	387.555	761.19	0.0010835	2.67E-04	11.6284	0.9	336.583	761.19	0.00101995	1.61E-04	11.6284
0.95	371.941	800.342	0.00112709	2.41E-04	11.9929	0.95	349.885	800.342	0.00106026	1.38E-04	11.9929
1	385.836	838.995	0.0011692	2.17E-04	12.3459	1	362.709	838.995	0.00109912	1.17E-04	12.3459
1.05	399.247	877.123	0.00120984	1.95E-04	12.688	1.05	375.056	877.123	0.00113657	9.81E-05	12.688
1.1	412.184	914.703	0.00124904	1.74E-04	13.0198	1.1	386.965	914.703	0.00117262	8.03E-05	13.0198
1.15	424.656	951.711	0.00128684	1.55E-04	13.3411	1.15	398.415	951.711	0.00120732	6.38E-05	13.3411
1.2	436.672	988.124	0.00132325	1.37E-04	13.6526	1.2	409.425	988.124	0.00124068	4.86E-05	13.5526
1.25	448.24	1023.92	0.0013583	1.20E-04	13.9546	1.25	420.006	1023.92	0.00127274	3.47E-05	13.9546
1.3	459.369	1059.08	0.00139203	1.05E-04	14.2472	1.3	430.166	1059.08	0.00130353	2.18E-05	14.2472
1.35	470.068	1093.57	0.00142445	9.05E-05	14.5307	1.35	439.915	1093.57	0.00133308	1.01E-05	14.5307
1.4	480.345	1127.38	0.00145559	7.72E-05	14.8052	1.4	449.262	1127.38	0.0013614	-6.62E-07	14.8052
1.45	490.211	1160.49	0.00148549	6.60E-05	15.071	1.45	458.217	1160.49	0.00138854	-1.05E-05	15.071
1.5	499.673	1192.87	0.00151416	5.37E-05	15.328	1.5	466.79	1192.87	0.00141451	-1.94E-05	15.328
1.55	508.739	1224.5	0.00154163	4.34E-05	15.5766	1.55	474.988	1224.5	0.00143936	-2.73E-05	15.5766
1.6	517.419	1255.37	0.00156794	3.38E-05	15.8168	1.6	482.821	1255.37	0.00146309	-3.44E-05	15.8168
1.55	525.721	1285.45	0.00159309	2.52E-05	16.0487	1.65	490.299	1285.46	0.00148576	-4.07E-05	16.0487
1.7	533.654	1314.74	0.00161713	1.73E-05	16.2724	1.7	497.43	1314.74	0.00160737	-4.63E-05	16.2724
1.75	541.225	1343.2	0.00164008	1.00E-05	16.4879	1.75	504.224	1343.2	0.00152795	-5.12E-05	16.4879
1.8	548.445	1370.82	0.00166195	3.66E-05	16.6955	1.8	510.689	1370.82	0.00154754	-5.53E-05	16.6955
1.85	555.319	1397.59	0.00168279	-2.06E-06	16.895	1.85	516.833	1397.59	0.00156616	-5.87E-05	16.895
1.9	561.858	1423.48	0.0017026	-7.21E-05	17.0867	1.9	522.666	1423.48	0.00158384	-6.15E-05	17.0867
1.95	568.069	1448.48	0.00172142	-1.17E-05	17.2705	1.96	528.195	1448.48	0.00160059	-6.38E-05	17.2705
2	573.958	1472.57	0.00173927	-1.55E-05	17.4464	2	533.429	1472.57	0.00161645	-6.55E-05	17.4464
2.05	579.535	1495.75	0.00175617	-1.88E-05	17.6147	2.05	538.376	1495.75	0.00163144	-6.63E-05	17.6147
2.1	584.806	1517.99	0.00177214	-2.16E-05	17.7752	2.1	543.042	1517.99	0.00164558	-6.70E-05	17.7752
2.15	589.779	1539.28	0.00178721	-2.38E-05	17.928	2.15	547.437	1539.28	0.0016569	-6.71E-05	17.928
2.2	594.45	1559.61	0.00180139	-2.56E-05	18.0731	2.2	551.566	1559.61	0.00167141	-6.65E-05	18.0731
2.25	596.856	1578.97	0.00181472	-2.69E-05	18.2107	2.25	555.438	1578.97	0.00168315	-6.57E-05	18.2107
2.3	602.974	1597.34	0.00182719	-2.78E-05	18.3406	2.3	559.059	1597.34	0.00169412	-6.44E-05	18.3406
2.35	606.82	1614.71	0.00183885	-2.82E-05	18.4629	2.35	562.434	1614.71	0.00170435	-6.25E-05	18.4629
2.4	610.4	1631.07	0.0018497	-2.63E-05	18.5777	2.4	565.571	1631.07	0.00171385	-6.05E-05	18.5777
2.45	613.718	1646.41	0.00185975	-2.79E-05	18.6849	2.45	568.475	1646.41	0.00172265	-5.79E-05	18.6849
2.5	616.782	1660.72	0.00186904	-2.73E-05	18.7846	2.5	571.152	1660.72	0.00173076	-5.52E-05	18.7846
2.55	619.595	1674	0.00187756	-2.54E-05	18.8768	2.55	573.607	1674	0.0017382	-5.21E-05	18.8768
2.6	622.162	1686.23	0.00188534	-2.52E-05	18.9615	2.6	575.844	1686.23	0.00174498	-4.88E-05	18.9615
2.65	624.488	1697.4	0.00189239	-2.37E-05	19.0387	2.65	577.869	1697.4	0.00175112	-4.49E-05	19.0387
2.7	626.577	1707.52	0.00189872	-2.19E-05	19.1084	2.7	579.684	1707.52	0.00175662	-4.11E-05	19.1084
2.75	628.431	1716.66	0.00190434	-2.01E-05	19.1707	2.75	581.295	1716.66	0.0017615	-3.70E-05	19.1707
2.8	630.054	1724.54	0.00190926	-1.79E-05	19.2255	2.8	582.704	1724.54	0.00176577	-3.27E-05	19.2255
2.85	631.451	1731.43	0.00191349	-1.56E-05	19.2728	2.85	583.914	1731.43	0.00176944	-2.83E-05	19.2728
2.9	632.621	1737.25	0.00191703	-1.31E-05	19.3127	2.9	584.929	1737.25	0.00177251	-2.37E-05	19.3127
2.95	633.569	1741.96	0.00191991	-1.06E-05	19.3451	2.95	585.749	1741.96	0.001775	-1.89E-05	19.3451
3	634.295	1745.62	0.00192211	-7.99E-06	19.3701	3	586.377	1745.62	0.0017769	-1.41E-05	19.3701
3.05	634.801	1748.17	0.00192364	-5.17E-06	19.3876	3.05	586.814	1748.17	0.00177823	-9.22E-06	19.3876
3.1	635.088	1749.62	0.00192451	-2.45E-06	19.3977	3.1	587.062	1749.62	0.00177897	-4.29E-05	19.3977
3.15	635.156	1749.96	0.00192471	2.72E-07	19.4004	3.15	587.12	1749.96	0.00177915	6.49E-07	19.4004
3.2	635.005	1749.25	0.00192426	3.22E-06	19.3956	3.2	586.989	1749.25	0.00177876	5.62E-06	19.3956
3.25	634.636	1747.43	0.00192314	5.83E-06	19.3834	3.25	586.669	1747.43	0.00177779	1.04E-05	19.3834
3.3	634.047	1744.51	0.00192135	8.57E-06	19.3637	3.3	586.159	1744.51	0.00177624	1.54E-05	19.3637
3.35	633.237	1740.51	0.0019189	1.12E-05	19.3366	3.35	585.457	1740.51	0.00177411	2.02E-05	19.3366
3.4	632.206	1735.41	0.00191578	1.37E-05	19.302	3.4	584.563	1735.41	0.0017714	2.49E-05	19.3021
3.45	630.951	1729.23	0.00191197	1.61E-05	19.2601	3.45	583.474	1729.23	0.0017681	2.93E-05	19.2601
3.5	629.47	1721.98	0.00190748	1.84E-05	19.2106	3.5	582.188	1721.98	0.00176421	3.39E-05	19.2106

PHI=0.2957						KO=0.9, NU=1.52					
T	FHEEL	F	Q2	P2	ALPHA	T	FHEEL	F	Q2	P2	ALPHA
0	0	0	0	0	0	0	0	0	0	0	0
0.05	26.2275	43.7454	7.95E-05	0.00173599	1.97445	0.05	26.9894	43.7454	8.18E-05	0.00602467	2.85554
0.1	47.9074	87.4635	1.45E-04	0.00124652	3.01511	0.1	47.4907	87.4635	1.44E-04	0.00233235	5.26195
0.15	70.1096	131.127	2.12E-04	0.00102211	3.90145	0.15	68.1061	131.127	2.06E-04	0.00161808	7.04984
0.2	91.5427	174.708	2.77E-04	8.47E-04	4.67469	0.2	86.9742	174.708	2.64E-04	0.00115757	8.60148
0.25	112.238	218.181	3.40E-04	7.20E-04	5.37107	0.25	104.378	218.181	3.16E-04	8.15E-04	10.01
0.3	132.227	261.517	4.01E-04	6.22E-04	6.0119	0.3	120.403	261.517	3.65E-04	5.44E-04	11.3152
0.35	151.558	304.689	4.59E-04	5.42E-04	6.60961	0.35	135.139	304.689	4.10E-04	3.19E-04	12.5401
0.4	170.254	347.671	5.16E-04	4.75E-04	7.17231	0.4	148.652	347.671	4.50E-04	1.28E-04	13.6995
0.45	188.338	390.436	5.71E-04	4.17E-04	7.7056	0.45	161.002	390.436	4.88E-04	-3.80E-05	14.8036
0.5	205.83	432.957	6.24E-04	3.67E-04	8.21357	0.5	172.244	432.957	5.22E-04	-1.84E-04	15.86
0.55	222.746	475.207	6.75E-04	3.22E-04	8.69932	0.55	182.427	475.207	5.53E-04	-3.13E-04	16.8742
0.6	239.101	517.16	7.25E-04	2.82E-04	9.16522	0.6	191.599	517.16	5.81E-04	-4.29E-04	17.8505
0.65	254.909	558.79	7.72E-04	2.46E-04	9.61316	0.65	199.804	558.79	6.05E-04	-5.33E-04	18.7924
0.7	270.181	600.071	8.19E-04	2.14E-04	10.0447	0.7	207.085	600.071	6.28E-04	-6.26E-04	19.7025
0.75	284.93	640.977	8.63E-04	1.84E-04	10.461	0.75	213.483	640.977	6.47E-04	-7.10E-04	20.5832
0.8	299.167	681.482	9.07E-04	1.57E-04	10.8632	0.8	219.04	681.482	6.64E-04	-7.85E-04	21.4362
0.85	312.903	721.561	9.48E-04	1.31E-04	11.2521	0.85	223.794	721.561	6.78E-04	-8.53E-04	22.2632
0.9	326.149	761.19	9.88E-04	1.09E-04	11.6284	0.9	227.785	761.19	6.90E-04	-9.14E-04	23.0653
0.95	338.913	800.342	0.00102701	8.75E-05	11.9929	0.95	231.051	800.342	7.00E-04	-9.69E-04	23.8438
1	351.208	838.995	0.00106427	6.80E-05	12.3459	1	233.531	838.995	7.08E-04	-0.00101721	24.5995
1.05	363.042	877.123	0.00110013	5.02E-05	12.688	1.05	235.561	877.123	7.14E-04	-0.00105983	25.3333
1.1	374.426	914.703	0.00113462	3.38E-05	13.0195	1.1	238.878	914.703	7.18E-04	-0.0010971	26.0459
1.15	385.369	951.711	0.00116779	1.87E-05	13.3411	1.15	237.62	951.711	7.20E-04	-0.0011292	26.7378
1.2	395.882	986.124	0.00119964	4.84E-06	13.6526	1.2	237.822	986.124	7.21E-04	-0.00115649	27.4097
1.25	405.974	1023.92	0.00123022	-7.75E-06	13.9546	1.25	237.519	1023.92	7.20E-04	-0.00117911	28.0619
1.3	415.654	1069.08	0.00125956	-1.94E-05	14.2472	1.3	238.748	1059.08	7.17E-04	-0.00119736	28.6948
1.35	424.933	1093.57	0.00128768	-2.98E-05	14.5307	1.35	235.542	1093.57	7.14E-04	-0.0012113	29.3089
1.4	433.82	1127.38	0.00131461	-3.93E-05	14.8052	1.4	233.937	1127.38	7.09E-04	-0.0012212	29.9043
1.45	442.325	1160.49	0.00134038	-4.79E-05	15.071	1.45	231.965	1160.49	7.03E-04	-0.00122728	30.4815
1.5	450.458	1192.87	0.00136502	-5.55E-05	15.328	1.5	229.659	1192.87	6.95E-04	-0.00122953	31.0405
1.55	458.226	1224.5	0.00138856	-6.23E-05	15.5756	1.55	227.053	1224.5	6.88E-04	-0.00122828	31.5818
1.6	465.641	1255.37	0.00141103	-6.82E-05	15.8168	1.6	224.178	1255.37	6.79E-04	-0.00122349	32.1053
1.65	472.712	1285.46	0.00143246	-7.35E-05	16.0487	1.65	221.065	1285.46	6.70E-04	-0.00121538	32.6113
1.7	479.447	1314.74	0.00145287	-7.78E-05	16.2724	1.7	217.744	1314.74	6.60E-04	-0.00120418	33.0999
1.75	485.856	1343.2	0.00147229	-8.16E-05	16.4879	1.75	214.246	1343.2	6.49E-04	-0.00118983	33.5712
1.8	491.949	1370.82	0.00149075	-8.45E-05	16.6955	1.8	210.599	1370.82	6.38E-04	-0.00117249	34.0255
1.85	497.732	1397.59	0.00150828	-8.68E-05	16.895	1.85	206.832	1397.59	6.27E-04	-0.00115241	34.4626
1.9	503.216	1423.48	0.00152449	-8.85E-05	17.0867	1.9	202.972	1423.48	6.15E-04	-0.00112963	34.8828
1.95	508.409	1448.48	0.00154063	-8.96E-05	17.2705	1.95	199.045	1448.48	6.03E-04	-0.00110416	35.2861
2	513.319	1472.57	0.00155551	-9.02E-05	17.4464	2	195.077	1472.57	5.91E-04	-0.00107629	35.6726
2.05	517.954	1495.75	0.00156956	-9.00E-05	17.6147	2.05	191.093	1495.75	5.79E-04	-0.00104603	36.0423
2.1	522.323	1517.99	0.0015828	-8.95E-05	17.7752	2.1	187.117	1517.99	5.67E-04	-0.00101338	36.3953
2.15	526.432	1539.28	0.00159525	-8.85E-05	17.928	2.15	183.171	1539.28	5.55E-04	-9.79E-04	36.7316
2.2	530.289	1559.61	0.00160694	-8.69E-05	18.0731	2.2	179.277	1559.61	5.43E-04	-9.42E-04	37.0513
2.25	533.902	1578.97	0.00161768	-8.48E-05	18.2107	2.25	175.458	1578.97	5.32E-04	-9.03E-04	37.3544
2.3	537.277	1597.34	0.00162811	-8.25E-05	18.3406	2.3	171.731	1597.34	5.20E-04	-8.63E-04	37.6408
2.35	540.421	1614.71	0.00163764	-7.97E-05	18.4629	2.35	168.116	1614.71	5.09E-04	-8.21E-04	37.9108
2.4	543.34	1631.07	0.00164648	-7.65E-05	18.5777	2.4	164.632	1631.07	4.99E-04	-7.77E-04	38.1642
2.45	546.039	1646.41	0.00165466	-7.29E-05	18.6849	2.45	161.295	1646.41	4.89E-04	-7.31E-04	38.401
2.5	548.525	1660.72	0.0016622	-6.90E-05	18.7846	2.5	158.122	1660.72	4.79E-04	-6.85E-04	38.6214
2.55	550.803	1674	0.0016691	-6.48E-05	18.8768	2.55	165.125	1674	4.70E-04	-6.38E-04	38.8252
2.6	552.878	1686.23	0.00167539	-6.03E-05	18.9615	2.6	152.32	1686.23	4.62E-04	-5.87E-04	39.0126
2.65	554.753	1697.4	0.00168107	-5.56E-05	19.0387	2.65	149.719	1697.4	4.54E-04	-5.37E-04	39.1835
2.7	556.435	1707.52	0.00168617	-5.07E-05	19.1084	2.7	147.334	1707.52	4.46E-04	-4.85E-04	39.338
2.75	567.925	1716.56	0.00169068	-4.53E-05	19.1707	2.75	145.174	1716.56	4.40E-04	-4.33E-04	39.4769
2.8	559.228	1724.54	0.00169463	-4.00E-05	19.2255	2.8	143.25	1724.54	4.34E-04	-3.80E-04	39.6974
2.85	560.347	1731.43	0.00169802	-3.45E-05	19.2728	2.85	141.569	1731.43	4.29E-04	-3.26E-04	39.7025
2.9	561.284	1737.25	0.00170086	-2.88E-05	19.3127	2.9	140.139	1737.25	4.25E-04	-2.71E-04	39.7911
2.95	562.042	1741.98	0.00170316	-2.30E-05	19.3451	2.95	138.966	1741.98	4.21E-04	-2.16E-04	39.8633
3	562.622	1745.62	0.00170491	-1.71E-05	19.3701	3	138.054	1745.62	4.18E-04	-1.61E-04	39.919
3.05	563.025	1748.17	0.00170614	-1.13E-05	19.3876	3.05	137.407	1748.17	4.16E-04	-1.05E-04	39.9583
3.1	563.254	1749.62	0.00170683	-5.24E-05	19.3977	3.1	137.028	1749.62	4.15E-04	-4.96E-05	39.9811
3.15	563.307	1749.98	0.00170699	8.10E-07	19.4004	3.15	136.918	1749.98	4.15E-04	6.09E-06	39.9875
3.2	563.186	1749.25	0.00170662	6.79E-06	19.3956	3.2	137.079	1749.25	4.15E-04	6.21E-05	39.9774
3.25	562.889	1747.43	0.00170573	1.28E-05	19.3834	3.25	137.508	1747.43	4.17E-04	1.18E-04	39.9509
3.3	562.418	1744.51	0.0017043	1.87E-05	19.3637	3.3	138.204	1744.51	4.19E-04	1.74E-04	39.908
3.35	561.769	1740.51	0.00170233	2.46E-05	19.3366	3.35	139.165	1740.51	4.22E-04	2.29E-04	39.8486
3.4	560.943	1735.41	0.00169983	3.03E-05	19.302	3.4	140.386	1735.41	4.25E-04	2.83E-04	39.7727
3.45	559.938	1729.23	0.00169678	3.60E-05	19.2601	3.45	141.862	1729.23	4.30E-04	3.38E-04	39.6805
3.5	558.747	1721.98	0.00169317	4.13E-05	19.2106	3.5	143.586	1721.98	4.35E-04	3.92E-04	39.5718

KO=0.9, NU=1.63						KO=1.95, NU=1.52					
T	FHEEL	F	Q2	P2	ALPHA	T	FHEEL	F	Q2	P2	ALPHA
0	0	0	0	0	0	0	0	0	0	0	0
0.05	27.5616	43.7454	8.36E-05	0.00541798	2.79603	0.05	27.4125	43.7454	8.31E-05	0.00259837	2.03047
0.1	48.1782	87.4635	1.45E-04	0.00215777	4.74448	0.1	50.0739	87.4635	1.52E-04	0.0017386	3.25055
0.15	89.5908	131.127	2.11E-04	0.00150387	6.21272	0.15	72.991	131.127	2.21E-04	0.00136773	4.2934
0.2	89.6737	174.708	2.72E-04	0.00114188	7.45756	0.2	95.0171	174.708	2.88E-04	0.00115616	5.21573
0.25	108.604	218.181	3.29E-04	8.85E-04	8.59404	0.25	116.152	218.181	3.52E-04	9.82E-04	6.05615
0.3	126.448	261.517	3.83E-04	6.88E-04	9.62891	0.3	136.43	261.517	4.13E-04	8.45E-04	6.83635
0.35	143.282	304.689	4.34E-04	5.27E-04	10.5932	0.35	155.895	304.689	4.72E-04	7.32E-04	7.5694
0.4	159.156	347.671	4.82E-04	3.93E-04	11.5003	0.4	174.581	347.671	5.29E-04	6.36E-04	8.26382
0.45	174.116	390.436	5.28E-04	2.78E-04	12.3596	0.45	192.514	390.436	5.83E-04	5.52E-04	8.92556
0.5	188.205	432.957	5.70E-04	1.78E-04	13.1778	0.5	209.719	432.957	6.36E-04	4.78E-04	9.55893
0.55	201.456	475.207	6.10E-04	9.00E-05	13.96	0.55	226.217	475.207	6.85E-04	4.12E-04	10.1672
0.6	213.905	517.16	6.48E-04	1.21E-05	14.7101	0.6	242.029	517.16	7.33E-04	3.52E-04	10.7529
0.65	225.583	558.79	6.84E-04	-5.75E-05	15.4311	0.65	257.174	558.79	7.79E-04	2.98E-04	11.3181
0.7	236.519	600.071	7.17E-04	-1.20E-04	16.1256	0.7	271.668	600.071	8.23E-04	2.48E-04	11.8643
0.75	245.742	640.977	7.48E-04	-1.76E-04	16.7956	0.75	285.53	640.977	8.65E-04	2.03E-04	12.3929
0.8	256.278	681.482	7.77E-04	-2.26E-04	17.4427	0.8	298.775	681.482	9.05E-04	1.61E-04	12.905
0.85	265.155	721.561	8.04E-04	-2.72E-04	18.0684	0.85	311.421	721.561	9.44E-04	1.23E-04	13.4015
0.9	273.398	761.19	8.28E-04	-3.13E-04	18.6739	0.9	323.482	761.19	9.80E-04	8.80E-05	13.8831
0.95	281.033	800.342	8.52E-04	-3.49E-04	19.2602	0.95	334.976	800.342	0.00101508	5.56E-05	14.3505
1	288.084	838.995	8.73E-04	-3.82E-04	19.8281	1	345.919	838.995	0.00104824	2.56E-05	14.8043
1.05	294.577	877.123	8.93E-04	-4.12E-04	20.3784	1.05	356.325	877.123	0.00107977	-1.66E-06	15.245
1.1	300.535	914.703	9.11E-04	-4.36E-04	20.9118	1.1	366.21	914.703	0.00110973	-2.69E-05	15.6729
1.15	305.982	951.711	9.27E-04	-4.61E-04	21.4288	1.15	375.592	951.711	0.00113616	-5.00E-05	16.0885
1.2	310.942	988.124	9.42E-04	-4.81E-04	21.9299	1.2	384.484	988.124	0.0011651	-7.11E-05	16.492
1.25	315.438	1023.92	9.56E-04	-4.99E-04	22.4156	1.25	392.904	1023.92	0.00119062	-9.04E-05	16.8837
1.3	319.494	1059.08	9.68E-04	-5.13E-04	22.8862	1.3	400.866	1059.08	0.00121475	-1.08E-04	17.2638
1.35	323.132	1093.57	9.79E-04	-5.26E-04	23.3421	1.35	408.386	1093.57	0.00123753	-1.24E-04	17.6327
1.4	326.374	1127.36	9.89E-04	-5.36E-04	23.7836	1.4	415.481	1127.36	0.00125903	-1.36E-04	17.9903
1.45	329.244	1160.49	9.98E-04	-5.43E-04	24.211	1.45	422.165	1160.49	0.00127929	-1.50E-04	18.337
1.5	331.762	1192.87	0.00100534	-5.49E-04	24.6244	1.5	428.454	1192.87	0.00129835	-1.61E-04	18.6728
1.55	333.95	1224.5	0.00101197	-5.52E-04	25.0242	1.55	434.363	1224.5	0.00131625	-1.71E-04	18.9979
1.6	335.831	1255.37	0.00101767	-5.54E-04	25.4105	1.6	439.908	1255.37	0.00133305	-1.79E-04	19.3123
1.65	337.424	1285.45	0.0010225	-5.54E-04	25.7834	1.65	445.103	1285.45	0.0013488	-1.85E-04	19.6163
1.7	338.749	1314.74	0.00102651	-5.52E-04	26.1431	1.7	449.964	1314.74	0.00136353	-1.92E-04	19.9097
1.75	339.828	1343.2	0.00102978	-5.48E-04	26.4898	1.75	454.505	1343.2	0.00137729	-1.96E-04	20.1929
1.8	340.679	1370.82	0.00103236	-5.42E-04	26.8235	1.8	458.741	1370.82	0.00139012	-1.99E-04	20.4657
1.85	341.322	1397.59	0.00103431	-5.35E-04	27.1445	1.85	462.686	1397.59	0.00140208	-2.01E-04	20.7282
1.9	341.776	1423.48	0.00103568	-5.26E-04	27.4527	1.9	466.353	1423.48	0.00141319	-2.02E-04	20.9806
1.95	342.058	1448.48	0.00103654	-5.16E-04	27.7483	1.95	469.757	1448.48	0.00142351	-2.02E-04	21.2228
2	342.185	1472.57	0.00103693	-5.05E-04	28.0314	2	472.911	1472.57	0.00143306	-2.01E-04	21.455
2.05	342.177	1495.75	0.0010369	-4.92E-04	28.3019	2.05	475.827	1495.75	0.0014419	-1.99E-04	21.677
2.1	342.048	1517.99	0.00103651	-4.78E-04	28.5601	2.1	478.519	1517.99	0.00145006	-1.97E-04	21.889
2.15	341.815	1539.28	0.0010358	-4.63E-04	28.8058	2.15	480.999	1539.28	0.00145757	-1.93E-04	22.091
2.2	341.493	1569.61	0.00103483	-4.45E-04	29.0393	2.2	483.277	1569.61	0.00146448	-1.88E-04	22.2829
2.25	341.097	1578.97	0.00103363	-4.29E-04	29.2605	2.25	485.387	1578.97	0.00147081	-1.83E-04	22.4649
2.3	340.64	1597.34	0.00103224	-4.11E-04	29.4695	2.3	487.278	1597.34	0.0014766	-1.77E-04	22.6369
2.35	340.137	1614.71	0.00103072	-3.91E-04	29.6663	2.35	489.021	1614.71	0.00148188	-1.70E-04	22.799
2.4	339.599	1631.07	0.00102909	-3.71E-04	29.851	2.4	490.605	1631.07	0.00148568	-1.62E-04	22.9511
2.45	339.039	1646.41	0.00102739	-3.50E-04	30.0235	2.45	492.042	1646.41	0.00149104	-1.54E-04	23.0933
2.5	338.468	1660.72	0.00102566	-3.28E-04	30.1839	2.5	493.338	1660.72	0.00149496	-1.45E-04	23.2255
2.55	337.896	1674	0.00102393	-3.05E-04	30.3322	2.55	494.503	1674	0.00149849	-1.36E-04	23.3479
2.6	337.334	1686.23	0.00102222	-2.82E-04	30.4685	2.6	495.544	1686.23	0.00150165	-1.26E-04	23.4603
2.65	336.791	1697.4	0.00102058	-2.56E-04	30.5928	2.65	496.468	1697.4	0.00150445	-1.16E-04	23.5629
2.7	336.273	1707.52	0.00101901	-2.33E-04	30.705	2.7	497.282	1707.52	0.00150692	-1.05E-04	23.6555
2.75	335.791	1716.56	0.00101755	-2.08E-04	30.8052	2.75	497.992	1716.56	0.00150907	-9.45E-05	23.7382
2.8	335.349	1724.54	0.00101621	-1.83E-04	30.8935	2.8	498.604	1724.54	0.00151092	-8.33E-05	23.8111
2.85	334.954	1731.43	0.00101501	-1.57E-04	30.9697	2.85	499.121	1731.43	0.00151249	-7.17E-05	23.874
2.9	334.612	1737.25	0.00101397	-1.31E-04	31.034	2.9	499.549	1737.25	0.00151379	-5.99E-05	23.9271
2.95	334.325	1741.98	0.00101311	-1.04E-04	31.0863	2.95	499.891	1741.98	0.00151482	-4.79E-05	23.9702
3	334.099	1745.62	0.00101242	-7.74E-05	31.1266	3	500.149	1745.62	0.00151556	-3.56E-05	24.0035
3.05	333.938	1748.17	0.00101193	-5.05E-05	31.155	3.05	500.326	1748.17	0.00151614	-2.33E-05	24.0269
3.1	333.837	1749.62	0.00101163	-2.36E-05	31.1714	3.1	500.423	1749.62	0.00151643	-1.09E-05	24.0404
3.15	333.804	1749.98	0.00101153	3.32E-06	31.1756	3.15	500.441	1749.98	0.00151649	1.63E-06	24.044
3.2	333.837	1749.25	0.00101163	3.04E-05	31.1683	3.2	500.361	1749.25	0.00151563	1.41E-05	24.0377
3.25	333.935	1747.43	0.00101192	5.73E-05	31.1489	3.25	500.241	1747.43	0.00151588	2.65E-05	24.0216
3.3	334.097	1744.51	0.00101242	8.41E-05	31.1175	3.3	500.021	1744.51	0.00151522	3.87E-05	23.9955
3.35	334.322	1740.51	0.0010131	1.11E-04	31.0741	3.35	499.72	1740.51	0.00151513	5.09E-05	23.9596
3.4	334.605	1735.41	0.00101396	1.37E-04	31.0188	3.4	499.334	1735.41	0.00151313	6.30E-05	23.9138
3.45	334.944	1729.23	0.00101498	1.63E-04	30.9515	3.45	498.851	1729.23	0.00151117	7.47E-05	23.8581
3.5	335.333	1721.98	0.00101616	1.89E-04	30.8722	3.5	498.297	1721.98	0.00150999	8.61E-05	23.7925

KO=1.95, NU=1.75						KO=3.0, NU=1.63					
T	FHEEL	F	Q2	P2	ALPHA	T	FHEEL	F	Q2	P2	ALPHA
0	0	0	0	0	0	0	0	0	0	0	0
0.05	27.4302	43.7454	8.31E-05	0.00152438	1.91257	0.05	26.2764	43.7454	7.95E-05	0.00106102	1.51394
0.1	50.3989	87.4635	1.53E-04	0.00131392	2.80148	0.1	50.9164	87.4635	1.64E-04	0.00130369	2.32189
0.15	74.2798	131.127	2.25E-04	0.00111914	3.56108	0.15	75.2671	131.127	2.28E-04	0.00107163	3.00587
0.2	97.3921	174.708	2.95E-04	9.43E-04	4.21178	0.2	98.8413	174.708	3.00E-04	9.26E-04	3.59703
0.25	119.897	218.181	3.63E-04	8.22E-04	4.79165	0.25	121.651	218.181	3.69E-04	8.20E-04	4.13039
0.3	141.823	261.517	4.30E-04	7.31E-04	5.32087	0.3	144.305	261.517	4.37E-04	7.39E-04	4.62148
0.35	163.198	304.689	4.95E-04	6.57E-04	5.81108	0.35	165.227	304.689	5.04E-04	6.73E-04	5.07971
0.4	184.044	347.671	5.58E-04	5.97E-04	6.26986	0.4	187.633	347.671	5.69E-04	6.17E-04	5.51119
0.45	204.376	390.436	6.19E-04	5.45E-04	6.70243	0.45	208.537	390.436	6.32E-04	5.69E-04	5.92021
0.5	224.208	432.957	6.79E-04	5.00E-04	7.11259	0.5	228.948	432.957	6.94E-04	5.27E-04	6.30986
0.55	243.551	475.207	7.38E-04	4.61E-04	7.5032	0.55	248.874	475.207	7.64E-04	4.90E-04	6.6825
0.6	262.412	517.16	7.95E-04	4.26E-04	7.87646	0.6	268.322	517.16	8.13E-04	4.57E-04	7.03995
0.65	280.801	558.79	8.51E-04	3.94E-04	8.23412	0.65	287.298	558.79	8.71E-04	4.26E-04	7.38364
0.7	298.723	600.071	9.05E-04	3.85E-04	8.5776	0.7	305.806	600.071	9.27E-04	3.98E-04	7.71475
0.75	316.186	640.977	9.58E-04	3.39E-04	8.90804	0.75	323.852	640.977	9.81E-04	3.73E-04	8.03422
0.8	333.193	681.482	0.00100968	3.15E-04	9.22641	0.8	341.439	681.482	0.00103466	3.49E-04	8.34284
0.85	349.752	721.561	0.00105965	2.93E-04	9.5335	0.85	358.571	721.561	0.00108658	3.27E-04	8.64129
0.9	365.865	761.19	0.00110868	2.72E-04	9.82999	0.9	375.253	761.19	0.00113713	3.06E-04	8.93011
0.95	381.538	800.342	0.00115618	2.53E-04	10.1165	0.95	391.488	800.342	0.00118633	2.87E-04	9.20979
1	396.775	838.995	0.00120235	2.35E-04	10.3934	1	407.278	838.995	0.00123418	2.69E-04	9.48073
1.05	411.581	877.123	0.00124722	2.19E-04	10.6513	1.05	422.629	877.123	0.00128069	2.52E-04	9.7433
1.1	425.95	914.703	0.00129079	2.03E-04	10.9205	1.1	437.543	914.703	0.00132589	2.35E-04	9.9978
1.15	439.916	951.711	0.00133308	1.89E-04	11.1713	1.15	452.025	951.711	0.00136977	2.21E-04	10.2445
1.2	453.454	988.124	0.0013741	1.75E-04	11.414	1.2	466.077	988.124	0.00141235	2.07E-04	10.4836
1.25	466.577	1023.92	0.00141387	1.63E-04	11.6488	1.25	479.703	1023.92	0.00145365	1.94E-04	10.7164
1.3	479.289	1059.08	0.00145239	1.51E-04	11.8761	1.3	492.908	1059.08	0.00149366	1.81E-04	10.94
1.35	491.595	1093.57	0.00148968	1.40E-04	12.096	1.35	505.694	1093.57	0.00153241	1.69E-04	11.1576
1.4	503.499	1127.38	0.00152576	1.29E-04	12.3086	1.4	518.066	1127.38	0.0015699	1.58E-04	11.3682
1.45	515.006	1160.49	0.00156062	1.19E-04	12.5142	1.45	530.028	1160.49	0.00160615	1.47E-04	11.5722
1.5	526.118	1192.87	0.0015943	1.10E-04	12.7128	1.5	541.583	1192.87	0.00164116	1.37E-04	11.7695
1.55	536.842	1224.5	0.00162679	1.01E-04	12.9046	1.55	552.735	1224.5	0.00167495	1.28E-04	11.9603
1.6	547.18	1255.37	0.00155812	9.34E-05	13.0898	1.6	563.49	1255.37	0.00170755	1.19E-04	12.1445
1.65	557.137	1285.46	0.00168829	8.58E-05	13.2684	1.65	573.85	1285.46	0.00173894	1.10E-04	12.3226
1.7	566.717	1314.74	0.00171732	7.87E-05	13.4405	1.7	583.819	1314.74	0.00176915	1.02E-04	12.4943
1.75	575.924	1343.2	0.00174523	7.20E-05	13.6062	1.75	593.403	1343.2	0.00179819	9.51E-05	12.6597
1.8	584.763	1370.82	0.00177201	6.58E-05	13.7656	1.8	602.603	1370.82	0.00182807	8.80E-05	12.819
1.85	593.237	1397.59	0.00179769	6.00E-05	13.9187	1.85	611.426	1397.59	0.00185828	8.12E-05	12.9722
1.9	601.351	1423.48	0.00182228	5.47E-05	14.0657	1.9	619.874	1423.48	0.00187841	7.51E-05	13.1193
1.95	609.108	1448.48	0.00184578	4.95E-05	14.2065	1.95	627.951	1448.48	0.00190268	6.91E-05	13.2604
2	616.512	1472.57	0.00186822	4.50E-05	14.3412	2	635.663	1472.57	0.00192625	6.36E-05	13.3954
2.05	623.568	1495.75	0.0018895	4.07E-05	14.4699	2.05	643.012	1495.75	0.00194852	5.85E-05	13.5245
2.1	630.278	1517.99	0.00190994	3.67E-05	14.5927	2.1	650.001	1517.99	0.0019697	5.35E-05	13.6477
2.15	636.648	1539.28	0.00192924	3.30E-05	14.7094	2.15	658.637	1539.28	0.00198981	4.90E-05	13.765
2.2	642.88	1559.61	0.00194751	2.97E-05	14.8203	2.2	662.92	1559.61	0.00200885	4.49E-05	13.8764
2.25	648.377	1578.97	0.00196478	2.65E-05	14.9253	2.25	668.656	1578.97	0.00202683	4.07E-05	13.982
2.3	653.743	1597.34	0.00198104	2.35E-05	15.0244	2.3	674.445	1597.34	0.00204378	3.71E-05	14.0817
2.35	658.782	1614.71	0.00199631	2.10E-05	15.1176	2.35	679.696	1614.71	0.00205969	3.35E-05	14.1756
2.4	663.495	1631.07	0.00201059	1.87E-05	15.2051	2.4	684.608	1631.07	0.00207457	3.05E-05	14.2636
2.45	667.887	1646.41	0.00202039	1.64E-05	15.2868	2.45	689.184	1646.41	0.00208844	2.74E-05	14.3459
2.5	671.95	1660.72	0.00203624	1.45E-05	15.3627	2.5	693.429	1660.72	0.0021013	2.46E-05	14.4224
2.55	675.716	1674	0.00204762	1.25E-05	15.4329	2.55	697.343	1674	0.00211316	2.19E-05	14.4932
2.6	679.159	1686.23	0.00205806	1.09E-05	15.4974	2.6	700.931	1686.23	0.00212403	1.96E-05	14.5582
2.65	682.29	1697.4	0.00206764	9.44E-05	15.5561	2.65	704.194	1697.4	0.00213392	1.73E-05	14.6174
2.7	686.111	1707.52	0.0020761	8.19E-05	15.6091	2.7	707.134	1707.52	0.00214283	1.50E-05	14.6709
2.75	687.624	1716.56	0.00208371	6.86E-05	15.6564	2.75	709.753	1716.56	0.00215077	1.32E-05	14.7187
2.8	689.832	1724.54	0.0020904	5.74E-05	15.6981	2.8	712.053	1724.54	0.00215774	1.11E-05	14.7607
2.85	691.735	1731.43	0.00209617	4.67E-05	15.734	2.85	714.037	1731.43	0.00216375	9.18E-05	14.797
2.9	693.335	1737.25	0.00210102	3.77E-05	15.7643	2.9	715.705	1737.25	0.0021688	7.75E-05	14.8276
2.95	694.633	1741.98	0.00210495	3.00E-05	15.7889	2.95	717.057	1741.98	0.0021729	5.93E-05	14.8524
3	695.629	1745.62	0.00210797	2.11E-05	15.8079	3	718.096	1745.62	0.00217606	4.37E-05	14.8716
3.05	696.326	1748.17	0.00211008	1.30E-05	15.8212	3.05	718.822	1748.17	0.00217825	2.83E-05	14.885
3.1	696.722	1749.62	0.00211128	5.35E-07	15.8288	3.1	719.235	1749.62	0.0021795	1.32E-05	14.8927
3.15	696.819	1749.98	0.00211157	-7.34E-08	15.8308	3.15	719.336	1749.98	0.00217981	-4.93E-07	14.8947
3.2	695.616	1749.25	0.00211096	-9.89E-07	15.8271	3.2	719.125	1749.25	0.00217917	-1.79E-06	14.891
3.25	696.114	1747.43	0.00210944	-1.70E-05	15.8178	3.25	718.801	1747.43	0.00217758	-3.42E-05	14.8816
3.3	695.312	1744.51	0.00210701	-2.48E-05	15.8028	3.3	717.785	1744.51	0.00217505	-4.87E-05	14.8665
3.35	694.208	1740.51	0.00210366	-3.33E-06	15.7822	3.35	716.614	1740.51	0.00217156	-6.47E-05	14.8456
3.4	692.604	1735.41	0.0020994	-4.29E-05	15.7559	3.4	715.151	1735.41	0.00216713	-6.42E-05	14.8191
3.45	691.097	1729.23	0.00209423	-5.13E-05	15.7239	3.45	713.373	1729.23	0.00216173	-1.00E-05	14.7868
3.5	689.086	1721.98	0.00208814	-6.13E-05	15.6863	3.5	711.278	1721.98	0.00215539	-1.18E-05	14.7488

KO=3.0, NU=1.75					
T	FHEEL	F	Q2	P2	ALPHA
0	0	0	0	0	0
0.05	25.9651	43.7454	7.87E-05	7.69E-04	1.47326
0.1	51.1017	87.4635	1.55E-04	0.00122342	2.19615
0.15	75.635	131.127	2.29E-04	9.61E-04	2.79127
0.2	99.5471	174.708	3.02E-04	8.36E-04	3.29812
0.25	122.971	218.181	3.73E-04	7.43E-04	3.75051
0.3	145.927	261.517	4.42E-04	6.73E-04	4.16359
0.35	168.432	304.689	5.10E-04	6.17E-04	4.54636
0.4	190.498	347.671	5.77E-04	5.71E-04	4.90467
0.45	212.136	390.436	6.43E-04	5.31E-04	5.24256
0.5	233.35	432.957	7.07E-04	4.96E-04	5.56298
0.55	254.147	475.207	7.70E-04	4.66E-04	5.86816
0.6	274.529	517.16	8.32E-04	4.38E-04	6.1598
0.65	294.498	558.79	8.92E-04	4.13E-04	6.43928
0.7	314.058	600.071	9.52E-04	3.91E-04	6.70768
0.75	333.207	640.977	0.00100972	3.70E-04	6.96591
0.8	351.948	681.482	0.00106651	3.51E-04	7.2147
0.85	370.281	721.561	0.00112205	3.33E-04	7.4547
0.9	388.205	761.19	0.00117638	3.16E-04	7.68641
0.95	405.725	800.342	0.00122947	3.00E-04	7.91031
1	422.835	838.995	0.00128132	2.85E-04	8.12677
1.05	439.537	877.123	0.00133193	2.71E-04	8.33613
1.1	455.833	914.703	0.00138131	2.56E-04	8.53869
1.15	471.721	951.711	0.00142946	2.48E-04	8.73471
1.2	487.203	988.124	0.00147637	2.34E-04	8.9244
1.25	502.277	1023.92	0.00152205	2.23E-04	9.10797
1.3	516.944	1059.08	0.0015665	2.12E-04	9.2856
1.35	531.205	1093.57	0.00160971	2.02E-04	9.45744
1.4	545.05	1127.38	0.0016517	1.92E-04	9.62363
1.45	558.509	1150.49	0.00169245	1.82E-04	9.7843
1.5	571.553	1192.87	0.00173198	1.73E-04	9.93956
1.55	584.192	1224.5	0.00177028	1.65E-04	10.0895
1.6	596.427	1255.37	0.00180735	1.56E-04	10.2342
1.65	608.256	1265.45	0.00184321	1.48E-04	10.3738
1.7	619.687	1314.74	0.00187784	1.41E-04	10.5083
1.75	630.713	1343.2	0.00191125	1.33E-04	10.6379
1.8	641.338	1370.82	0.00194345	1.26E-04	10.7624
1.85	651.563	1397.59	0.00197443	1.20E-04	10.8821
1.9	661.388	1423.48	0.00200421	1.13E-04	10.997
1.95	670.815	1448.48	0.00203277	1.07E-04	11.1071
2	679.844	1472.57	0.00206013	1.01E-04	11.2124
2.05	688.477	1495.75	0.00208629	9.49E-05	11.313
2.1	696.714	1517.99	0.00211125	8.93E-05	11.4089
2.15	704.556	1539.28	0.00213502	8.38E-05	11.5002
2.2	712.006	1559.61	0.00215759	7.85E-05	11.5868
2.25	719.063	1578.97	0.00217898	7.34E-05	11.6688
2.3	725.727	1597.34	0.00219917	6.84E-05	11.7463
2.35	732.001	1614.71	0.00221819	6.36E-05	11.8192
2.4	737.886	1631.07	0.00223602	5.89E-05	11.8876
2.45	743.382	1646.41	0.00225267	5.43E-05	11.9514
2.5	748.491	1660.72	0.00226815	5.00E-05	12.0108
2.55	753.212	1674	0.00228245	4.57E-05	12.0656
2.6	757.547	1686.23	0.0022956	4.15E-05	12.116
2.65	761.497	1697.4	0.00230757	3.72E-05	12.1619
2.7	765.062	1707.52	0.00231837	3.33E-05	12.2033
2.75	768.243	1716.56	0.00232801	2.93E-05	12.2403
2.8	771.041	1724.54	0.00233649	2.54E-05	12.2728
2.85	773.456	1731.43	0.00234381	2.15E-05	12.3009
2.9	775.488	1737.25	0.00234996	1.79E-05	12.3245
2.95	777.139	1741.98	0.00235497	1.41E-05	12.3438
3	778.408	1745.62	0.00235881	1.03E-05	12.3586
3.05	779.295	1748.17	0.0023615	6.70E-06	12.3689
3.1	779.801	1749.62	0.00236303	3.00E-06	12.3749
3.15	779.926	1749.98	0.00236341	-6.56E-07	12.3764
3.2	779.67	1749.25	0.00236264	-4.28E-06	12.3736
3.25	779.032	1747.43	0.0023607	-7.93E-06	12.3662
3.3	778.014	1744.51	0.00235762	-1.16E-05	12.3545
3.35	776.613	1740.51	0.00235337	-1.53E-05	12.3384
3.4	774.831	1735.41	0.00234797	-1.91E-05	12.3178
3.45	772.667	1729.23	0.00234142	-2.29E-05	12.2928
3.5	770.12	1721.98	0.0023337	-2.67E-05	12.2633

First Condition Data: Nominal Case					
T	FHEEL	F	Q2	P2	ALPHA
0	0	0	0	0	0
0.05	27.4646	43.7454	8.33E-05	0.0020643	1.9745
0.1	50.279	87.4635	1.52E-04	0.00149844	3.01512
0.15	73.6717	131.127	2.23E-04	0.00124332	3.90145
0.2	96.2986	174.708	2.92E-04	0.00104624	4.67469
0.25	118.183	218.181	3.58E-04	9.02E-04	5.37107
0.3	139.368	261.517	4.22E-04	7.92E-04	6.0119
0.35	159.885	304.689	4.85E-04	7.02E-04	6.60962
0.4	179.766	347.671	5.45E-04	6.27E-04	7.17231
0.45	199.029	390.436	6.03E-04	5.62E-04	7.7056
0.5	217.695	432.957	6.60E-04	5.06E-04	8.21357
0.55	235.777	475.207	7.14E-04	4.55E-04	8.69932
0.6	253.291	517.16	7.68E-04	4.11E-04	9.16522
0.65	270.247	558.79	8.19E-04	3.70E-04	9.61316
0.7	286.66	600.071	8.69E-04	3.33E-04	10.0447
0.75	302.538	640.977	9.17E-04	2.99E-04	10.481
0.8	317.893	681.462	9.63E-04	2.69E-04	10.8632
0.85	332.735	721.561	0.00100829	2.40E-04	11.2521
0.9	347.073	761.19	0.00105174	2.14E-04	11.6284
0.95	360.916	800.342	0.00109369	1.90E-04	11.9929
1	374.275	838.995	0.00113417	1.67E-04	12.3459
1.05	387.159	877.123	0.00117321	1.46E-04	12.688
1.1	399.576	914.703	0.00121084	1.27E-04	13.0196
1.15	411.537	951.711	0.00124708	1.09E-04	13.3411
1.2	423.049	988.124	0.00128197	9.27E-05	13.6526
1.25	434.123	1023.92	0.00131552	7.74E-05	13.9546
1.3	444.787	1059.08	0.00134778	6.33E-05	14.2472
1.35	454.99	1093.57	0.00137876	5.02E-05	14.5307
1.4	464.802	1127.38	0.00140849	3.82E-05	14.8052
1.44	472.381	1153.92	0.0014314	2.93E-05	15.0185
Second Condition Data: Nominal Case					
Runtime	FHEEL	F	T		
1.44	472.362	1153.92	0		
1.49	465.927	1186.45	0.05		
1.54	499.091	1218.24	0.1		
1.59	511.616	1249.26	0.15		
1.64	524.063	1279.51	0.2		
1.69	536.155	1308.95	0.25		
1.74	547.838	1337.58	0.3		
1.79	559.235	1365.37	0.35		
1.84	570.275	1392.3	0.4		
1.89	580.942	1418.37	0.45		
1.94	591.259	1443.55	0.5		
1.99	601.205	1467.83	0.55		
2.04	610.771	1491.19	0.6		
2.09	619.958	1513.82	0.65		
2.14	628.758	1535.1	0.7		
2.19	637.164	1555.62	0.75		
2.24	645.172	1575.18	0.8		
2.29	652.777	1593.74	0.85		
2.34	659.974	1611.31	0.9		
2.39	666.759	1627.88	0.95		
2.44	673.127	1643.42	1		
2.49	679.073	1657.94	1.05		
2.54	684.598	1671.43	1.1		
2.59	689.691	1683.86	1.15		
2.64	694.355	1695.25	1.2		
2.69	698.584	1705.58	1.25		
2.74	702.378	1714.84	1.3		
2.79	705.732	1723.03	1.35		
2.84	708.645	1730.14	1.4		
2.89	711.116	1736.17	1.45		
2.94	713.142	1741.12	1.5		
2.99	714.722	1744.98	1.55		
3.04	715.856	1747.74	1.6		
3.09	716.542	1749.42	1.65		
3.14	716.78	1750	1.7		
3.19	716.57	1749.49	1.75		
3.24	715.913	1747.88	1.8		
3.29	714.809	1745.18	1.85		
3.34	713.256	1741.4	1.9		
3.39	711.259	1736.52	1.95		
3.44	708.818	1730.56	2		
3.49	705.933	1723.51	2.05		
3.5	705.303	1721.98	2.06		

L1=0.31						L1=0.32					
T	FHEEL	F	Q2	P2	ALPHA	T	FHEEL	F	Q2	P2	ALPHA
0	0	0	0	0	0	0	0	0	0	0	0
0.05	29.2686	43.7454	9.44E-05	0.00205606	1.97458	0.05	28.3192	43.7454	8.85E-05	0.00206022	1.97454
0.1	53.5141	87.4635	1.73E-04	0.00152189	3.01514	0.1	51.8696	87.4635	1.62E-04	0.00151643	3.01512
0.15	78.4111	131.127	2.53E-04	0.00126754	3.90145	0.15	75.9661	131.127	2.37E-04	0.00125128	3.90145
0.2	102.515	174.708	3.31E-04	0.00106917	4.67469	0.2	99.3089	174.708	3.10E-04	0.0010573	4.67469
0.25	125.809	218.181	4.05E-04	9.24E-04	5.37107	0.25	121.877	218.181	3.81E-04	9.12E-04	5.37107
0.3	148.358	261.517	4.79E-04	8.12E-04	6.0119	0.3	143.72	261.517	4.49E-04	8.02E-04	6.0119
0.35	170.2	304.689	5.49E-04	7.22E-04	6.60961	0.35	164.882	304.689	5.15E-04	7.12E-04	6.60962
0.4	191.363	347.671	6.17E-04	6.46E-04	7.17231	0.4	185.383	347.671	5.79E-04	6.36E-04	7.17231
0.45	211.87	390.436	6.83E-04	5.81E-04	7.7056	0.45	205.249	390.436	6.41E-04	5.71E-04	7.7056
0.5	231.739	432.957	7.48E-04	5.24E-04	8.21357	0.5	224.498	432.957	7.02E-04	5.14E-04	8.21367
0.65	250.989	475.207	8.10E-04	4.73E-04	8.69932	0.55	243.145	475.207	7.50E-04	4.64E-04	8.69932
0.6	269.632	517.16	8.70E-04	4.27E-04	9.16522	0.6	261.205	517.16	8.16E-04	4.19E-04	9.16522
0.65	287.683	558.79	9.28E-04	3.86E-04	9.61316	0.65	278.693	558.79	8.71E-04	3.78E-04	9.61316
0.7	305.154	600.071	9.84E-04	3.49E-04	10.0447	0.7	295.618	600.071	9.24E-04	3.41E-04	10.0447
0.75	322.057	640.977	0.00103889	3.15E-04	10.461	0.75	311.992	640.977	9.75E-04	3.07E-04	10.461
0.8	338.402	681.482	0.00109162	2.83E-04	10.8632	0.8	327.827	681.482	0.00102446	2.76E-04	10.8632
0.85	354.201	721.561	0.00114259	2.54E-04	11.2521	0.85	343.133	721.561	0.00107229	2.47E-04	11.2521
0.9	369.465	761.19	0.00119182	2.27E-04	11.6284	0.9	357.919	761.19	0.0011185	2.20E-04	11.6284
0.95	384.201	800.342	0.00123936	2.03E-04	11.9929	0.95	372.195	800.342	0.00116311	1.96E-04	11.9929
1	398.422	838.995	0.00128523	1.80E-04	12.3459	1	385.971	838.995	0.00120516	1.73E-04	12.3459
1.05	412.137	877.123	0.00132947	1.59E-04	12.688	1.05	399.256	877.123	0.00124768	1.52E-04	12.688
1.1	425.355	914.703	0.00137211	1.39E-04	13.0196	1.1	412.063	914.703	0.0012877	1.33E-04	13.0196
1.15	438.087	951.711	0.00141319	1.21E-04	13.3411	1.15	424.397	951.711	0.00132624	1.15E-04	13.3411
1.2	450.343	988.124	0.00145272	1.04E-04	13.6526	1.2	436.27	988.124	0.00136334	9.78E-05	13.6526
1.25	462.131	1023.92	0.00149074	8.78E-05	13.9546	1.25	447.689	1023.92	0.00139903	8.23E-05	13.9546
1.3	473.461	1059.08	0.0015273	7.32E-05	14.2472	1.3	458.666	1059.08	0.00143333	6.81E-05	14.2472
1.35	484.344	1093.57	0.0015624	5.97E-05	14.5307	1.35	469.209	1093.57	0.00146628	5.47E-05	14.5307
1.4	494.789	1127.38	0.00159609	4.74E-05	14.8052	1.4	479.327	1127.38	0.0014979	4.26E-05	14.8052
1.44	502.837	1153.92	0.00162205	3.82E-05	15.0185	1.44	487.123	1153.92	0.00152226	3.35E-05	15.0185
1.44	502.835	1153.92				1.44	487.123	1153.92			
1.49	517.244	1186.45				1.49	500.917	1186.45			
1.54	531.223	1218.24				1.54	514.466	1218.24			
1.59	544.778	1249.26				1.59	527.666	1249.26			
1.64	557.944	1279.51				1.64	540.481	1279.51			
1.69	570.747	1308.95				1.69	552.917	1308.95			
1.74	583.202	1337.68				1.74	564.992	1337.68			
1.79	595.305	1365.37				1.79	576.715	1365.37			
1.84	607.049	1392.3				1.84	588.085	1392.3			
1.89	618.418	1418.37				1.89	599.094	1418.37			
1.94	629.401	1443.65				1.94	609.732	1443.65			
1.99	639.99	1467.83				1.99	619.99	1467.83			
2.04	650.177	1491.19				2.04	629.859	1491.19			
2.09	659.957	1513.62				2.09	639.333	1513.62			
2.14	669.324	1535.1				2.14	648.407	1535.1			
2.19	678.272	1555.62				2.19	657.076	1555.62			
2.24	686.796	1575.18				2.24	665.334	1575.18			
2.29	694.891	1593.74				2.29	673.176	1593.74			
2.34	702.553	1611.31				2.34	680.598	1611.31			
2.39	709.775	1627.88				2.39	687.694	1627.88			
2.44	716.554	1643.42				2.44	694.161	1643.42			
2.49	722.885	1657.94				2.49	700.296	1657.94			
2.54	728.763	1671.43				2.54	705.99	1671.43			
2.59	734.187	1683.86				2.59	711.244	1683.86			
2.64	739.152	1695.25				2.64	716.053	1695.25			
2.69	743.655	1705.56				2.69	720.415	1705.56			
2.74	747.693	1714.84				2.74	724.327	1714.84			
2.79	751.264	1723.03				2.79	727.787	1723.03			
2.84	754.355	1730.14				2.84	730.791	1730.14			
2.89	756.994	1736.17				2.89	733.338	1736.17			
2.94	759.151	1741.12				2.94	735.427	1741.12			
2.99	780.833	1744.98				2.99	737.057	1744.98			
3.04	762.04	1747.74				3.04	738.226	1747.74			
3.09	762.771	1749.42				3.09	738.934	1749.42			
3.14	763.024	1750				3.14	739.18	1750			
3.19	762.801	1749.49				3.19	738.964	1749.49			
3.24	762.101	1747.88				3.24	738.286	1747.88			
3.29	760.925	1745.18				3.29	737.146	1745.18			
3.34	759.273	1741.4				3.34	735.546	1741.4			
3.39	757.147	1736.52				3.39	733.487	1736.52			
3.44	754.548	1730.56				3.44	730.968	1730.56			
3.49	751.477	1723.51				3.49	727.993	1723.51			

L1=0.34							L1=0.35						
T	FHEEL	F	Q2	P2	ALPHA		T	FHEEL	F	Q2	P2	ALPHA	
0	0	0	0	0	0	0	0	0	0	0	0	0	0
0.05	26.7062	43.7454	7.85E-05	0.00205117	1.97445		0.05	25.9296	43.7454	7.41E-05	0.00203515	1.97442	
0.1	48.8104	87.4635	1.44E-04	0.00149622	3.01511		0.1	47.4127	87.4635	1.35E-04	0.00148046	3.0151	
0.15	71.4962	131.127	2.10E-04	0.00123437	3.90148		0.15	69.4544	131.127	1.98E-04	0.00122279	3.90145	
0.2	93.4664	174.708	2.75E-04	0.00103515	4.67469		0.2	90.7967	174.708	2.59E-04	0.0010271	4.67469	
0.25	114.706	218.181	3.37E-04	8.93E-04	5.37107		0.25	111.428	218.181	3.18E-04	8.85E-04	5.37107	
0.3	135.267	261.517	3.98E-04	7.83E-04	6.0119		0.3	131.402	261.517	3.75E-04	7.75E-04	6.0119	
0.35	155.183	304.689	4.56E-04	6.94E-04	6.60961		0.35	150.749	304.689	4.31E-04	6.86E-04	6.60961	
0.4	174.478	347.671	5.13E-04	6.19E-04	7.17231		0.4	169.493	347.671	4.84E-04	6.11E-04	7.17231	
0.45	193.176	390.436	5.68E-04	5.54E-04	7.7056		0.45	187.656	390.436	5.36E-04	5.47E-04	7.7056	
0.5	211.292	432.957	6.21E-04	4.98E-04	8.21357		0.5	205.265	432.957	5.86E-04	4.91E-04	8.21357	
0.55	228.842	475.207	6.73E-04	4.48E-04	8.69932		0.55	222.304	475.207	6.35E-04	4.41E-04	8.69932	
0.6	245.841	517.16	7.23E-04	4.03E-04	9.18522		0.6	238.817	517.16	6.82E-04	3.97E-04	9.16522	
0.65	262.299	558.79	7.71E-04	3.63E-04	9.61316		0.65	254.805	558.79	7.28E-04	3.57E-04	9.61316	
0.7	278.229	600.071	8.18E-04	3.26E-04	10.0447		0.7	270.279	600.071	7.72E-04	3.20E-04	10.0447	
0.75	293.64	640.977	8.64E-04	2.93E-04	10.461		0.75	285.25	640.977	8.15E-04	2.87E-04	10.461	
0.8	308.543	681.482	9.07E-04	2.62E-04	10.8632		0.8	299.728	681.482	8.56E-04	2.56E-04	10.8632	
0.85	322.948	721.561	9.50E-04	2.34E-04	11.2521		0.85	313.721	721.561	8.96E-04	2.28E-04	11.2521	
0.9	336.864	761.19	9.91E-04	2.08E-04	11.6284		0.9	327.24	761.19	9.35E-04	2.03E-04	11.6284	
0.95	350.301	800.342	0.0010303	1.84E-04	11.9929		0.95	340.293	800.342	9.72E-04	1.79E-04	11.9929	
1	363.267	838.995	0.00106843	1.62E-04	12.3459		1	352.888	838.995	0.00100825	1.57E-04	12.3459	
1.05	375.772	877.123	0.00110521	1.41E-04	12.688		1.05	365.035	877.123	0.00104296	1.36E-04	12.688	
1.1	387.824	914.703	0.00114066	1.22E-04	13.0196		1.1	376.744	914.703	0.00107641	1.17E-04	13.0196	
1.15	399.433	951.711	0.0011748	1.04E-04	13.3411		1.15	388.02	951.711	0.00110863	9.98E-05	13.3411	
1.2	410.606	988.124	0.00120767	8.80E-05	13.6526		1.2	398.875	988.124	0.00113964	8.37E-05	13.6526	
1.25	421.355	1023.92	0.00123928	7.29E-05	13.9546		1.25	409.316	1023.92	0.00116947	6.88E-05	13.9546	
1.3	431.685	1059.08	0.00126966	5.89E-05	14.2472		1.3	419.352	1059.08	0.00119815	5.50E-05	14.2472	
1.35	441.608	1093.57	0.00129885	4.61E-05	14.5307		1.35	428.991	1093.57	0.00122569	4.23E-05	14.5307	
1.4	451.131	1127.38	0.00132686	3.43E-05	14.8052		1.4	438.242	1127.38	0.00125212	3.05E-05	14.8052	
1.44	458.469	1153.92	0.00134844	2.55E-05	15.0185		1.44	445.369	1153.92	0.00127248	2.19E-05	15.0185	
1.44	458.47	1153.92					1.44	445.368	1153.92				
1.49	471.847	1186.45					1.49	458.276	1186.45				
1.54	484.181	1218.24					1.54	470.558	1218.24				
1.59	496.695	1249.26					1.59	482.428	1249.26				
1.54	508.622	1279.51					1.64	494.087	1279.51				
1.69	520.372	1308.95					1.69	505.491	1308.95				
1.74	531.737	1337.58					1.74	516.558	1337.58				
1.79	542.786	1365.37					1.79	527.281	1365.37				
1.84	553.499	1392.3					1.84	537.679	1392.3				
1.89	563.857	1418.37					1.89	547.748	1418.37				
1.94	573.871	1443.65					1.94	557.474	1443.65				
1.99	583.52	1467.83					1.99	566.85	1467.83				
2.04	592.809	1491.19					2.04	575.871	1491.19				
2.09	601.724	1513.62					2.09	584.532	1513.62				
2.14	610.265	1535.1					2.14	592.829	1535.1				
2.19	618.424	1555.62					2.19	600.755	1555.62				
2.24	626.197	1575.18					2.24	608.306	1575.18				
2.29	633.578	1593.74					2.29	615.476	1593.74				
2.34	640.563	1611.31					2.34	622.262	1611.31				
2.39	647.148	1627.88					2.39	628.658	1627.88				
2.44	653.329	1643.42					2.44	634.662	1643.42				
2.49	659.101	1657.94					2.49	640.269	1657.94				
2.54	664.461	1671.43					2.54	645.477	1671.43				
2.59	669.406	1683.86					2.59	650.28	1683.86				
2.64	673.933	1695.25					2.64	654.677	1695.25				
2.69	678.038	1705.68					2.69	658.666	1705.58				
2.74	681.72	1714.84					2.74	662.242	1714.84				
2.79	684.976	1723.03					2.79	665.405	1723.03				
2.84	687.803	1730.14					2.84	668.152	1730.14				
2.89	690.201	1736.17					2.89	670.481	1736.17				
2.94	692.167	1741.12					2.94	672.391	1741.12				
2.99	693.701	1744.98					2.99	673.881	1744.98				
3.04	694.801	1747.74					3.04	674.95	1747.74				
3.09	695.467	1749.42					3.09	675.597	1749.42				
3.14	695.698	1750					3.14	675.821	1750				
3.19	695.495	1749.49					3.19	675.624	1749.49				
3.24	694.857	1747.88					3.24	675.004	1747.88				
3.29	693.785	1745.18					3.29	673.962	1745.18				
3.34	692.278	1741.4					3.34	672.499	1741.4				
3.39	690.34	1736.52					3.39	670.616	1738.52				
3.44	687.97	1730.56					3.44	668.313	1730.56				
3.49	685.17	1723.51					3.49	665.593	1723.51				

L3=0.12						L3=0.13					
T	FHEEL	F	Q2	P2	ALPHA	T	FHEEL	F	Q2	P2	ALPHA
0	0	0	0	0	0	0	0	0	0	0	0
0.05	24.432	43.7454	7.40E-05	0.00173682	1.76853	0.05	25.9319	43.7454	7.86E-05	0.00189642	1.87208
0.1	46.261	87.4635	1.37E-04	0.00123648	2.73636	0.1	47.7631	87.4635	1.45E-04	0.00136768	2.87755
0.15	66.3541	131.127	2.01E-04	0.00102097	3.54617	0.15	70.0088	131.127	2.12E-04	0.00113145	3.72645
0.2	86.7088	174.708	2.63E-04	8.67E-04	4.25024	0.2	91.4963	174.708	2.77E-04	9.56E-04	4.46561
0.25	106.398	218.181	3.22E-04	7.55E-04	4.88423	0.25	112.28	218.181	3.40E-04	8.29E-04	5.13126
0.3	125.451	261.517	3.80E-04	6.70E-04	5.48754	0.3	132.394	261.517	4.01E-04	7.32E-04	5.74376
0.35	143.899	304.689	4.36E-04	6.00E-04	6.01154	0.35	151.874	304.689	4.60E-04	6.52E-04	6.31502
0.4	161.769	347.671	4.90E-04	5.42E-04	6.52362	0.4	170.745	347.671	5.17E-04	5.85E-04	6.85278
0.45	179.08	390.436	5.43E-04	4.92E-04	7.00893	0.45	189.028	390.436	5.73E-04	5.28E-04	7.36244
0.5	195.847	432.957	5.93E-04	4.48E-04	7.47118	0.5	206.739	432.957	6.26E-04	4.78E-04	7.84789
0.55	212.087	475.207	6.43E-04	4.09E-04	7.91319	0.55	223.895	475.207	6.78E-04	4.33E-04	8.3121
0.6	227.81	517.16	6.90E-04	3.73E-04	8.33713	0.6	240.508	517.16	7.29E-04	3.94E-04	8.75733
0.65	243.029	558.79	7.36E-04	3.42E-04	8.74472	0.65	256.59	558.79	7.78E-04	3.58E-04	9.1854
0.7	257.755	600.071	7.81E-04	3.13E-04	9.13736	0.7	272.153	600.071	8.25E-04	3.25E-04	9.59776
0.75	271.997	640.977	8.24E-04	2.86E-04	9.51617	0.75	287.207	640.977	8.70E-04	2.95E-04	9.99561
0.8	285.765	681.482	8.66E-04	2.62E-04	9.88211	0.8	301.762	681.482	9.14E-04	2.67E-04	10.3799
0.85	299.068	721.561	9.06E-04	2.39E-04	10.236	0.85	315.828	721.561	9.57E-04	2.42E-04	10.7516
0.9	311.915	761.19	9.46E-04	2.18E-04	10.5784	0.9	329.414	761.19	9.98E-04	2.18E-04	11.1112
0.95	324.316	800.342	9.83E-04	1.99E-04	10.91	0.95	342.528	800.342	0.00103797	1.96E-04	11.4595
1	336.277	838.995	0.00101902	1.81E-04	11.2312	1	355.182	838.995	0.00107631	1.76E-04	11.7969
1.05	347.808	877.123	0.00105396	1.64E-04	11.5425	1.05	367.382	877.123	0.00111328	1.58E-04	12.1238
1.1	358.918	914.703	0.00108763	1.49E-04	11.8442	1.1	379.138	914.703	0.0011489	1.40E-04	12.4407
1.15	369.614	951.711	0.00112004	1.34E-04	12.1366	1.15	390.459	951.711	0.00118321	1.24E-04	12.7478
1.2	379.906	988.124	0.00115123	1.20E-04	12.4201	1.2	401.353	988.124	0.00121622	1.09E-04	13.0456
1.25	389.801	1023.92	0.00118121	1.08E-04	12.6949	1.25	411.83	1023.92	0.00124797	9.47E-05	13.3341
1.3	399.308	1059.08	0.00121002	9.60E-05	12.9611	1.3	421.898	1059.08	0.00127848	8.19E-05	13.6137
1.36	408.435	1093.57	0.00123768	8.48E-05	13.219	1.35	431.566	1093.57	0.00130778	6.98E-05	13.8846
1.4	417.192	1127.38	0.00126422	7.46E-05	13.4688	1.4	440.843	1127.38	0.00133589	5.87E-05	14.147
1.45	425.585	1160.48	0.00128965	6.52E-05	13.7106	1.45	449.736	1160.49	0.00136284	4.84E-05	14.4009
1.5	433.623	1192.87	0.00131401	5.64E-05	13.9445	1.5	458.256	1192.87	0.00138865	3.90E-05	14.6466
1.55	441.315	1224.5	0.00133732	4.82E-05	14.1706	1.55	466.409	1224.5	0.00141336	3.03E-05	14.8841
1.6	448.669	1255.37	0.0013596	4.08E-05	14.3891	1.58	471.131	1243.12	0.00142767	2.54E-05	15.0227
1.65	455.692	1285.46	0.00138089	3.38E-05	14.6001	1.58	471.131	1243.12			
1.7	462.394	1314.74	0.00140119	2.75E-05	14.8036	1.63	483.042	1273.52			
1.75	468.781	1343.2	0.00142055	2.18E-05	14.9998	1.68	494.38	1303.13			
1.76	470.022	1348.79	0.00142431	2.06E-05	15.0381	1.73	505.088	1331.92			
1.76	470.022	1348.79				1.78	515.785	1369.88			
1.81	480.414	1376.24				1.83	526.089	1386.98			
1.86	489.738	1402.83				1.88	535.994	1413.23			
1.91	498.377	1428.55				1.93	545.635	1438.59			
1.96	507.233	1453.37				1.98	554.916	1463.05			
2.01	515.583	1477.28				2.03	563.835	1486.59			
2.06	523.53	1500.27				2.08	572.419	1509.21			
2.11	531.272	1522.33				2.13	580.641	1530.88			
2.16	538.636	1543.43				2.18	588.495	1551.6			
2.21	545.646	1563.56				2.23	595.987	1571.34			
2.26	552.343	1582.72				2.28	603.104	1590.11			
2.31	558.684	1600.89				2.33	609.844	1607.88			
2.36	564.671	1618.06				2.38	616.203	1624.65			
2.41	570.313	1634.22				2.43	622.177	1640.4			
2.46	575.596	1649.36				2.48	627.763	1655.12			
2.51	580.518	1663.46				2.53	632.956	1668.81			
2.56	585.078	1676.53				2.58	637.753	1681.46			
2.61	589.272	1688.55				2.63	642.152	1693.06			
2.66	593.099	1699.51				2.68	646.15	1703.6			
2.71	596.554	1709.41				2.73	649.743	1713.07			
2.76	599.637	1718.24				2.78	652.931	1721.48			
2.81	602.345	1726				2.83	655.71	1728.8			
2.86	604.676	1732.68				2.88	658.08	1735.05			
2.91	606.629	1738.28				2.93	660.038	1740.22			
2.96	608.204	1742.79				2.98	661.584	1744.29			
3.01	609.398	1748.21				3.03	662.717	1747.28			
3.06	610.211	1748.54				3.08	663.435	1749.17			
3.11	610.643	1749.78				3.13	663.739	1749.97			
3.16	610.694	1749.93				3.18	663.628	1749.68			
3.21	610.363	1748.98				3.23	663.102	1748.29			
3.26	609.65	1746.93				3.28	662.161	1745.81			
3.31	608.556	1743.8				3.33	660.808	1742.24			
3.36	607.082	1739.58				3.38	659.041	1737.58			
3.41	606.229	1734.26				3.43	656.861	1731.84			
3.46	602.997	1727.87				3.48	654.272	1725.01			

L3=0.15						L3=0.16					
T	FHEEL	F	Q2	P2	ALPHA	T	FHEEL	F	Q2	P2	ALPHA
0	0	0	0	0	0	0	0	0	0	0	0
0.05	29.0988	43.7454	8.82E-05	0.00224535	2.07612	0.05	30.7808	43.7454	9.33E-05	0.00244576	2.17722
0.1	52.8141	87.4635	1.60E-04	0.00162863	3.14963	0.1	55.3757	87.4635	1.68E-04	0.00175931	3.28159
0.15	77.3413	131.127	2.34E-04	0.00135558	4.07171	0.15	81.0174	131.127	2.46E-04	0.001467	4.2377
0.2	101.114	174.708	3.06E-04	0.00113693	4.87809	0.2	105.941	174.708	3.21E-04	0.00122803	5.07631
0.25	124.105	218.181	3.76E-04	9.75E-04	5.60437	0.25	130.044	218.181	3.94E-04	0.00104769	5.83175
0.3	146.364	261.517	4.44E-04	8.52E-04	6.27275	0.3	153.384	261.517	4.65E-04	9.10E-04	6.52698
0.35	167.928	304.689	5.09E-04	7.51E-04	6.8962	0.35	176.001	304.689	5.33E-04	7.98E-04	7.1755
0.4	188.826	347.671	5.72E-04	6.66E-04	7.48313	0.4	197.924	347.671	6.00E-04	7.04E-04	7.78605
0.46	209.08	390.436	6.34E-04	5.94E-04	8.03941	0.46	219.175	390.436	6.64E-04	6.23E-04	8.36474
0.5	228.708	432.957	6.93E-04	5.30E-04	8.56929	0.5	239.774	432.957	7.27E-04	5.52E-04	8.91597
0.55	247.727	475.207	7.51E-04	4.74E-04	9.07599	0.55	259.737	475.207	7.87E-04	4.90E-04	9.44309
0.6	266.15	517.16	8.07E-04	4.24E-04	9.562	0.6	279.08	517.16	8.46E-04	4.34E-04	9.94868
0.65	283.992	558.79	8.61E-04	3.79E-04	10.0293	0.65	297.817	558.79	9.02E-04	3.84E-04	10.4348
0.7	301.265	600.071	9.13E-04	3.38E-04	10.4794	0.7	315.959	600.071	9.57E-04	3.38E-04	10.9031
0.75	317.979	640.977	9.64E-04	3.00E-04	10.9137	0.75	333.519	640.977	0.00101066	2.97E-04	11.3549
0.8	334.146	681.482	0.00101256	2.66E-04	11.3333	0.8	350.508	681.482	0.00106214	2.59E-04	11.7914
0.85	349.775	721.661	0.00105992	2.34E-04	11.739	0.85	366.936	721.661	0.00111193	2.24E-04	12.2134
0.9	364.877	761.19	0.00110569	2.05E-04	12.1316	0.9	382.814	761.19	0.00116004	1.92E-04	12.6219
0.95	379.462	800.342	0.00114989	1.78E-04	12.5117	0.95	398.152	800.342	0.00120662	1.62E-04	13.0174
1	393.54	838.995	0.00119255	1.54E-04	12.88	1	412.96	838.995	0.0012514	1.35E-04	13.4005
1.05	407.12	877.123	0.0012337	1.31E-04	13.2369	1.05	427.249	877.123	0.00129469	1.10E-04	13.7718
1.1	420.212	914.703	0.00127337	1.09E-04	13.5829	1.1	441.027	914.703	0.00133645	8.69E-05	14.1317
1.15	432.825	951.711	0.00131159	8.99E-05	13.9182	1.15	454.306	951.711	0.00137668	6.57E-05	14.4806
1.2	444.969	988.124	0.00134839	7.19E-05	14.2432	1.2	467.094	988.124	0.00141544	4.61E-05	14.8187
1.25	456.653	1023.92	0.0013838	5.52E-05	14.5582	1.23	474.535	1009.68	0.00143798	3.50E-04	15.0166
1.3	467.887	1059.08	0.00141784	3.99E-05	14.8635	1.23	474.533	1009.68			
1.33	474.415	1079.85	0.00143762	3.13E-05	15.042	1.28	491.317	1045.09			
1.33	474.415	1079.85				1.33	507.863	1079.85			
1.38	490.069	1113.94				1.38	523.714	1113.94			
1.43	504.886	1147.33				1.43	539.449	1147.33			
1.48	518.928	1180				1.48	554.856	1180			
1.53	533.136	1211.94				1.53	569.832	1211.94			
1.58	546.876	1243.12				1.58	584.501	1243.12			
1.63	560.174	1273.52				1.63	598.805	1273.52			
1.68	573.236	1303.13				1.68	612.716	1303.13			
1.73	585.905	1331.92				1.73	626.256	1331.92			
1.78	598.187	1359.88				1.78	639.405	1359.88			
1.83	610.121	1386.98				1.83	652.149	1386.98			
1.88	621.666	1413.23				1.88	664.488	1413.23			
1.93	632.817	1438.59				1.93	676.413	1438.59			
1.98	643.579	1463.05				1.98	687.913	1463.05			
2.03	653.937	1486.59				2.03	698.984	1486.59			
2.08	663.885	1509.21				2.08	709.619	1509.21			
2.13	673.419	1530.88				2.13	719.81	1530.88			
2.18	682.532	1551.6				2.18	729.55	1551.6			
2.23	691.219	1571.34				2.23	738.836	1571.34			
2.28	699.473	1590.11				2.28	747.659	1590.11			
2.33	707.291	1607.88				2.33	756.014	1507.88			
2.38	714.666	1624.65				2.38	763.898	1624.65			
2.43	721.595	1640.4				2.43	771.304	1640.4			
2.48	728.073	1655.12				2.48	778.228	1655.12			
2.53	734.096	1668.81				2.53	784.665	1668.81			
2.58	739.66	1681.46				2.58	790.613	1681.46			
2.63	744.761	1693.06				2.63	796.066	1693.06			
2.68	749.398	1703.6				2.68	801.022	1703.6			
2.73	753.566	1713.07				2.73	805.477	1713.07			
2.78	757.262	1721.48				2.78	809.428	1721.48			
2.83	760.486	1728.8				2.83	812.874	1728.8			
2.88	763.235	1735.05				2.88	815.812	1735.05			
2.93	765.506	1740.22				2.93	818.24	1740.22			
2.98	767.299	1744.29				2.98	820.156	1744.29			
3.03	768.613	1747.28				3.03	821.56	1747.28			
3.08	769.446	1749.17				3.08	822.461	1749.17			
3.13	769.798	1749.97				3.13	822.827	1749.97			
3.18	769.669	1749.68				3.18	822.689	1749.68			
3.23	769.059	1748.29				3.23	822.038	1748.29			
3.28	767.968	1745.81				3.28	820.872	1746.81			
3.33	766.398	1742.24				3.33	819.193	1742.24			
3.38	764.349	1737.58				3.38	817.002	1737.58			
3.43	761.822	1731.84				3.43	814.301	1731.84			
3.48	758.818	1725.01				3.48	811.091	1725.01			

PHI=0.2269						PHI=0.2443					
T	FHEEL	F	Q2	P2	ALPHA	T	FHEEL	F	Q2	P2	ALPHA
0	0	0	0	0	0	0	0	0	0	0	0
0.05	28.7335	43.7454	8.71E-05	0.00239012	1.97454	0.05	28.1121	43.7454	8.52E-05	0.00222801	1.97452
0.1	52.6351	87.4635	1.60E-04	0.00174899	3.01513	0.1	51.4625	87.4635	1.56E-04	0.00162426	3.01513
0.15	77.2111	131.127	2.34E-04	0.00146327	3.90145	0.15	75.4486	131.127	2.29E-04	0.00135377	3.90145
0.2	101.028	174.708	3.06E-04	0.00124425	4.67469	0.2	98.6736	174.708	2.99E-04	0.00114569	4.67469
0.25	124.099	218.181	3.76E-04	0.00108376	5.37107	0.25	121.153	218.181	3.67E-04	9.93E-04	5.37107
0.3	146.471	261.517	4.44E-04	9.61E-04	6.0119	0.3	142.934	261.517	4.33E-04	8.77E-04	6.0119
0.35	168.175	304.689	5.10E-04	8.62E-04	6.60962	0.35	164.047	304.689	4.97E-04	7.82E-04	6.60962
0.4	189.238	347.671	5.73E-04	7.78E-04	7.17231	0.4	184.521	347.671	5.59E-04	7.03E-04	7.17231
0.45	209.68	390.436	6.35E-04	7.07E-04	7.7056	0.45	204.376	390.436	6.19E-04	6.35E-04	7.7056
0.5	229.518	432.957	6.96E-04	6.44E-04	8.21357	0.5	223.629	432.957	6.78E-04	5.75E-04	8.21357
0.65	248.766	475.207	7.54E-04	5.88E-04	8.69932	0.65	242.297	475.207	7.34E-04	5.22E-04	8.69932
0.6	267.436	517.16	8.10E-04	5.39E-04	9.16522	0.6	260.391	517.16	7.89E-04	4.75E-04	9.16522
0.65	285.546	558.79	8.65E-04	4.94E-04	9.61316	0.65	277.925	558.79	8.42E-04	4.32E-04	9.61316
0.7	303.099	600.071	9.18E-04	4.53E-04	10.0447	0.7	294.909	600.071	8.94E-04	3.93E-04	10.0447
0.75	320.109	640.977	9.70E-04	4.15E-04	10.461	0.75	311.355	640.977	9.44E-04	3.57E-04	10.461
0.8	336.584	681.482	0.00101995	3.81E-04	10.8632	0.8	327.271	681.482	9.92E-04	3.25E-04	10.8632
0.85	352.534	721.561	0.00106828	3.49E-04	11.2521	0.85	342.668	721.561	0.00103839	2.95E-04	11.2521
0.9	367.967	761.19	0.00111505	3.19E-04	11.6284	0.9	357.555	761.19	0.0010835	2.67E-04	11.6284
0.95	382.893	800.342	0.00116028	2.92E-04	11.9929	0.95	371.941	800.342	0.00112709	2.41E-04	11.9929
1	397.321	838.995	0.001204	2.66E-04	12.3459	1	385.836	838.995	0.0011692	2.17E-04	12.3459
1.05	411.257	877.123	0.00124623	2.43E-04	12.688	1.05	399.247	877.123	0.00120984	1.95E-04	12.688
1.1	424.713	914.703	0.00128701	2.20E-04	13.0196	1.1	412.184	914.703	0.00124904	1.74E-04	13.0196
1.15	437.694	951.711	0.00132635	2.00E-04	13.3411	1.15	424.656	951.711	0.00128684	1.65E-04	13.3411
1.2	450.212	988.124	0.00136428	1.81E-04	13.6526	1.2	436.672	988.124	0.00132325	1.37E-04	13.6526
1.25	462.272	1023.92	0.00140082	1.63E-04	13.9546	1.25	448.24	1023.92	0.0013583	1.20E-04	13.9546
1.3	473.885	1059.08	0.00143601	1.46E-04	14.2472	1.3	459.369	1059.08	0.00139203	1.05E-04	14.2472
1.35	485.058	1093.57	0.00146987	1.30E-04	14.5307	1.35	470.068	1093.57	0.00142445	9.05E-05	14.5307
1.4	495.8	1127.38	0.00150242	1.16E-04	14.8062	1.4	480.346	1127.38	0.00145559	7.72E-05	14.8052
1.45	506.12	1160.49	0.0015337	1.03E-04	15.071	1.45	490.211	1160.49	0.00148549	6.50E-05	15.071
1.5	516.025	1192.87	0.00156371	8.99E-05	15.328	1.5	499.673	1192.87	0.00151416	5.37E-05	15.328
1.65	525.526	1224.5	0.0015925	7.85E-05	15.5768	1.65	508.739	1224.5	0.00154163	4.34E-05	15.5766
1.6	534.628	1255.37	0.00162009	6.78E-05	15.8168	1.6	517.419	1255.37	0.00156794	3.38E-05	15.8168
1.65	543.342	1285.46	0.00164649	5.80E-05	16.0487	1.65	525.721	1285.46	0.00159309	2.52E-05	16.0487
1.7	651.675	1314.74	0.00167174	4.89E-05	16.2724	1.7	538.643	1314.74			
1.75	659.636	1343.2	0.00169587	4.05E-05	16.4879	1.75	550.364	1343.2			
1.8	567.233	1370.82	0.00171689	3.30E-05	16.6955	1.8	561.288	1370.82			
1.85	574.473	1397.59	0.00174083	2.61E-05	16.895	1.85	572.47	1397.59			
1.88	578.649	1413.23	0.00175348	2.22E-05	17.011	1.9	583.084	1423.48			
1.88	578.648	1413.23				1.95	593.235	1448.48			
1.93	589.197	1436.59				2	603.157	1472.57			
1.98	599.334	1463.06				2.05	612.65	1495.75			
2.03	608.843	1486.59				2.1	621.739	1517.99			
2.08	618.147	1509.21				2.15	630.473	1539.28			
2.13	627.05	1530.88				2.2	638.8	1659.61			
2.18	635.503	1651.6				2.25	646.723	1578.97			
2.23	643.602	1571.34				2.3	654.25	1597.34			
2.28	651.293	1590.11				2.35	661.355	1614.71			
2.33	658.565	1607.88				2.4	668.065	1631.07			
2.38	665.435	1624.65				2.45	674.349	1646.41			
2.43	671.887	1640.4				2.5	680.212	1660.72			
2.48	677.917	1655.12				2.55	685.649	1674			
2.63	683.526	1668.81				2.6	690.658	1686.23			
2.68	688.707	1681.46				2.65	695.235	1697.4			
2.63	693.456	1693.06				2.7	699.378	1707.52			
2.68	697.774	1703.6				2.75	703.084	1716.56			
2.73	701.654	1713.07				2.8	706.35	1724.54			
2.78	706.097	1721.48				2.85	709.175	1731.43			
2.83	708.098	1728.8				2.9	711.657	1737.25			
2.88	710.657	1735.05				2.95	713.494	1741.98			
2.93	712.772	1740.22				3	714.984	1745.62			
2.98	714.442	1744.29				3.05	716.029	1748.17			
3.03	715.665	1747.28				3.1	716.625	1749.62			
3.08	716.44	1749.17				3.15	716.774	1749.98			
3.13	716.768	1749.97				3.2	716.475	1749.25			
3.18	716.648	1749.68				3.25	715.728	1747.43			
3.23	716.081	1748.29				3.3	714.533	1744.51			
3.28	715.065	1745.81				3.35	712.893	1740.51			
3.33	713.603	1742.24				3.4	710.807	1735.41			
3.38	711.695	1737.58				3.45	708.276	1729.23			
3.43	709.341	1731.84				3.5	705.303	1721.98			
3.48	706.545	1725.01									

PHI=0.2793						PHI=0.2967					
T	FHEEL	F	Q2	P2	ALPHA	T	FHEEL	F	Q2	P2	ALPHA
0	0	0	0	0	0	0	0	0	0	0	0
0.05	26.8553	43.7454	8.14E-05	0.00189995	1.97447	0.05	26.2275	43.7454	7.95E-05	0.00173599	1.97445
0.1	49.0916	87.4635	1.49E-04	0.00137227	3.01511	0.1	47.9074	87.4635	1.45E-04	0.00124652	3.01511
0.15	71.8881	131.127	2.18E-04	0.00113255	3.90145	0.15	70.1096	131.127	2.12E-04	0.00102211	3.90145
0.2	93.9168	174.708	2.85E-04	9.47E-04	4.67469	0.2	91.5427	174.708	2.77E-04	8.47E-04	4.67469
0.25	115.204	218.181	3.49E-04	8.11E-04	5.37107	0.25	112.236	218.181	3.40E-04	7.20E-04	5.37107
0.3	135.79	261.517	4.11E-04	7.07E-04	6.0119	0.3	132.227	261.517	4.01E-04	6.22E-04	6.0119
0.35	155.713	304.689	4.72E-04	6.22E-04	6.60961	0.35	151.558	304.689	4.59E-04	5.42E-04	6.60961
0.4	175	347.671	5.30E-04	5.51E-04	7.17231	0.4	170.254	347.671	5.16E-04	4.75E-04	7.17231
0.45	193.673	390.436	5.87E-04	4.90E-04	7.7056	0.45	188.338	390.436	5.71E-04	4.17E-04	7.7056
0.5	211.75	432.957	6.42E-04	4.36E-04	8.21357	0.5	205.83	432.957	6.24E-04	3.67E-04	8.21357
0.55	229.247	475.207	6.95E-04	3.89E-04	8.69932	0.55	222.746	475.207	6.75E-04	3.22E-04	8.69932
0.6	246.18	517.16	7.46E-04	3.46E-04	9.16522	0.6	239.101	517.16	7.25E-04	2.82E-04	9.16522
0.65	262.56	558.79	7.96E-04	3.08E-04	9.61316	0.65	254.909	558.79	7.72E-04	2.46E-04	9.61316
0.7	278.4	600.071	8.44E-04	2.73E-04	10.0447	0.7	270.181	600.071	8.19E-04	2.14E-04	10.0447
0.75	293.712	640.977	8.90E-04	2.41E-04	10.461	0.75	284.93	640.977	8.63E-04	1.64E-04	10.461
0.8	308.506	681.482	9.35E-04	2.12E-04	10.8632	0.8	299.167	681.482	9.07E-04	1.57E-04	10.8632
0.85	322.793	721.561	9.78E-04	1.86E-04	11.2521	0.85	312.903	721.561	9.48E-04	1.31E-04	11.2521
0.9	336.583	761.19	0.00101995	1.61E-04	11.6284	0.9	326.149	761.19	9.88E-04	1.09E-04	11.6284
0.95	349.885	800.342	0.00106026	1.38E-04	11.9929	0.95	338.913	800.342	0.00102701	8.75E-05	11.9929
1	362.709	838.995	0.00109912	1.17E-04	12.3459	1	351.208	838.995	0.00106427	6.80E-05	12.3459
1.05	375.066	877.123	0.00113657	9.81E-05	12.685	1.05	363.042	877.123	0.00110013	5.02E-05	12.688
1.1	386.965	914.703	0.00117262	8.03E-05	13.0196	1.1	374.426	914.703	0.00113462	3.38E-05	13.0196
1.15	398.415	951.711	0.00120732	6.38E-05	13.3411	1.15	389.751	951.711			
1.2	409.425	988.124	0.00124068	4.86E-05	13.6526	1.2	404.84	988.124			
1.25	420.006	1023.92	0.00127274	3.47E-05	13.9546	1.25	419.328	1023.92			
1.26	422.071	1031	0.001279	3.19E-05	14.0139	1.3	433.771	1059.08			
1.26	422.07	1031				1.35	447.938	1093.57			
1.31	436.576	1066.03				1.4	461.746	1127.38			
1.36	450.816	1100.39				1.45	475.317	1160.49			
1.41	464.443	1134.06				1.5	488.588	1192.87			
1.46	477.985	1167.02				1.55	501.536	1224.5			
1.51	491.224	1199.26				1.6	514.183	1255.37			
1.56	504.081	1230.74				1.65	526.508	1285.46			
1.61	516.672	1261.45				1.7	538.499	1314.74			
1.66	528.937	1291.38				1.75	550.157	1343.2			
1.71	540.855	1320.5				1.8	561.471	1370.82			
1.76	552.447	1348.79				1.85	572.433	1397.59			
1.81	563.692	1376.24				1.9	583.037	1423.46			
1.86	574.582	1402.83				1.95	593.278	1448.48			
1.91	585.115	1428.55				2	603.147	1472.57			
1.96	595.282	1453.37				2.05	612.64	1495.75			
2.01	605.076	1477.28				2.1	621.749	1517.99			
2.06	614.493	1500.27				2.15	630.471	1539.28			
2.11	623.525	1522.33				2.2	638.798	1559.61			
2.16	632.168	1543.43				2.25	646.726	1578.97			
2.21	640.415	1563.56				2.3	654.249	1597.34			
2.26	648.263	1582.72				2.35	661.364	1614.71			
2.31	655.705	1600.89				2.4	668.066	1631.07			
2.36	662.738	1618.06				2.45	674.349	1646.41			
2.41	669.356	1634.22				2.5	680.212	1660.72			
2.46	675.556	1649.36				2.55	685.649	1674			
2.51	681.334	1663.46				2.6	690.658	1686.23			
2.56	686.686	1676.53				2.65	695.235	1697.4			
2.61	691.608	1688.55				2.7	699.378	1707.52			
2.66	696.099	1699.51				2.75	703.084	1716.56			
2.71	700.155	1709.41				2.8	706.35	1724.54			
2.76	703.772	1718.24				2.85	709.175	1731.43			
2.81	706.951	1726				2.9	711.557	1737.25			
2.86	709.687	1732.68				2.95	713.494	1741.98			
2.91	711.979	1738.28				3	714.984	1745.62			
2.96	713.827	1742.79				3.05	716.029	1748.17			
3.01	715.229	1748.21				3.1	716.625	1749.62			
3.06	716.184	1748.54				3.15	716.774	1749.98			
3.11	716.691	1749.78				3.2	716.475	1749.25			
3.16	716.75	1749.93				3.25	715.728	1747.43			
3.21	716.361	1748.96				3.3	714.534	1744.51			
3.26	715.525	1745.93				3.35	712.893	1740.51			
3.31	714.241	1743.8				3.4	710.807	1735.41			
3.36	712.511	1739.58				3.45	708.276	1729.23			
3.41	710.336	1734.26				3.5	705.303	1721.98			
3.46	707.717	1727.87									
3.51	704.655	1720.39									

KO=0.9, NU=1.52						KO=0.9, NU=1.63					
T	FHEEL	F	Q2	P2	ALPHA	T	FHEEL	F	Q2	P2	ALPHA
0	0	0	0	0	0	0	0	0	0	0	0
0.05	26.9894	43.7454	8.18E-05	0.00602467	2.85554	0.05	27.5816	43.7454	8.36E-05	0.00541798	2.79603
0.1	47.4907	87.4635	1.44E-04	0.00233235	5.26195	0.1	46.1782	87.4635	1.46E-04	0.0021577	4.74448
0.15	68.1061	131.127	2.06E-04	0.00161808	7.04984	0.15	69.5908	131.127	2.11E-04	0.00150387	6.21272
0.2	86.9742	174.708	2.64E-04	0.00115757	8.60146	0.2	89.6737	174.708	2.72E-04	0.00114188	7.46756
0.25	104.378	218.181	3.16E-04	8.15E-04	10.01	0.25	108.604	218.181	3.29E-04	8.85E-04	8.59404
0.3	120.403	261.517	3.65E-04	5.44E-04	11.3152	0.3	126.448	261.517	3.83E-04	6.88E-04	9.62891
0.35	135.139	304.689	4.10E-04	3.19E-04	12.5401	0.35	143.282	304.689	4.34E-04	5.27E-04	10.5932
0.4	146.652	347.671	4.50E-04	1.28E-04	13.6995	0.4	159.158	347.671	4.82E-04	3.93E-04	11.5003
0.45	161.002	390.436	4.88E-04	-3.80E-05	14.8036	0.45	174.116	390.436	5.28E-04	2.78E-04	12.3596
0.46	163.337	398.961	4.94E-04	-6.85E-05	15.0185	0.5	188.205	432.957	5.70E-04	1.78E-04	13.1778
0.46	163.337	398.961				0.55	201.456	475.207	6.10E-04	9.00E-05	13.96
0.51	180.52	441.429				0.6	213.905	517.16	6.46E-04	1.21E-05	14.7101
0.56	198.283	463.622				0.62	218.867	533.853	6.62E-04	-1.66E-05	15.0018
0.61	215.219	525.513				0.62	218.668	533.853			
0.66	232.2	567.075				0.67	235.427	575.346			
0.71	249.189	608.283				0.72	252.634	616.46			
0.76	265.858	649.111				0.77	269.188	657.228			
0.81	282.406	689.533				0.82	285.66	697.566			
0.86	298.812	729.524				0.87	302.087	737.468			
0.91	314.992	769.059				0.92	318.208	776.909			
0.96	330.987	808.114				0.97	334.153	815.865			
1.01	346.782	846.663				1.02	349.92	854.31			
1.06	362.352	884.683				1.07	365.439	892.222			
1.11	377.698	922.151				1.12	380.737	929.576			
1.16	392.809	959.042				1.17	395.803	966.349			
1.21	407.673	995.334				1.22	410.616	1002.52			
1.26	422.283	1031				1.27	425.174	1038.06			
1.31	436.629	1066.03				1.32	439.467	1072.95			
1.36	450.703	1100.39				1.37	453.464	1107.18			
1.41	464.494	1134.06				1.42	467.218	1140.71			
1.46	477.995	1167.02				1.47	480.861	1173.53			
1.51	491.198	1199.26				1.52	493.802	1205.61			
1.56	504.093	1230.74				1.57	506.635	1236.94			
1.61	516.674	1261.45				1.62	519.152	1267.5			
1.66	528.931	1291.38				1.67	531.343	1297.27			
1.71	540.858	1320.5				1.72	543.204	1326.22			
1.76	552.448	1346.79				1.77	554.724	1354.35			
1.81	563.691	1376.24				1.82	565.898	1381.63			
1.86	574.583	1402.83				1.87	576.718	1408.05			
1.91	585.115	1428.55				1.92	587.178	1433.59			
1.96	595.282	1453.37				1.97	597.27	1458.23			
2.01	605.076	1477.28				2.02	606.99	1461.96			
2.06	614.493	1500.27				2.07	616.33	1504.76			
2.11	623.525	1522.33				2.12	625.285	1526.62			
2.16	632.168	1543.43				2.17	633.849	1547.53			
2.21	640.415	1563.56				2.22	642.017	1567.47			
2.26	646.263	1582.72				2.27	649.784	1586.43			
2.31	655.705	1600.89				2.32	657.145	1604.41			
2.36	662.738	1618.06				2.37	664.094	1621.37			
2.41	669.356	1634.22				2.42	670.63	1637.33			
2.46	675.556	1649.36				2.47	676.745	1652.26			
2.51	681.334	1683.46				2.52	682.438	1666.16			
2.56	686.686	1676.53				2.57	687.705	1679.02			
2.61	691.608	1688.55				2.62	692.541	1690.82			
2.66	696.099	1699.51				2.67	696.945	1701.58			
2.71	700.154	1709.41				2.72	700.913	1711.26			
2.76	703.772	1718.24				2.77	704.443	1719.88			
2.81	706.95	1726				2.82	707.533	1727.43			
2.86	709.687	1732.68				2.87	710.181	1733.89			
2.91	711.98	1738.28				2.92	712.385	1739.27			
2.96	713.828	1742.79				2.97	714.144	1743.56			
3.01	715.229	1746.21				3.02	715.456	1746.77			
3.06	716.164	1746.54				3.07	716.321	1746.88			
3.11	716.691	1749.76				3.12	716.739	1749.9			
3.16	716.75	1749.93				3.17	716.708	1749.82			
3.21	716.361	1746.98				3.22	716.23	1748.66			
3.26	715.525	1746.93				3.27	715.304	1746.39			
3.31	714.241	1743.8				3.32	713.931	1743.04			
3.36	712.511	1739.58				3.37	712.112	1738.6			
3.41	710.336	1734.26				3.42	709.846	1733.07			
3.46	707.717	1727.87				3.47	707.14	1726.46			
3.51	704.655	1720.39				3.51	704.655	1720.39			

		KO=1.95, NU=1.52								KO=1.95, NU=1.75			
T	FHEEL	F	Q2	P2	ALPHA	T	FHEEL	F	Q2	P2	ALPHA		
0	0	0	0	0	0	0	0	0	0	0	0		
0.05	27.4125	43.7454	8.31E-05	0.00259837	2.03047	0.05	27.4302	43.7454	8.31E-05	0.00152438	1.91257		
0.1	50.0739	87.4835	1.52E-04	0.0017386	3.25055	0.1	50.3989	87.4635	1.53E-04	0.00131392	2.80148		
0.15	72.991	131.127	2.21E-04	0.00138773	4.2934	0.15	74.2798	131.127	2.25E-04	0.00111914	3.56108		
0.2	95.0171	174.708	2.88E-04	0.00115616	5.21573	0.2	97.3921	174.708	2.95E-04	9.43E-04	4.21178		
0.25	116.152	218.181	3.52E-04	9.82E-04	6.05615	0.25	119.897	218.181	3.63E-04	8.22E-04	4.79165		
0.3	136.43	261.517	4.13E-04	8.48E-04	6.83635	0.3	141.823	261.517	4.30E-04	7.31E-04	5.32087		
0.35	155.895	304.689	4.72E-04	7.32E-04	7.5694	0.35	163.198	304.689	4.95E-04	6.57E-04	5.81108		
0.4	174.581	347.671	5.29E-04	6.36E-04	8.26382	0.4	184.044	347.671	5.58E-04	5.97E-04	6.26986		
0.45	192.514	390.436	5.83E-04	5.52E-04	8.92556	0.45	204.376	390.436	6.19E-04	5.45E-04	6.70243		
0.5	209.719	432.957	6.36E-04	4.78E-04	9.55893	0.5	224.208	432.957	6.79E-04	5.00E-04	7.11259		
0.55	226.217	475.207	6.86E-04	4.12E-04	10.1672	0.55	243.551	475.207	7.38E-04	4.61E-04	7.5032		
0.6	242.029	517.16	7.33E-04	3.52E-04	10.7529	0.6	262.412	517.16	7.95E-04	4.26E-04	7.87648		
0.65	257.174	558.79	7.79E-04	2.98E-04	11.3181	0.65	280.801	558.79	8.51E-04	3.94E-04	8.23412		
0.7	271.668	600.071	8.23E-04	2.48E-04	11.8643	0.7	298.723	600.071	9.05E-04	3.65E-04	8.5776		
0.75	285.53	640.977	8.65E-04	2.03E-04	12.3929	0.75	316.186	640.977	9.58E-04	3.39E-04	8.90804		
0.8	298.775	681.482	9.05E-04	1.61E-04	12.905	0.8	333.193	681.482	0.00100968	3.15E-04	9.22641		
0.85	311.421	721.561	9.44E-04	1.23E-04	13.4015	0.85	349.752	721.561	0.00105985	2.93E-04	9.5335		
0.9	323.482	761.19	9.80E-04	8.80E-05	13.8831	0.9	365.885	781.19	0.00110868	2.72E-04	9.82999		
0.95	334.976	800.342	0.00101508	5.56E-05	14.3505	0.95	381.538	800.342	0.00115618	2.53E-04	10.1165		
1	345.919	838.995	0.00104824	2.58E-05	14.8043	1	396.775	838.995	0.00120235	2.35E-04	10.3934		
1.03	352.225	861.936	0.00106735	9.06E-06	15.0703	1.05	411.581	877.123	0.00124722	2.19E-04	10.6613		
1.03	352.226	861.936				1.1	425.96	914.703	0.00129079	2.03E-04	10.9205		
1.08	368.605	899.738				1.15	439.916	951.711	0.00133308	1.89E-04	11.1713		
1.13	384.023	936.978				1.2	453.454	988.124	0.0013741	1.75E-04	11.414		
1.18	398.594	973.632				1.25	466.577	1023.92	0.00141387	1.63E-04	11.6488		
1.23	413.574	1009.68				1.3	479.289	1059.08	0.00145239	1.51E-04	11.8781		
1.28	428.11	1045.09				1.35	491.595	1093.57	0.00148968	1.40E-04	12.096		
1.33	442.247	1079.85				1.4	503.499	1127.38	0.00152576	1.29E-04	12.3086		
1.38	456.26	1113.94				1.45	515.006	1160.49	0.00156062	1.19E-04	12.5142		
1.43	469.943	1147.33				1.5	528.118	1192.87	0.0015943	1.10E-04	12.7128		
1.48	483.302	1180				1.55	536.842	1224.5	0.00162679	1.01E-04	12.9046		
1.53	496.395	1211.94				1.6	547.18	1255.37	0.00165812	9.34E-05	13.0898		
1.58	509.167	1243.12				1.65	557.137	1285.48	0.00168829	8.58E-05	13.2684		
1.63	521.614	1273.52				1.7	566.717	1314.74	0.00171732	7.87E-05	13.4405		
1.68	533.743	1303.13				1.75	575.924	1343.2	0.00174523	7.20E-05	13.6062		
1.73	545.535	1331.92				1.8	584.763	1370.82	0.00177201	6.58E-05	13.7656		
1.78	556.986	1359.88				1.85	593.237	1397.59	0.00179769	6.00E-05	13.9187		
1.83	568.091	1386.98				1.9	601.351	1423.48	0.00182228	5.47E-05	14.0657		
1.88	578.839	1413.23				1.95	609.108	1448.48	0.00184578	4.96E-05	14.2065		
1.93	589.226	1438.59				2	616.512	1472.57	0.00186822	4.50E-05	14.3412		
1.98	599.244	1483.05				2.05	623.568	1495.75	0.0018896	4.07E-05	14.4899		
2.03	608.888	1486.59				2.1	630.278	1517.99	0.00190994	3.67E-05	14.5927		
2.08	618.152	1509.21				2.15	638.648	1539.28	0.00192924	3.30E-05	14.7094		
2.13	627.029	1530.88				2.2	642.68	1559.61	0.00194751	2.97E-05	14.8203		
2.18	635.515	1551.6				2.25	648.377	1578.97	0.00196478	2.65E-05	14.9253		
2.23	643.603	1571.34				2.29	652.696	1593.74	0.00197787	2.42E-05	15.005		
2.28	651.289	1590.11				2.29	652.697	1593.74					
2.33	658.568	1607.88				2.34	659.95	1611.31					
2.38	665.435	1624.65				2.39	666.804	1627.88					
2.43	671.886	1640.4				2.44	673.107	1643.42					
2.48	677.918	1655.12				2.49	679.088	1657.94					
2.53	683.526	1668.81				2.54	684.606	1671.43					
2.58	688.706	1681.48				2.59	689.687	1683.86					
2.63	693.457	1693.06				2.64	694.354	1695.25					
2.68	697.773	1703.6				2.69	698.587	1705.58					
2.73	701.655	1713.07				2.74	702.377	1714.84					
2.78	705.096	1721.48				2.79	705.732	1723.03					
2.83	708.099	1728.8				2.84	708.645	1730.14					
2.88	710.657	1735.05				2.89	711.116	1736.17					
2.93	712.772	1740.22				2.94	713.142	1741.12					
2.98	714.442	1744.29				2.99	714.722	1744.98					
3.03	715.665	1747.28				3.04	715.855	1747.74					
3.08	716.441	1749.17				3.09	716.542	1749.42					
3.13	716.768	1749.97				3.14	716.78	1750					
3.18	716.648	1749.68				3.19	716.571	1749.49					
3.23	716.081	1748.29				3.24	715.913	1747.88					
3.28	715.065	1745.81				3.29	714.809	1745.18					
3.33	713.603	1742.24				3.34	713.257	1741.4					
3.38	711.695	1737.58				3.39	711.259	1736.52					
3.43	709.341	1731.84				3.44	708.818	1730.56					
3.48	706.545	1725.01				3.49	705.933	1723.51					
3.51	704.655	1720.39											

KO=3.00, NU=1.63						KO=3.00, NU=1.75					
T	FHEEL	F	Q2	P2	ALPHA	T	FHEEL	F	Q2	P2	ALPHA
0	0	0	0	0	0	0	0	0	0	0	0
0.05	26.2764	43.7454	7.96E-05	0.00105102	1.51394	0.05	25.9651	43.7454	7.87E-05	7.69E-04	1.47326
0.1	50.9154	87.4635	1.54E-04	0.00130369	2.32189	0.1	51.1017	87.4635	1.55E-04	0.00122342	2.19615
0.15	75.2671	131.127	2.28E-04	0.00107163	3.00587	0.15	75.635	131.127	2.29E-04	9.61E-04	2.79127
0.2	98.8413	174.708	3.00E-04	9.26E-04	3.59703	0.2	99.5471	174.708	3.02E-04	8.35E-04	3.29812
0.25	121.851	218.181	3.69E-04	8.20E-04	4.13039	0.25	122.971	218.181	3.73E-04	7.43E-04	3.75051
0.3	144.305	261.517	4.37E-04	7.39E-04	4.62148	0.3	145.927	261.517	4.42E-04	6.73E-04	4.16359
0.35	156.227	304.689	5.04E-04	6.73E-04	5.07971	0.35	168.432	304.689	5.10E-04	6.17E-04	4.54636
0.4	187.633	347.671	5.69E-04	6.17E-04	5.51119	0.4	190.498	347.671	5.77E-04	5.71E-04	4.90467
0.45	208.637	390.436	6.32E-04	5.69E-04	5.92021	0.45	212.135	390.436	6.43E-04	5.31E-04	5.24256
0.5	228.948	432.957	6.94E-04	5.27E-04	6.30986	0.5	233.35	432.957	7.07E-04	4.96E-04	5.56298
0.55	248.874	475.207	7.54E-04	4.90E-04	6.6825	0.55	254.147	475.207	7.70E-04	4.56E-04	5.86816
0.6	268.322	517.16	8.13E-04	4.57E-04	7.03995	0.6	274.529	517.16	8.32E-04	4.38E-04	6.1598
0.65	287.298	558.79	8.71E-04	4.26E-04	7.38364	0.65	294.498	558.79	8.92E-04	4.13E-04	6.43928
0.7	305.806	600.071	9.27E-04	3.98E-04	7.71475	0.7	314.058	600.071	9.52E-04	3.91E-04	6.70768
0.75	323.852	640.977	9.81E-04	3.73E-04	8.03422	0.75	333.207	640.977	0.00100972	3.70E-04	6.96591
0.8	341.439	681.482	0.00103466	3.49E-04	8.34284	0.8	351.948	681.482	0.00106651	3.51E-04	7.2147
0.85	358.571	721.561	0.00108658	3.27E-04	8.64129	0.85	370.281	721.561	0.00112205	3.33E-04	7.4547
0.9	375.263	761.19	0.00113713	3.05E-04	8.93011	0.9	388.205	761.19	0.00117638	3.16E-04	7.68641
0.95	391.488	800.342	0.00118633	2.87E-04	9.20979	0.95	405.725	800.342	0.00122947	3.00E-04	7.91031
1	407.278	838.995	0.00123418	2.69E-04	9.48073	1	422.835	838.995	0.00128132	2.85E-04	8.12677
1.05	422.629	877.123	0.00128069	2.52E-04	9.7433	1.05	439.637	877.123	0.00133193	2.71E-04	8.33613
1.1	437.543	914.703	0.00132589	2.35E-04	9.9978	1.1	455.833	914.703	0.00138131	2.58E-04	8.53869
1.15	452.025	951.711	0.00136977	2.21E-04	10.2445	1.15	471.721	951.711	0.00142946	2.46E-04	8.73471
1.2	466.077	988.124	0.00141235	2.07E-04	10.4836	1.2	487.203	988.124	0.00147637	2.34E-04	8.9244
1.25	479.703	1023.92	0.00145365	1.94E-04	10.7154	1.25	502.277	1023.92	0.00152205	2.23E-04	9.10797
1.3	492.908	1059.08	0.00149356	1.81E-04	10.94	1.3	516.944	1059.08	0.0015665	2.12E-04	9.2856
1.35	505.694	1093.57	0.00163241	1.69E-04	11.1576	1.35	631.205	1093.57	0.00160971	2.02E-04	9.45744
1.4	518.066	1127.38	0.0015699	1.58E-04	11.3582	1.4	545.05	1127.38	0.0016517	1.92E-04	9.62363
1.45	530.028	1160.49	0.00160615	1.47E-04	11.5722	1.45	558.509	1160.49	0.00169245	1.82E-04	9.7843
1.5	541.583	1192.87	0.00164116	1.37E-04	11.7695	1.5	571.553	1192.87	0.00173198	1.73E-04	9.93956
1.55	552.735	1224.5	0.00167496	1.28E-04	11.9603	1.55	584.192	1224.5	0.00177028	1.65E-04	10.0895
1.6	563.49	1255.37	0.00170755	1.19E-04	12.1446	1.6	596.427	1255.37	0.00180735	1.56E-04	10.2342
1.65	573.85	1285.46	0.00173894	1.10E-04	12.3226	1.65	608.258	1285.46	0.00184321	1.48E-04	10.3738
1.7	583.819	1314.74	0.00176915	1.02E-04	12.4943	1.7	619.687	1314.74	0.00187784	1.41E-04	10.5083
1.75	593.403	1343.2	0.00179819	9.51E-05	12.6597	1.75	630.713	1343.2	0.00191125	1.33E-04	10.6379
1.8	602.603	1370.82	0.00182607	8.80E-05	12.819	1.8	641.338	1370.82	0.00194345	1.26E-04	10.7624
1.85	611.426	1397.59	0.0018528	8.12E-05	12.9722	1.85	651.563	1397.59	0.00197443	1.20E-04	10.8821
1.9	619.874	1423.48	0.00187841	7.51E-05	13.1193	1.9	661.388	1423.48	0.00200421	1.13E-04	10.997
1.95	627.951	1448.48	0.00190268	6.91E-05	13.2604	1.95	670.815	1448.48	0.00203277	1.07E-04	11.1071
2	635.663	1472.57	0.00192625	6.35E-05	13.3954	2	679.844	1472.57	0.00206013	1.01E-04	11.2124
2.05	643.012	1496.75	0.00194852	5.85E-05	13.5245	2.05	688.477	1496.75	0.00208629	9.49E-05	11.313
2.1	650.001	1517.99	0.0019697	5.35E-05	13.6477	2.1	696.714	1517.99	0.00211125	8.93E-05	11.4089
2.15	656.637	1539.28	0.00198981	4.90E-05	13.765	2.15	704.556	1539.28	0.00213502	8.38E-05	11.5002
2.2	662.92	1559.61	0.00200885	4.49E-05	13.8764	2.2	712.006	1559.61	0.00215759	7.85E-05	11.5868
2.25	668.856	1578.97	0.00202683	4.07E-05	13.982	2.25	719.063	1578.97	0.00217898	7.34E-05	11.6688
2.3	674.446	1597.34	0.00204378	3.71E-05	14.0817	2.3	725.727	1597.34	0.00219917	6.84E-05	11.7463
2.35	679.696	1614.71	0.00205969	3.35E-05	14.1756	2.35	732.001	1614.71	0.00221819	6.35E-05	11.8192
2.4	684.608	1631.07	0.00207457	3.05E-05	14.2636	2.4	737.886	1631.07	0.00223602	5.89E-05	11.8876
2.45	689.184	1646.41	0.00208844	2.74E-05	14.3459	2.45	743.382	1646.41	0.00225267	5.43E-05	11.9514
2.5	693.429	1660.72	0.0021013	2.46E-05	14.4224	2.5	748.491	1660.72	0.00226815	5.00E-05	12.0108
2.65	697.343	1674	0.00211316	2.19E-05	14.4932	2.55	753.212	1674	0.00228246	4.57E-05	12.0656
2.6	700.931	1686.23	0.00212403	1.96E-05	14.5582	2.6	757.547	1686.23	0.0022956	4.15E-05	12.116
2.65	704.194	1697.4	0.00213392	1.73E-05	14.6174	2.65	761.497	1697.4	0.00230757	3.72E-05	12.1619
2.7	707.134	1707.52	0.00214283	1.50E-05	14.6709	2.7	765.062	1707.52	0.00231837	3.33E-05	12.2033
2.75	709.753	1716.56	0.00215077	1.32E-05	14.7187	2.75	768.243	1716.56	0.00232801	2.93E-05	12.2403
2.8	712.053	1724.54	0.00215774	1.11E-05	14.7607	2.8	771.041	1724.54	0.00233649	2.54E-05	12.2728
2.85	714.037	1731.43	0.00216375	9.18E-06	14.797	2.85	773.456	1731.43	0.00234381	2.15E-05	12.3009
2.9	715.705	1737.25	0.0021668	7.75E-06	14.8276	2.9	775.488	1737.25	0.00234996	1.79E-05	12.3245
2.95	717.057	1741.98	0.0021729	5.93E-06	14.8524	2.95	777.139	1741.98	0.00235497	1.41E-05	12.3438
3	718.096	1745.62	0.00217605	4.37E-06	14.8716	3	778.408	1745.62	0.00235881	1.03E-05	12.3586
3.05	718.822	1748.17	0.00217825	2.83E-06	14.886	3.05	779.295	1748.17	0.0023515	6.70E-06	12.3589
3.1	719.235	1749.62	0.0021795	1.32E-06	14.8927	3.1	779.801	1749.62	0.00236303	3.00E-06	12.3749
3.15	719.336	1749.98	0.00217981	-4.93E-07	14.8947	3.15	779.926	1749.98	0.00236341	-6.68E-07	12.3764
3.2	719.125	1749.25	0.00217917	-1.79E-06	14.891	3.2	779.67	1749.25	0.00236264	-4.28E-06	12.3736
3.25	718.601	1747.43	0.00217758	-3.42E-06	14.8816	3.25	779.032	1747.43	0.0023607	-7.93E-06	12.3662
3.3	717.765	1744.51	0.00217505	-4.87E-06	14.8665	3.3	778.014	1744.51	0.00235762	-1.16E-05	12.3545
3.35	716.614	1740.51	0.00217156	-6.47E-06	14.8456	3.35	776.613	1740.51	0.00235337	-1.53E-05	12.3384
3.4	715.151	1735.41	0.00216713	-8.42E-06	14.8191	3.4	774.831	1735.41	0.00234797	-1.91E-05	12.3178
3.45	713.373	1729.23	0.00216173	-1.00E-05	14.7868	3.45	772.567	1729.23	0.00234142	-2.29E-05	12.2928
3.5	711.278	1721.98	0.00215539	-1.18E-05	14.7488	3.5	770.12	1721.98	0.0023337	-2.67E-05	12.2633